Energy-Stable Galerkin Reduced Order Models for Prediction and Control of Fluid Systems

I. Kalashnikova[1], S. Arunajatesan[2], B. van Bloemen Waanders[1]

[1] Numerical Analysis & Applications Department, Sandia National Laboratories*, Albuquerque, NM, U.S.A.
[2] Aerosciences Department, Sandia National Laboratories*, Albuquerque, NM, U.S.A.

SIAM Conference on Computational Science & Engineering (CS&E13)
Boston, Massachusetts
February 25 - March 1, 2013

* Sandia is a multiprogram laboratory operated by Sandia Corporation, a Lockheed Martin Company, for the United States Department of Energy under Contract DE-AC04-94AL85000.

Target Cavity Flow Control Problem

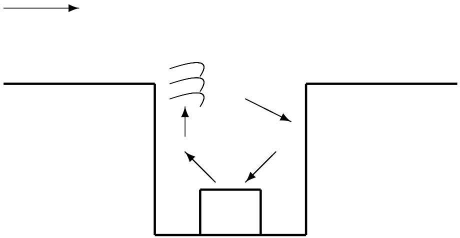

- **Configuration/Plant:** compressible non-linear fluid flow over open cavity containing components.

Target Cavity Flow Control Problem

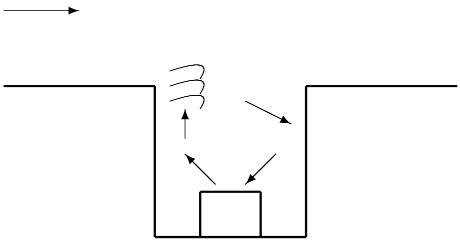

- **Configuration/Plant:** compressible non-linear fluid flow over open cavity containing components.
- **Physical Control Problem:** using upstream actuation, control oscillations within cavity caused by pressure fluctuations propagating between downstream wall and shear layer.

Target Cavity Flow Control Problem

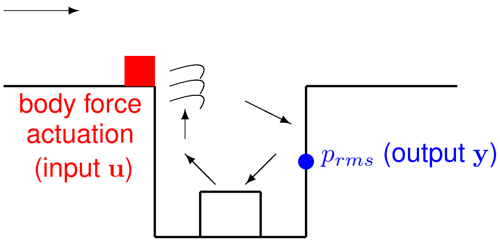

- **Configuration/Plant:** compressible non-linear fluid flow over open cavity containing components.
- **Physical Control Problem:** using upstream actuation, control oscillations within cavity caused by pressure fluctuations propagating between downstream wall and shear layer.
- **Mathematical Control Problem:** compute optimal body-force actuation input $\mathbf{u}_{opt}$ to minimize the RMS pressure halfway up the downstream wall.

$$\text{input } \mathbf{u}: \quad \mathbf{q}^T = \begin{pmatrix} 0, & f(t), & 0 & 0 & 0 \end{pmatrix}^T$$

$$\text{output } \mathbf{y}: \quad p_{rms} = \sqrt{\frac{1}{K}\sum_{i=1}^{K}(p(t_k) - \bar{p})^2}$$

Sandia National Laboratories

ROM-Based Cavity Flow Control Road Map

1. Collect snapshots from non-linear high-fidelity CFD cavity simulation

$$\dot{\mathbf{x}} = \mathbf{f}(\mathbf{x}, \mathbf{u}_i), \qquad \mathbf{y}_i = \mathbf{h}(\mathbf{x}, \mathbf{u}_i)$$

for some set of inputs $\{\mathbf{u}_i(t)\}$, and construct empirical basis (POD, BPOD) from this snapshot set.

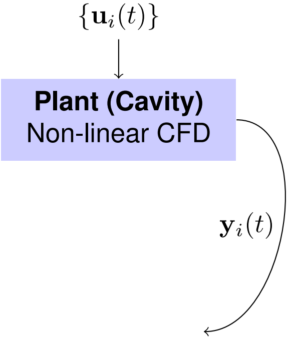

ROM-Based Cavity Flow Control Road Map

1. Collect snapshots from non-linear high-fidelity CFD cavity simulation

$$\dot{\mathbf{x}} = \mathbf{f}(\mathbf{x}, \mathbf{u}_i), \qquad \mathbf{y}_i = \mathbf{h}(\mathbf{x}, \mathbf{u}_i)$$

   for some set of inputs $\{\mathbf{u}_i(t)\}$, and construct empirical basis (POD, BPOD) from this snapshot set.

2. Build a ROM for the fluid system, or approximation of fluid system.

$\{\mathbf{u}_i(t)\}$

Plant (Cavity)
Non-linear CFD

$\mathbf{y}_i(t)$

Sandia National Laboratories

ROM-Based Cavity Flow Control Road Map

1. Collect snapshots from non-linear high-fidelity CFD cavity simulation

$$\dot{\mathbf{x}} = \mathbf{f}(\mathbf{x}, \mathbf{u}_i), \qquad \mathbf{y}_i = \mathbf{h}(\mathbf{x}, \mathbf{u}_i)$$

   for some set of inputs $\{\mathbf{u}_i(t)\}$, and construct empirical basis (POD, BPOD) from this snapshot set.

2. Build a ROM for the fluid system, or approximation of fluid system.

3. Compute optimal controller $\mathbf{u}_{opt}(t)$ using ROM.

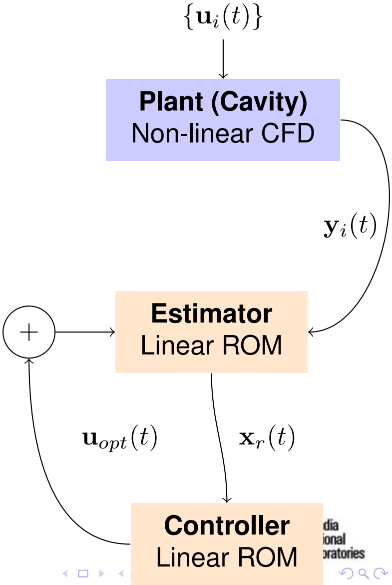

ROM-Based Cavity Flow Control Road Map

1. Collect snapshots from non-linear high-fidelity CFD cavity simulation

$$\dot{\mathbf{x}} = \mathbf{f}(\mathbf{x}, \mathbf{u}_i), \qquad \mathbf{y}_i = \mathbf{h}(\mathbf{x}, \mathbf{u}_i)$$

   for some set of inputs $\{\mathbf{u}_i(t)\}$, and construct empirical basis (POD, BPOD) from this snapshot set.

2. Build a ROM for the fluid system, or approximation of fluid system.

3. Compute optimal controller $\mathbf{u}_{opt}(t)$ using ROM.

4. Apply ROM-based controller to non-linear cavity problem.

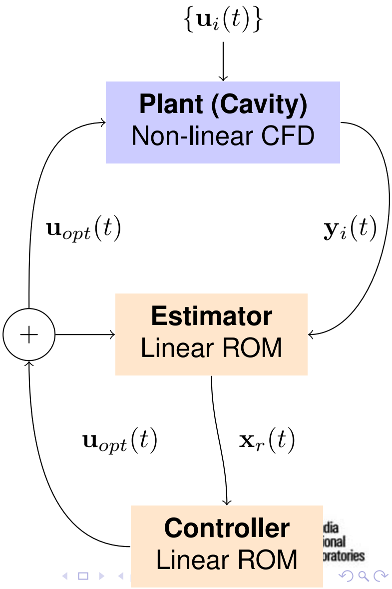

ROM-Based Cavity Flow Control Road Map

1. Collect snapshots from non-linear high-fidelity CFD cavity simulation

$$\dot{\mathbf{x}} = \mathbf{f}(\mathbf{x}, \mathbf{u}_i), \qquad \mathbf{y}_i = \mathbf{h}(\mathbf{x}, \mathbf{u}_i)$$

   for some set of inputs $\{\mathbf{u}_i(t)\}$, and construct empirical basis (POD, BPOD) from this snapshot set.

2. Build a ROM for the fluid system, or ***approximation of fluid system.***

3. Compute optimal controller $\mathbf{u}_{opt}(t)$ using ROM.

4. Apply ROM-based controller to non-linear cavity problem.

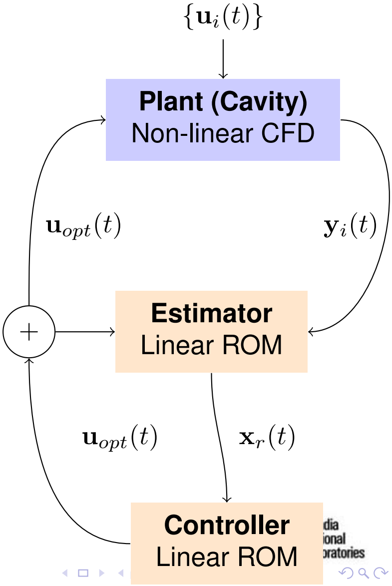

3D Full (Non-Linear) Compressible Navier-Stokes Equations

- 3D compressible Navier-Stokes equations:

$$\begin{aligned}
\rho \frac{Du_1}{dt} &= -\frac{\partial p}{\partial x_1} + \sum_{j=1}^{3} \frac{\partial}{\partial x_j} \left\{ \mu \left(\frac{\partial u_1}{\partial x_j} + \frac{\partial u_j}{\partial x_1} \right) + \lambda \delta_{1j} \nabla \cdot \mathbf{u} \right\}, \\
\rho \frac{Du_2}{dt} &= -\frac{\partial p}{\partial x_2} + \sum_{j=1}^{3} \frac{\partial}{\partial x_j} \left\{ \mu \left(\frac{\partial u_2}{\partial x_j} + \frac{\partial u_j}{\partial x_2} \right) + \lambda \delta_{2j} \nabla \cdot \mathbf{u} \right\}, \\
\rho \frac{Du_3}{dt} &= -\frac{\partial p}{\partial x_3} + \sum_{j=1}^{3} \frac{\partial}{\partial x_j} \left\{ \mu \left(\frac{\partial u_3}{\partial x_j} + \frac{\partial u_j}{\partial x_3} \right) + \lambda \delta_{3j} \nabla \cdot \mathbf{u} \right\}, \\
\rho C_v \frac{DT}{dt} &= -p \nabla \cdot \mathbf{u} + \sum_{i=1}^{3} \frac{\partial}{\partial x_i} \left(\kappa \frac{\partial T}{\partial x_i} \right), \\
\frac{D\rho}{\partial t} &= -\rho \nabla \cdot \mathbf{u}.
\end{aligned} \tag{1}$$

- ROM approach is based on local linearization of full non-linear equations (1):
    - Full non-linear equations (1) are solved to generate snapshots in high-fidelity code.
    - Linearized approximation of (1) is projected onto reduced basis modes in building the ROM.

Sandia National Laboratories

3D Linearized Compressible Navier-Stokes Equations

- Appropriate when a compressible fluid system can be described by viscous, small-amplitude perturbations about a steady-state mean (or base) flow.
- Linearization of full compressible Navier-Stokes equations:

$$\mathbf{q}^T(\mathbf{x},t) \equiv \left(\; u_1, \quad u_2, \quad u_3, \quad T, \quad \rho \; \right) \equiv \underbrace{\bar{\mathbf{q}}^T(\mathbf{x})}_{\text{mean}} + \underbrace{\mathbf{q}'^T(\mathbf{x},t)}_{\text{fluctuation}} \in \mathbb{R}^5$$

  - **Simplest linearization**: neglect $\nabla\bar{\mathbf{q}}$ terms (uniform base flow)

$$\mathbf{q}'_{,t} + \mathbf{A}_i(\bar{\mathbf{q}})\mathbf{q}'_{,i} - [\mathbf{K}_{ij}(\bar{\mathbf{q}})\mathbf{q}'_{,j}]_{,i} = \mathbf{F}$$

  - **More accurate linearization**: retain $\nabla\bar{\mathbf{q}}$ terms

$$\mathbf{q}'_{,t} + [\mathbf{A}_i(\bar{\mathbf{q}}) - \mathbf{K}_i^{vw}(\nabla\bar{\mathbf{q}})]\mathbf{q}'_{,i} - [\mathbf{K}_{ij}(\bar{\mathbf{q}})\mathbf{q}'_{,j}]_{,i} + \mathbf{C}(\nabla\bar{\mathbf{q}})\mathbf{q}' = \mathbf{F}$$

$\mathbf{A}_i(\bar{\mathbf{q}})$: convective flux matrices
$\mathbf{K}_{ij}(\bar{\mathbf{q}})$: diffusive flux matrices
$\mathbf{K}_i^{vw}(\bar{\mathbf{q}})$: viscous work matrices

Sandia National Laboratories

Outline

This talk focuses on how to construct a Galerkin ROM that is **stable** *a priori*

Energy-Stability

- **Practical Definition:** Numerical solution does not “blow up” in finite time.

Energy-Stability

- **Practical Definition:** Numerical solution does not “blow up” in finite time.
- **More Precise Definition:** Numerical discretization does not introduce any spurious instabilities inconsistent with natural instability modes supported by the governing continuous PDEs.

Energy-Stability

- **Practical Definition:** Numerical solution does not “blow up” in finite time.
- **More Precise Definition:** Numerical discretization does not introduce any spurious instabilities inconsistent with natural instability modes supported by the governing continuous PDEs.

Numerical solutions **must** maintain a proper energy balance

Energy-Stability

- **Practical Definition:** Numerical solution does not "blow up" in finite time.
- **More Precise Definition:** Numerical discretization does not introduce any spurious instabilities inconsistent with natural instability modes supported by the governing continuous PDEs.

Numerical solutions **must** maintain a proper energy balance

Linearized Compressible Navier-Stokes Equations:
$\frac{dE}{dt} \leq 0$
Non-increasing energy [5]

$\longleftarrow$ duality $\longrightarrow$

Compressible Navier-Stokes Equations:
$\frac{d}{dt} \int_\Omega \rho \eta d\Omega \geq 0$
Clausius-Duhem Inequality
Non-decreasing entropy [4]

Energy-Stability

- **Practical Definition:** Numerical solution does not “blow up” in finite time.
- **More Precise Definition:** Numerical discretization does not introduce any spurious instabilities inconsistent with natural instability modes supported by the governing continuous PDEs.

Numerical solutions **must** maintain a proper energy balance

Linearized Compressible Navier-Stokes Equations:

$$\frac{dE}{dt} \leq 0$$

Non-increasing energy [5]

⟵ duality ⟶

Compressible Navier-Stokes Equations:

$$\frac{d}{dt}\int_\Omega \rho\eta d\Omega \geq 0$$

Clausius-Duhem Inequality

Non-decreasing entropy [4]

- Analyzed using the **Energy Method**: Uses an equation for the evolution of numerical solution “energy” (or “entropy”) to determine stability.

Sandia National Laboratories

Connection to Lyapunov Stability*

$$\dot{\mathbf{x}}_N = \mathbf{f}_N(\mathbf{x}_N), \qquad \mathbf{x}_N \in \mathbb{R}^N$$

- **Lyapunov Stability:** If there exists a **Lyapunov function** V such that
  - $V > 0$ (positive-definite), and
  - $\frac{dV}{dt} = \frac{dV}{d\mathbf{x}}\mathbf{f}(\mathbf{x}) \leq 0$ (negative semi-definite along system trajectories)

  in $B_r(\mathbf{x}_s)$, then $\mathbf{x}_s$ is ***locally stable in the sense of Lyapunov*** [8].

- **Energy Stability:** Let

$$E_N \equiv \frac{1}{2}||\mathbf{x}_N||^2$$

denote the system energy. If

$$\frac{dE_N}{dt} \leq 0$$

the system is ***energy-stable***.

*Manuscript in preparation.

Sandia National Laboratories

Connection to Lyapunov Stability*

$$\dot{\mathbf{x}}_N = \mathbf{f}_N(\mathbf{x}_N), \qquad \mathbf{x}_N \in \mathbb{R}^N$$

- **Lyapunov Stability:** If there exists a **Lyapunov function** V such that
  - $V > 0$ (positive-definite), and
  - $\frac{dV}{dt} = \frac{dV}{d\mathbf{x}}\mathbf{f}(\mathbf{x}) \leq 0$ (negative semi-definite along system trajectories)

  in $B_r(\mathbf{x}_s)$, then $\mathbf{x}_s$ is ***locally stable in the sense of Lyapunov*** [8].

- **Energy Stability:** Let

$$E_N \equiv \frac{1}{2}||\mathbf{x}_N||^2$$

denote the system energy. If

$$\frac{dE_N}{dt} \leq 0$$

the system is ***energy-stable***.

Remark: System energy E_N satisfies the definition of a Lyapunov function!

*Manuscript in preparation.

Model Reduction Approach

High-Fidelity CFD Simulations:

Snapshot 1

Snapshot 2

⋮

Snapshot K

Step 1 →

Fluid Modal Decomposition (POD):

$$\mathbf{u}_M = \sum_{k=1}^{M} a_k(t)\boldsymbol{\phi}_k(\mathbf{x})$$

Step 2 →

Galerkin Projection of Fluid PDEs:

$$(\boldsymbol{\phi}_j, \dot{\mathbf{u}}_M + \nabla \cdot \mathbf{F}(\mathbf{u}_M)) = 0$$

“Small” ROM ODE System:

$$\dot{a}_k = f(a_1, \ldots, a_M)$$

Step 1: Constructing the Modes

High-Fidelity CFD Simulations:

Snapshot 1

Snapshot 2

⋮

Snapshot K

Step 1 →

Fluid Modal Decomposition (POD):

$$\mathbf{u}_M = \sum_{k=1}^{M} a_k(t)\boldsymbol{\phi}_k(\mathbf{x})$$

Step 2 →

Galerkin Projection of Fluid PDEs:

$$(\boldsymbol{\phi}_j, \dot{\mathbf{u}}_M + \nabla \cdot \mathbf{F}(\mathbf{u}_M)) = 0$$

"Small" ROM ODE System:

$$\dot{a}_k = f(a_1, \ldots, a_M)$$

- **POD basis** $\{\boldsymbol{\phi}_i\}_{i=1}^{M}$ with $M << K$ maximizes the energy in the projection of snapshots onto span$\{\boldsymbol{\phi}_i\}$.
- **POD SVD problem**:

$$\mathbf{X} = \mathbf{U}\boldsymbol{\Sigma}\mathbf{V}^T$$

$$(\boldsymbol{\phi}_1, \cdots, \boldsymbol{\phi}_M) = \mathbf{U}(:, 1:M)$$

Step 2: Galerkin Projection

High-Fidelity CFD Simulations:

Snapshot 1

Snapshot 2

⋮

Snapshot K

Step 1 →

Fluid Modal Decomposition (POD):

$$\mathbf{u}_M = \sum_{k=1}^{M} a_k(t)\boldsymbol{\phi}_k(\mathbf{x})$$

Step 2 →

Galerkin Projection of Fluid PDEs:

$$(\boldsymbol{\phi}_j, \dot{\mathbf{u}}_M + \nabla \cdot \mathbf{F}(\mathbf{u}_M)) = 0$$

“Small” ROM ODE System:

$$\dot{a}_k = f(a_1, \ldots, a_M)$$

Discrete vs. Continuous Projection

DISCRETE APPROACH

Governing Equations
$$\mathbf{u}_t = \mathcal{L}u$$
$\downarrow$

CFD Model
$$\dot{\mathbf{u}}_N = \mathbf{A}_N \mathbf{u}_N$$
$\downarrow$

Discrete Modal Basis Φ

$\downarrow$

Projection of CFD Model
(Matrix Operation)

$\downarrow$

ROM
$$\dot{\mathbf{a}} = \Phi^T \mathbf{A}_N \Phi \mathbf{a}$$

CONTINUOUS APPROACH

Governing Equations
$$\mathbf{u}_t = \mathcal{L}u$$
$\downarrow$

CFD Model
$$\dot{\mathbf{u}}_N = \mathbf{A}_N \mathbf{u}_N$$
$\downarrow$

Continuous Modal Basis* $\phi_j(\mathbf{x})$

$\downarrow$

Projection of Governing Equations
(Numerical Integration)

$\downarrow$

ROM
$$\dot{a}_j = (\phi_j, \mathcal{L}\phi_k) a_k$$

* Continuous functions space is defined using finite elements.

Energy-Stable ROM via Continuous Projection

Energy stability of the Galerkin ROM can be proven [1] following "symmetrization" the linearized compressible Navier-Stokes equations.

- Linearized compressible Navier-Stokes system is "symmetrizable" [5].
- Pre-multiply equations by symmetric positive definite matrix:

$$\mathbf{H} \equiv \begin{pmatrix} \bar{\rho} & 0 & 0 & 0 & 0 \\ 0 & \bar{\rho} & 0 & 0 & 0 \\ 0 & 0 & \rho & 0 & 0 \\ 0 & 0 & 0 & \frac{\bar{\rho}R}{\bar{T}(\gamma-1)} & 0 \\ 0 & 0 & 0 & 0 & \frac{R\bar{T}}{\bar{\rho}} \end{pmatrix} \Rightarrow \boxed{\mathbf{H}\mathbf{q}'_{,t} + \mathbf{H}\mathbf{A}_i\,\mathbf{q}'_{,i} - \mathbf{H}[\mathbf{K}_{ij}\mathbf{q}'_{,i}]_{,j} + \cdots = \mathbf{F}}$$

- $\mathbf{H}$ is called the "symmetrizer" of the system:
  - The convective flux matrices $\mathbf{H}\mathbf{A}_i$ are all symmetric.
  - The following augmented viscosity matrix

$$\mathbf{K}^S \equiv \begin{pmatrix} \mathbf{H}\mathbf{K}_{11} & \mathbf{H}\mathbf{K}_{12} & \mathbf{H}\mathbf{K}_{13} \\ \mathbf{H}\mathbf{K}_{21} & \mathbf{H}\mathbf{K}_{22} & \mathbf{H}\mathbf{K}_{23} \\ \mathbf{H}\mathbf{K}_{31} & \mathbf{H}\mathbf{K}_{32} & \mathbf{H}\mathbf{K}_{33} \end{pmatrix},$$

  is symmetric positive semi-definite.

Sandia National Laboratories

Symmetry Inner Product & A Stable Galerkin ROM

- Define the "symmetry" inner product and "symmetry" norm:

$$(\mathbf{q}'^{(1)}, \mathbf{q}'^{(2)})_{(\mathbf{H},\Omega)} \equiv \int_{\Omega} [\mathbf{q}'^{(1)}]^T \mathbf{H} \mathbf{q}'^{(2)} d\Omega, \qquad ||\mathbf{q}'||_{(\mathbf{H},\Omega)} \equiv (\mathbf{q}', \mathbf{q}')_{(\mathbf{H},\Omega)} \tag{2}$$

Symmetry Inner Product & A Stable Galerkin ROM

- Define the "symmetry" inner product and "symmetry" norm:

$$(\mathbf{q}'^{(1)}, \mathbf{q}'^{(2)})_{(\mathbf{H},\Omega)} \equiv \int_\Omega [\mathbf{q}'^{(1)}]^T \mathbf{H} \mathbf{q}'^{(2)} d\Omega, \qquad ||\mathbf{q}'||_{(\mathbf{H},\Omega)} \equiv (\mathbf{q}', \mathbf{q}')_{(\mathbf{H},\Omega)} \tag{2}$$

- Stability analysis reveals that the symmetry inner product (and *not* the L^2 inner product!) is the energy inner product for this equation set.

Symmetry Inner Product & A Stable Galerkin ROM

- Define the "symmetry" inner product and "symmetry" norm:

$$(\mathbf{q}'^{(1)}, \mathbf{q}'^{(2)})_{(\mathbf{H},\Omega)} \equiv \int_{\Omega} [\mathbf{q}'^{(1)}]^T \mathbf{H} \mathbf{q}'^{(2)} d\Omega, \qquad ||\mathbf{q}'||_{(\mathbf{H},\Omega)} \equiv (\mathbf{q}', \mathbf{q}')_{(\mathbf{H},\Omega)} \tag{2}$$

- Stability analysis reveals that the symmetry inner product (and *not* the L^2 inner product!) is the energy inner product for this equation set.
- **Uniform base flow case:** non-increasing energy in Galerkin approximation $\mathbf{q}'_M = \sum_{i=1}^{M} a_k(t)\boldsymbol{\phi}_k(\mathbf{x})$

$$\boxed{\frac{dE_M}{dt} \equiv \frac{1}{2}\frac{d}{dt}||\mathbf{q}'_M(\mathbf{x},t)||_{(\mathbf{H},\Omega)} \leq 0}$$

Sandia National Laboratories

Symmetry Inner Product & A Stable Galerkin ROM

- Define the "symmetry" inner product and "symmetry" norm:

$$(\mathbf{q}'^{(1)}, \mathbf{q}'^{(2)})_{(\mathbf{H},\Omega)} \equiv \int_{\Omega} [\mathbf{q}'^{(1)}]^T \mathbf{H} \mathbf{q}'^{(2)} d\Omega, \qquad ||\mathbf{q}'||_{(\mathbf{H},\Omega)} \equiv (\mathbf{q}', \mathbf{q}')_{(\mathbf{H},\Omega)} \tag{2}$$

- Stability analysis reveals that the symmetry inner product (and *not* the L^2 inner product!) is the energy inner product for this equation set.
- **Uniform base flow case:** non-increasing energy in Galerkin approximation $\mathbf{q}'_M = \sum_{i=1}^{M} a_k(t)\boldsymbol{\phi}_k(\mathbf{x})$

$$\boxed{\frac{dE_M}{dt} \equiv \frac{1}{2}\frac{d}{dt}||\mathbf{q}'_M(\mathbf{x},t)||_{(\mathbf{H},\Omega)} \leq 0}$$

- **General case:** Galerkin approximation satisfies same energy expression as solutions to the continuous PDEs

$$\boxed{||\mathbf{q}'_M(\mathbf{x},t)||_{(\mathbf{H},\Omega)} \leq e^{\beta t}||\mathbf{q}'_M(\mathbf{x},0)||_{(\mathbf{H},\Omega)}}$$

Sandia National Laboratories

Symmetry Inner Product & A Stable Galerkin ROM

- Define the "symmetry" inner product and "symmetry" norm:

$$(\mathbf{q}'^{(1)}, \mathbf{q}'^{(2)})_{(\mathbf{H},\Omega)} \equiv \int_\Omega [\mathbf{q}'^{(1)}]^T \mathbf{H} \mathbf{q}'^{(2)} d\Omega, \qquad ||\mathbf{q}'||_{(\mathbf{H},\Omega)} \equiv (\mathbf{q}', \mathbf{q}')_{(\mathbf{H},\Omega)} \tag{2}$$

- Stability analysis reveals that the symmetry inner product (and *not* the L^2 inner product!) is the energy inner product for this equation set.
- **Uniform base flow case:** non-increasing energy in Galerkin approximation $\mathbf{q}'_M = \sum_{i=1}^M a_k(t)\boldsymbol{\phi}_k(\mathbf{x})$

$$\frac{dE_M}{dt} \equiv \frac{1}{2}\frac{d}{dt}||\mathbf{q}'_M(\mathbf{x},t)||_{(\mathbf{H},\Omega)} \leq 0$$

- **General case:** Galerkin approximation satisfies same energy expression as solutions to the continuous PDEs

$$||\mathbf{q}'_M(\mathbf{x},t)||_{(\mathbf{H},\Omega)} \leq e^{\beta t}||\mathbf{q}'_M(\mathbf{x},0)||_{(\mathbf{H},\Omega)}$$

Practical Implication:
Symmetry inner product ensures Galerkin projection step of the ROM is stable (provided system is in stable state) for **any** basis!

Energy-Stable ROM via Discrete Projection

Symmetry inner product has discrete analog!

- Consider linear discrete (i.e., discretized in space) stable full order system

$$\dot{\mathbf{x}} = \mathbf{A}\mathbf{x} \tag{3}$$

- Lyapunov function for (3): $V(\mathbf{x}) = \mathbf{x}^T\mathbf{P}\mathbf{x}$ where $\mathbf{P}$ is the solution of the Ricatti equation:

$$\mathbf{A}^T\mathbf{P} + \mathbf{P}\mathbf{A} = -\mathbf{Q} \tag{4}$$

  - S.p.d. solution to (4) exists if $\mathbf{Q}$ is s.p.d. and $\mathbf{A}$ is stable [8].
  - Solution to (4) can be obtained using MATLAB control toolbox:

```
P = lyap(A', Q, [] speye(n, n));
```

- Discrete analog of symmetry inner-product: **Lyapunov inner product**

$$(\mathbf{x}_1, \mathbf{x}_2)_{\mathbf{P}} \equiv \mathbf{x}_1^T\mathbf{P}\mathbf{x}_2$$

Energy-Stable ROM via Discrete Projection

Symmetry inner product has discrete analog!

- Consider linear discrete (i.e., discretized in space) stable full order system

$$\dot{\mathbf{x}} = \mathbf{A}\mathbf{x} \tag{3}$$

- Lyapunov function for (3): $V(\mathbf{x}) = \mathbf{x}^T\mathbf{P}\mathbf{x}$ where $\mathbf{P}$ is the solution of the Ricatti equation:

$$\mathbf{A}^T\mathbf{P} + \mathbf{P}\mathbf{A} = -\mathbf{Q} \tag{4}$$

  - S.p.d. solution to (4) exists if $\mathbf{Q}$ is s.p.d. and $\mathbf{A}$ is stable [8].
  - Solution to (4) can be obtained using MATLAB control toolbox:

```
P = lyap(A', Q, [] speye(n, n));
```

- Discrete analog of symmetry inner-product: **Lyapunov inner product**

$$\boxed{(\mathbf{x}_1, \mathbf{x}_2)_{\mathbf{P}} \equiv \mathbf{x}_1^T\mathbf{P}\mathbf{x}_2}$$

- Can show: if ROM for (3) is constructed in Lyapunov inner product,

$$\frac{dE_M}{dt} \equiv \frac{1}{2}\frac{d}{dt}||\mathbf{x}_M||_2^2 \leq 0$$

Sandia National Laboratories

Energy-Stable ROM via Discrete Projection: vs. Continuous Projection

Symmetry Inner Product
(Continuous)

$$\boxed{(\mathbf{q}'^{(1)}, \mathbf{q}'^{(2)})_{(\mathbf{H},\Omega)} \equiv \int_\Omega [\mathbf{q}'^{(1)}]^T \mathbf{H} \mathbf{q}'^{(2)} d\Omega}$$

Lyapunov Inner Product
(Discrete)

$$\boxed{(\mathbf{x}_1, \mathbf{x}_2)_{\mathbf{P}} \equiv \mathbf{x}_1^T \mathbf{P} \mathbf{x}_2}$$

Sandia National Laboratories

Energy-Stable ROM via Discrete Projection: vs. Continuous Projection

Symmetry Inner Product
(Continuous)

$$\boxed{(\mathbf{q}'^{(1)}, \mathbf{q}'^{(2)})_{(\mathbf{H},\Omega)} \equiv \int_{\Omega} [\mathbf{q}'^{(1)}]^T \mathbf{H} \mathbf{q}'^{(2)} d\Omega}$$

- For linear system:

$$\mathbf{q}'_{,t} + \mathbf{A}_i \mathbf{q}'_{,i} - [\mathbf{K}_{ij} \mathbf{q}'_{,i}]_{,j} + \cdots = \mathbf{F}$$

Lyapunov Inner Product
(Discrete)

$$\boxed{(\mathbf{x}_1, \mathbf{x}_2)_{\mathbf{P}} \equiv \mathbf{x}_1^T \mathbf{P} \mathbf{x}_2}$$

- For linear system:

$$\mathbf{x}_{,t} = \mathbf{A}\mathbf{x}$$

Sandia National Laboratories

Energy-Stable ROM via Discrete Projection: vs. Continuous Projection

Symmetry Inner Product
(Continuous)

$$\boxed{(\mathbf{q}'^{(1)}, \mathbf{q}'^{(2)})_{(\mathbf{H},\Omega)} \equiv \int_{\Omega} [\mathbf{q}'^{(1)}]^T \mathbf{H} \mathbf{q}'^{(2)} d\Omega}$$

- For linear system:

$$\mathbf{q}'_{,t} + \mathbf{A}_i \mathbf{q}'_{,i} - [\mathbf{K}_{ij} \mathbf{q}'_{,i}]_{,j} + \cdots = \mathbf{F}$$

- Defined for unstable systems, but stability of ROM not guaranteed.

Lyapunov Inner Product
(Discrete)

$$\boxed{(\mathbf{x}_1, \mathbf{x}_2)_{\mathbf{P}} \equiv \mathbf{x}_1^T \mathbf{P} \mathbf{x}_2}$$

- For linear system:

$$\mathbf{x}_{,t} = \mathbf{A}\mathbf{x}$$

- Undefined for unstable systems.

Sandia National Laboratories

Energy-Stable ROM via Discrete Projection: vs. Continuous Projection

Symmetry Inner Product
(Continuous)

$$\left(\mathbf{q}'^{(1)}, \mathbf{q}'^{(2)}\right)_{(\mathbf{H},\Omega)} \equiv \int_\Omega [\mathbf{q}'^{(1)}]^T \mathbf{H} \mathbf{q}'^{(2)} d\Omega$$

- For linear system:

$$\mathbf{q}'_{,t} + \mathbf{A}_i \mathbf{q}'_{,i} - [\mathbf{K}_{ij}\mathbf{q}'_{,i}]_{,j} + \cdots = \mathbf{F}$$

- Defined for unstable systems, but stability of ROM not guaranteed.
- Induced by Lyapunov function for system.

Lyapunov Inner Product
(Discrete)

$$(\mathbf{x}_1, \mathbf{x}_2)_{\mathbf{P}} \equiv \mathbf{x}_1^T \mathbf{P} \mathbf{x}_2$$

- For linear system:

$$\mathbf{x}_{,t} = \mathbf{A}\mathbf{x}$$

- Undefined for unstable systems.
- Induced by Lyapunov function for system.

Sandia National Laboratories

Energy-Stable ROM via Discrete Projection: vs. Continuous Projection

Symmetry Inner Product
(Continuous)

$$\boxed{(\mathbf{q}'^{(1)}, \mathbf{q}'^{(2)})_{(\mathbf{H},\Omega)} \equiv \int_\Omega [\mathbf{q}'^{(1)}]^T \mathbf{H}\mathbf{q}'^{(2)} d\Omega}$$

- For linear system:

$$\mathbf{q}'_{,t} + \mathbf{A}_i \mathbf{q}'_{,i} - [\mathbf{K}_{ij}\mathbf{q}'_{,i}]_{,j} + \cdots = \mathbf{F}$$

- Defined for unstable systems, but stability of ROM not guaranteed.
- Induced by Lyapunov function for system.
- Equation-specific ($\Rightarrow$ embedded algorithm).
- Known analytically in closed form.

Lyapunov Inner Product
(Discrete)

$$\boxed{(\mathbf{x}_1, \mathbf{x}_2)_{\mathbf{P}} \equiv \mathbf{x}_1^T \mathbf{P} \mathbf{x}_2}$$

- For linear system:

$$\mathbf{x}_{,t} = \mathbf{A}\mathbf{x}$$

- Undefined for unstable systems.
- Induced by Lyapunov function for system.
- Black-box.
- Computed numerically by solving Ricatti equation ($\mathcal{O}(N^3)$ ops).

Implementation

- **Stability-Preserving Discrete Implementation of ROM:**
  - ROM is implemented in a C++ code that uses distributed vector and matrix data structures and parallel eigensolvers from the `Trilinos` project [7].
  - POD modes defined using piecewise smooth finite elements.
  - Gauss quadrature rules of sufficient accuracy are used to compute exactly inner products with the help of `libmesh` library.

ROM code is potentially compatible with any CFD code that can output a mesh and snapshot data stored at the nodes of this mesh.

- **High-fidelity CFD Code: SIGMA CFD**
  - Sandia in-house finite volume flow solver derived from LESLIE3D [6], a LES flow solver originally developed in the Computational Combustion Laboratory at Georgia Tech.
  - Solves the turbulent compressible flow equations using an explicit 2-4 MacCormack scheme.
  - A hybrid scheme coupling the MacCormack scheme to flux difference splitting schemes is employed to capture shocks.

Sandia National Laboratories

Driven Pulse in a Uniform Base Flow

- Uniform base flow in $\Omega = (-1, 1)^2$:

$$\bar{p} = 10.1325 \text{ Pa}$$
$$\bar{T} = 300 \text{ K}$$
$$\bar{\rho} = \frac{\bar{p}}{R\bar{T}} = 1.17 \times 10^{-4} \text{ kg/m}^3$$
$$\bar{u}_1 = \bar{u}_2 = \bar{u}_3 = 0.0 \text{ m/s}$$
$$\bar{c} = 347.9693 \text{ m/s}.$$

- Slip wall boundary conditions applied on all boundaries of Ω.

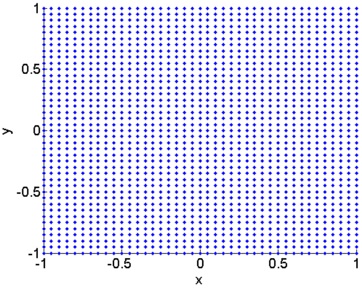

Driven Pulse in a Uniform Base Flow

- Uniform base flow in $\Omega = (-1,1)^2$:

$$\bar{p} = 10.1325 \text{ Pa}$$
$$\bar{T} = 300 \text{ K}$$
$$\bar{\rho} = \frac{\bar{p}}{RT} = 1.17 \times 10^{-4} \text{ kg/m}^3$$
$$\bar{u}_1 = \bar{u}_2 = \bar{u}_3 = 0.0 \text{ m/s}$$
$$\bar{c} = 347.9693 \text{ m/s}.$$

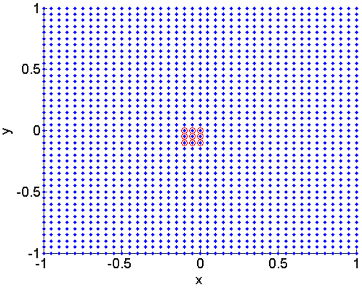

- Slip wall boundary conditions applied on all boundaries of Ω.
- Force for y–momentum equation drives the flow:

$$F_v(\mathbf{x},t) = \left(1 \times 10^{-4}\right)\cos(2000\pi t), \qquad \mathbf{x} \in (-0.1, 0)^2$$

Driven Pulse in a Uniform Base Flow

- Uniform base flow in $\Omega = (-1, 1)^2$:

$$\bar{p} = 10.1325 \text{ Pa}$$
$$\bar{T} = 300 \text{ K}$$
$$\bar{\rho} = \frac{\bar{p}}{R\bar{T}} = 1.17 \times 10^{-4} \text{ kg/m}^3$$
$$\bar{u}_1 = \bar{u}_2 = \bar{u}_3 = 0.0 \text{ m/s}$$
$$\bar{c} = 347.9693 \text{ m/s}.$$

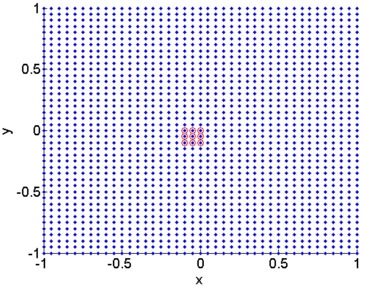

- Slip wall boundary conditions applied on all boundaries of Ω.
- Force for y–momentum equation drives the flow:

$$F_v(\mathbf{x}, t) = \left(1 \times 10^{-4}\right) \cos(2000\pi t), \qquad \mathbf{x} \in (-0.1, 0)^2$$

- High-fidelity CFD simulation run on 3362 node mesh until time $T = 0.5$ seconds.
- 2500 snapshots (saved every 2×10^{-5} seconds), used to construct a 20 mode POD basis.

Sandia National Laboratories

Uncontrolled Symmetry ROM Results

- Figure below shows:
  - ○: t vs. $a_i(t)$ (ROM coefficients).
  - $-$: t vs. $(\mathbf{q}'_{CFD}(\mathbf{x}, t), \boldsymbol{\phi}_i(\mathbf{x}))$ (projection of snapshots onto modes).
- Movie on right shows u-velocity snapshot (top) vs. 20 mode symmetry ROM solution for u (bottom).

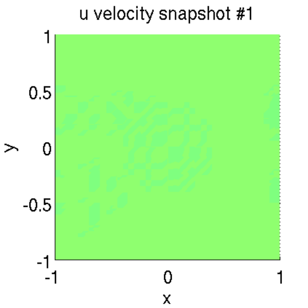

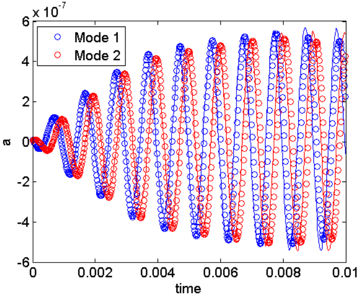

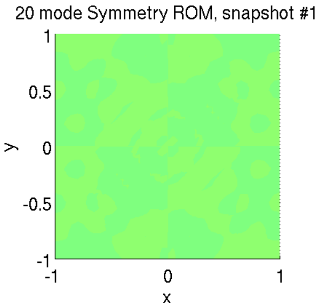

Uncontrolled Symmetry ROM Results

- Figure below shows:
  - $\circ$: t vs. $a_i(t)$ (ROM coefficients).
  - $-$: t vs. $(\mathbf{q}'_{CFD}(\mathbf{x},t), \boldsymbol{\phi}_i(\mathbf{x}))$ (projection of snapshots onto modes).
- Movie on right shows u-velocity snapshot (top) vs. 20 mode symmetry ROM solution for u (bottom).

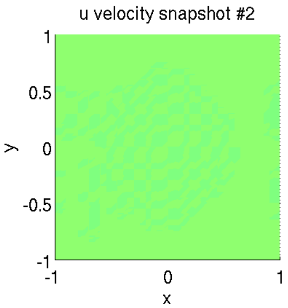

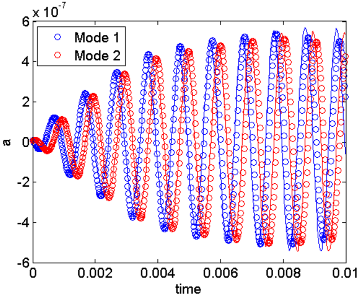

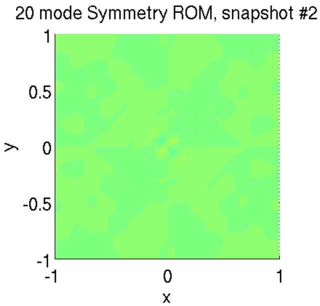

Uncontrolled Symmetry ROM Results

- Figure below shows:
  - $\circ$: t vs. $a_i(t)$ (ROM coefficients).
  - $-$: t vs. $(\mathbf{q}'_{CFD}(\mathbf{x},t), \boldsymbol{\phi}_i(\mathbf{x}))$ (projection of snapshots onto modes).
- Movie on right shows u-velocity snapshot (top) vs. 20 mode symmetry ROM solution for u (bottom).

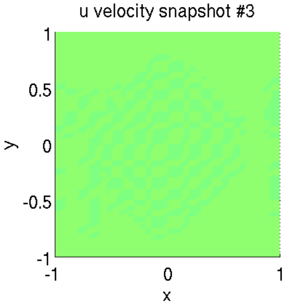

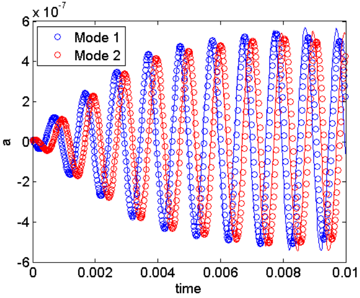

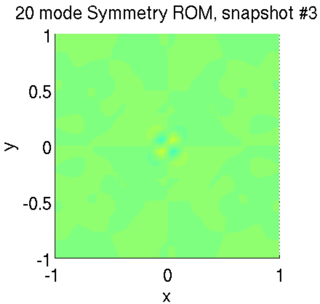

Uncontrolled Symmetry ROM Results

- Figure below shows:
  - ○: t vs. $a_i(t)$ (ROM coefficients).
  - $-$: t vs. $(\mathbf{q}'_{CFD}(\mathbf{x},t), \boldsymbol{\phi}_i(\mathbf{x}))$ (projection of snapshots onto modes).
- Movie on right shows u-velocity snapshot (top) vs. 20 mode symmetry ROM solution for u (bottom).

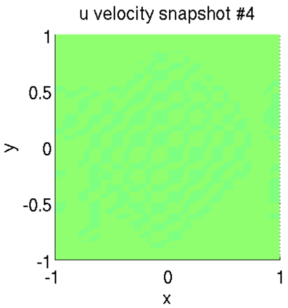

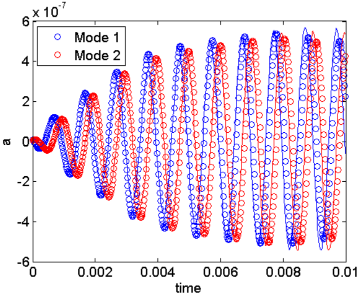

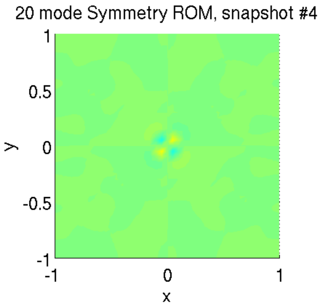

Uncontrolled Symmetry ROM Results

- Figure below shows:
  - $\circ$: t vs. $a_i(t)$ (ROM coefficients).
  - $-$: t vs. $(\mathbf{q}'_{CFD}(\mathbf{x}, t), \boldsymbol{\phi}_i(\mathbf{x}))$ (projection of snapshots onto modes).
- Movie on right shows u-velocity snapshot (top) vs. 20 mode symmetry ROM solution for u (bottom).

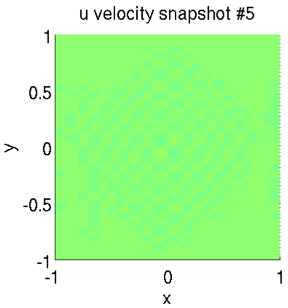

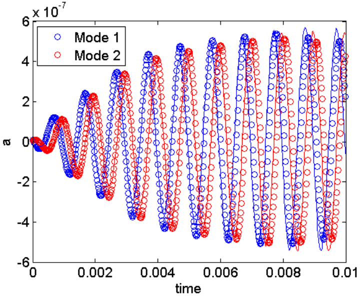

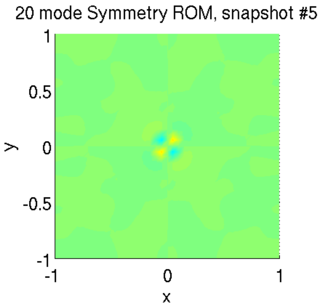

Uncontrolled Symmetry ROM Results

- Figure below shows:
  - $\circ$: t vs. $a_i(t)$ (ROM coefficients).
  - $-$: t vs. $(\mathbf{q}'_{CFD}(\mathbf{x},t), \boldsymbol{\phi}_i(\mathbf{x}))$ (projection of snapshots onto modes).
- Movie on right shows u-velocity snapshot (top) vs. 20 mode symmetry ROM solution for u (bottom).

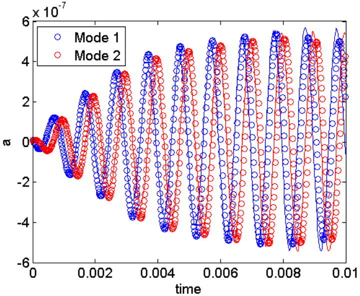

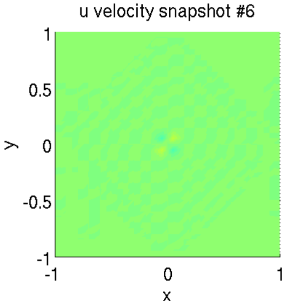

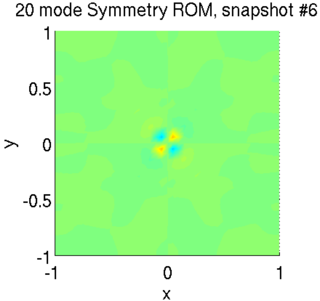

Uncontrolled Symmetry ROM Results

- Figure below shows:
  - $\circ$: t vs. $a_i(t)$ (ROM coefficients).
  - $-$: t vs. $(\mathbf{q}'_{CFD}(\mathbf{x},t), \boldsymbol{\phi}_i(\mathbf{x}))$ (projection of snapshots onto modes).
- Movie on right shows u-velocity snapshot (top) vs. 20 mode symmetry ROM solution for u (bottom).

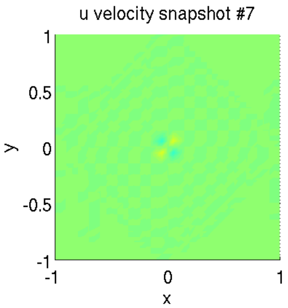

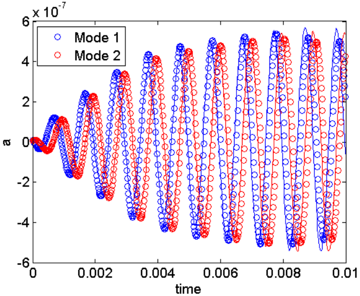

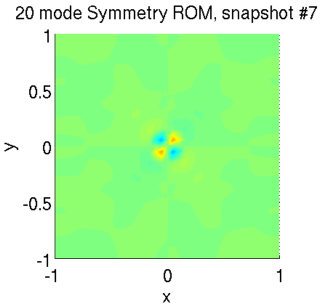

Uncontrolled Symmetry ROM Results

- Figure below shows:
  - $\circ$: t vs. $a_i(t)$ (ROM coefficients).
  - $-$: t vs. $(\mathbf{q}'_{CFD}(\mathbf{x}, t), \boldsymbol{\phi}_i(\mathbf{x}))$ (projection of snapshots onto modes).
- Movie on right shows u-velocity snapshot (top) vs. 20 mode symmetry ROM solution for u (bottom).

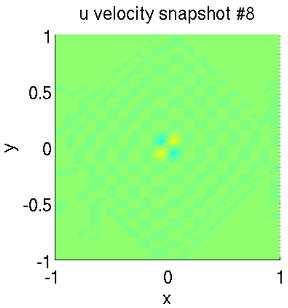

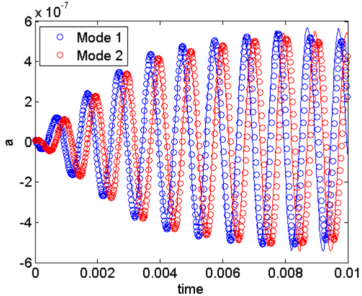

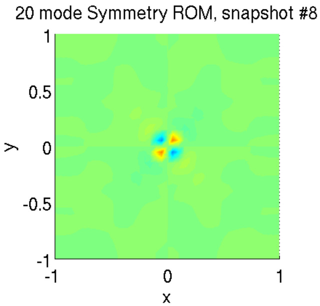

Uncontrolled Symmetry ROM Results

- Figure below shows:
  - $\circ$: t vs. $a_i(t)$ (ROM coefficients).
  - $-$: t vs. $(\mathbf{q}'_{CFD}(\mathbf{x}, t), \boldsymbol{\phi}_i(\mathbf{x}))$ (projection of snapshots onto modes).
- Movie on right shows u-velocity snapshot (top) vs. 20 mode symmetry ROM solution for u (bottom).

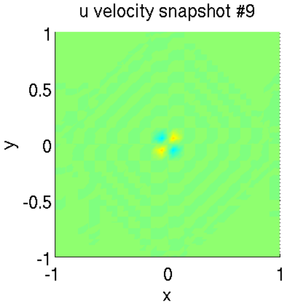

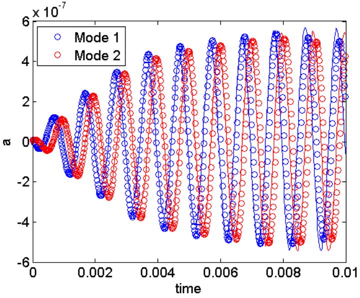

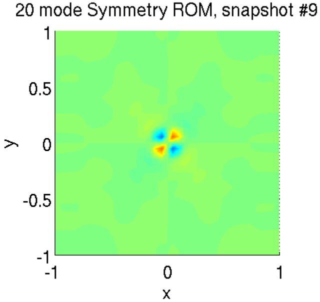

Uncontrolled Symmetry ROM Results

- Figure below shows:
  - ∘: t vs. $a_i(t)$ (ROM coefficients).
  - $-$: t vs. $(\mathbf{q}'_{CFD}(\mathbf{x},t), \boldsymbol{\phi}_i(\mathbf{x}))$ (projection of snapshots onto modes).
- Movie on right shows u-velocity snapshot (top) vs. 20 mode symmetry ROM solution for u (bottom).

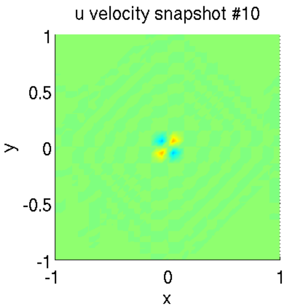

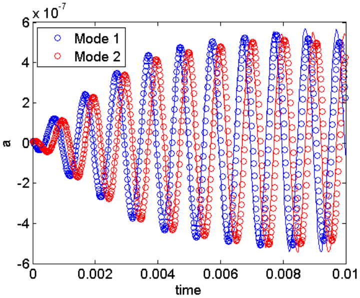

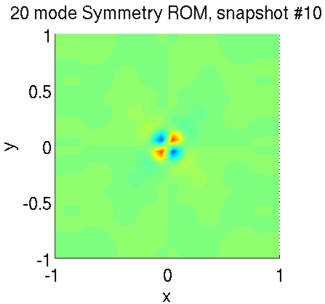

Uncontrolled Symmetry ROM Results

- Figure below shows:
  - $\circ$: t vs. $a_i(t)$ (ROM coefficients).
  - $-$: t vs. $(\mathbf{q}'_{CFD}(\mathbf{x},t), \boldsymbol{\phi}_i(\mathbf{x}))$ (projection of snapshots onto modes).
- Movie on right shows u-velocity snapshot (top) vs. 20 mode symmetry ROM solution for u (bottom).

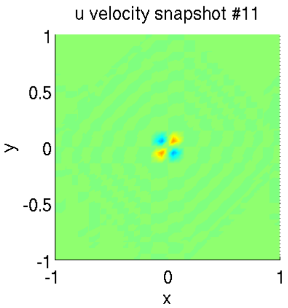

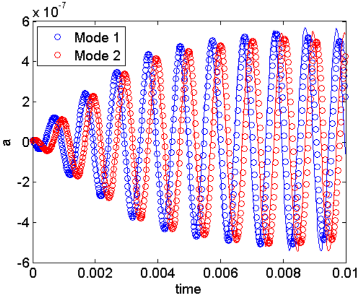

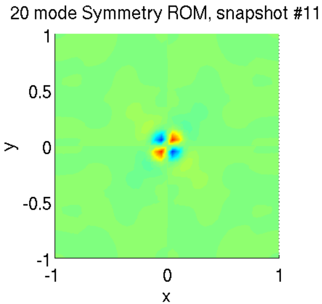

Uncontrolled Symmetry ROM Results

- Figure below shows:
  - ∘: t vs. $a_i(t)$ (ROM coefficients).
  - $-$: t vs. $(\mathbf{q}'_{CFD}(\mathbf{x},t), \boldsymbol{\phi}_i(\mathbf{x}))$ (projection of snapshots onto modes).
- Movie on right shows u-velocity snapshot (top) vs. 20 mode symmetry ROM solution for u (bottom).

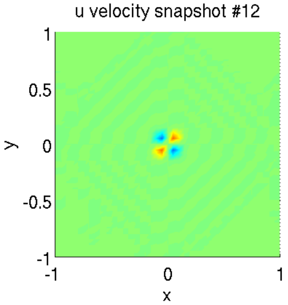

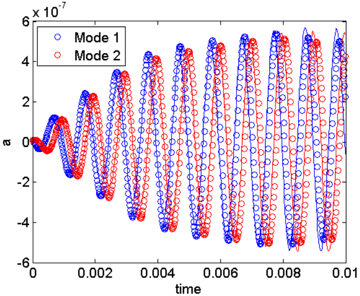

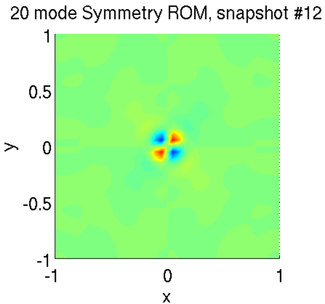

Uncontrolled Symmetry ROM Results

- Figure below shows:
  - $\circ$: t vs. $a_i(t)$ (ROM coefficients).
  - $-$: t vs. $(\mathbf{q}'_{CFD}(\mathbf{x},t), \boldsymbol{\phi}_i(\mathbf{x}))$ (projection of snapshots onto modes).
- Movie on right shows u-velocity snapshot (top) vs. 20 mode symmetry ROM solution for u (bottom).

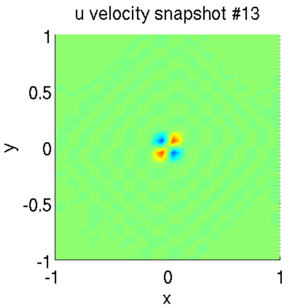

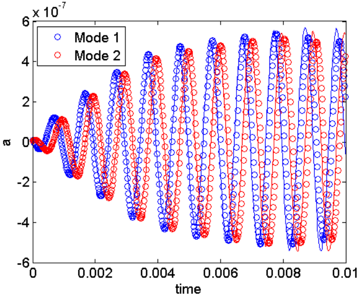

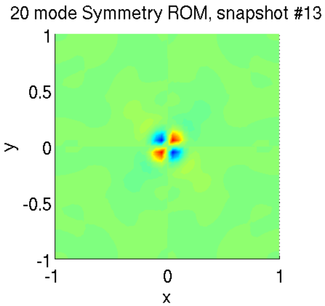

Uncontrolled Symmetry ROM Results

- Figure below shows:
  - ○: t vs. $a_i(t)$ (ROM coefficients).
  - $-$: t vs. $(\mathbf{q}'_{CFD}(\mathbf{x},t), \boldsymbol{\phi}_i(\mathbf{x}))$ (projection of snapshots onto modes).
- Movie on right shows u-velocity snapshot (top) vs. 20 mode symmetry ROM solution for u (bottom).

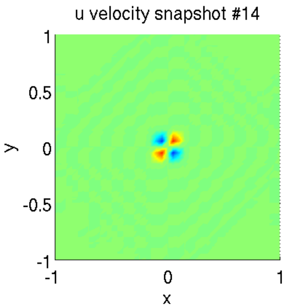

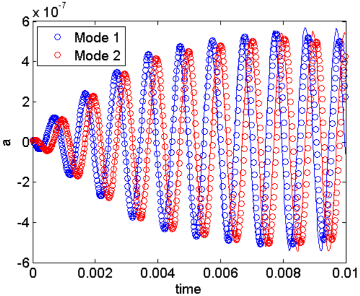

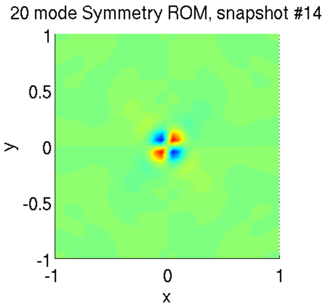

Uncontrolled Symmetry ROM Results

- Figure below shows:
  - $\circ$: t vs. $a_i(t)$ (ROM coefficients).
  - $-$: t vs. $(\mathbf{q}'_{CFD}(\mathbf{x}, t), \boldsymbol{\phi}_i(\mathbf{x}))$ (projection of snapshots onto modes).
- Movie on right shows u-velocity snapshot (top) vs. 20 mode symmetry ROM solution for u (bottom).

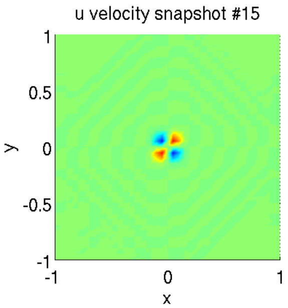

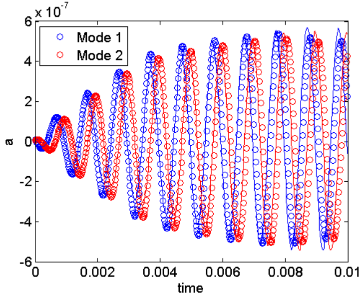

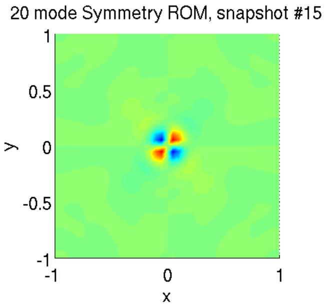

Uncontrolled Symmetry ROM Results

- Figure below shows:
  - ○: t vs. $a_i(t)$ (ROM coefficients).
  - $-$: t vs. $(\mathbf{q}'_{CFD}(\mathbf{x},t), \boldsymbol{\phi}_i(\mathbf{x}))$ (projection of snapshots onto modes).
- Movie on right shows u-velocity snapshot (top) vs. 20 mode symmetry ROM solution for u (bottom).

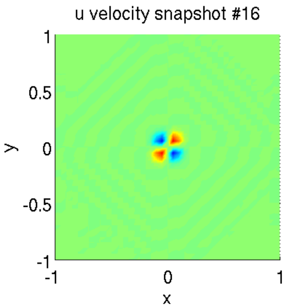

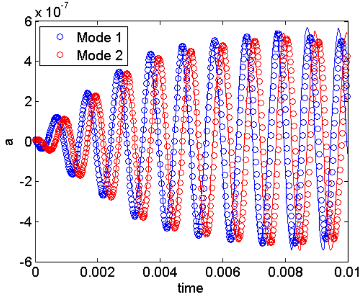

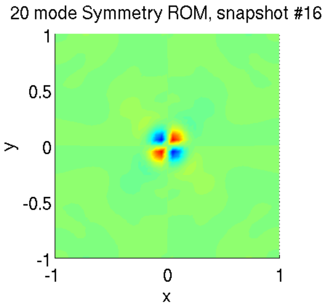

Uncontrolled Symmetry ROM Results

- Figure below shows:
  - $\circ$: t vs. $a_i(t)$ (ROM coefficients).
  - $-$: t vs. $(\mathbf{q}'_{CFD}(\mathbf{x},t), \boldsymbol{\phi}_i(\mathbf{x}))$ (projection of snapshots onto modes).
- Movie on right shows u-velocity snapshot (top) vs. 20 mode symmetry ROM solution for u (bottom).

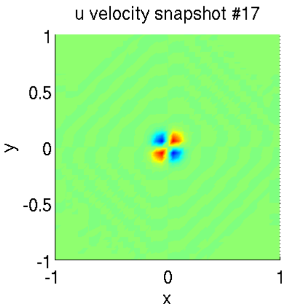

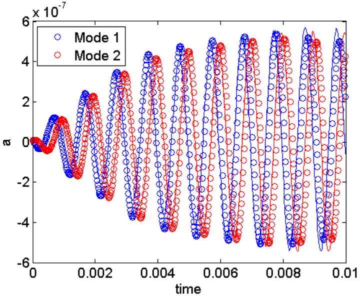

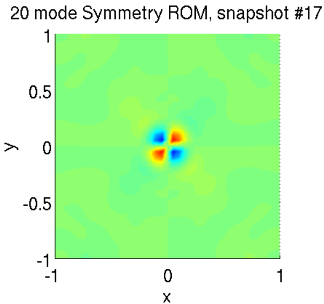

Uncontrolled Symmetry ROM Results

- Figure below shows:
  - $\circ$: t vs. $a_i(t)$ (ROM coefficients).
  - $-$: t vs. $(\mathbf{q}'_{CFD}(\mathbf{x}, t), \boldsymbol{\phi}_i(\mathbf{x}))$ (projection of snapshots onto modes).
- Movie on right shows u-velocity snapshot (top) vs. 20 mode symmetry ROM solution for u (bottom).

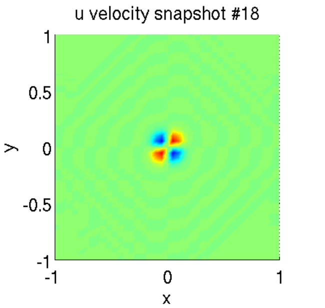

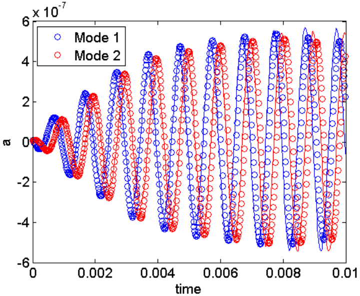

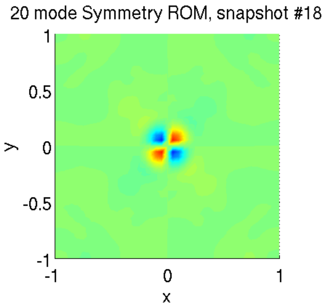

Uncontrolled Symmetry ROM Results

- Figure below shows:
  - ○: t vs. $a_i(t)$ (ROM coefficients).
  - $-$: t vs. $(\mathbf{q}'_{CFD}(\mathbf{x},t), \boldsymbol{\phi}_i(\mathbf{x}))$ (projection of snapshots onto modes).
- Movie on right shows u-velocity snapshot (top) vs. 20 mode symmetry ROM solution for u (bottom).

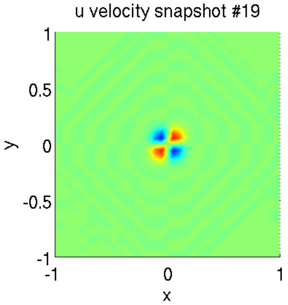

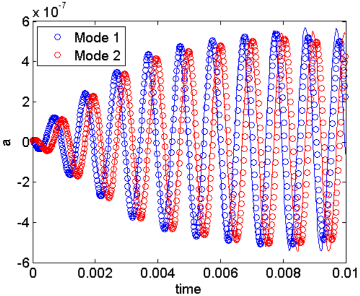

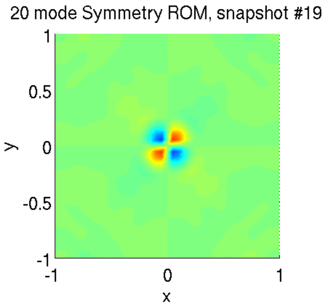

Uncontrolled Symmetry ROM Results

- Figure below shows:
  - $\circ$: t vs. $a_i(t)$ (ROM coefficients).
  - $-$: t vs. $(\mathbf{q}'_{CFD}(\mathbf{x}, t), \boldsymbol{\phi}_i(\mathbf{x}))$ (projection of snapshots onto modes).
- Movie on right shows u-velocity snapshot (top) vs. 20 mode symmetry ROM solution for u (bottom).

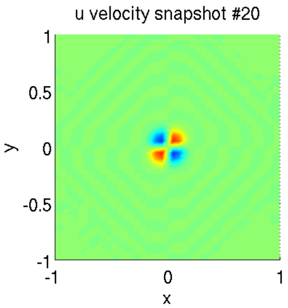

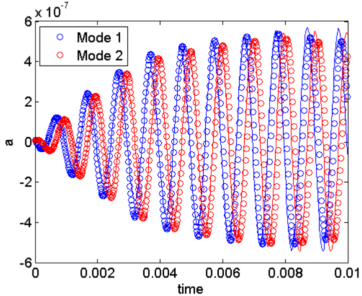

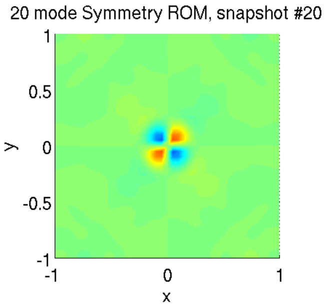

Uncontrolled Symmetry ROM Results

- Figure below shows:
  - $\circ$: t vs. $a_i(t)$ (ROM coefficients).
  - $-$: t vs. $(\mathbf{q}'_{CFD}(\mathbf{x},t), \boldsymbol{\phi}_i(\mathbf{x}))$ (projection of snapshots onto modes).
- Movie on right shows u-velocity snapshot (top) vs. 20 mode symmetry ROM solution for u (bottom).

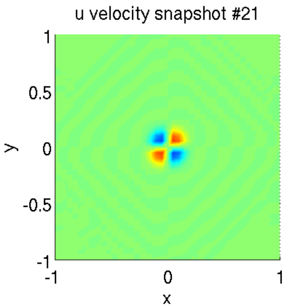

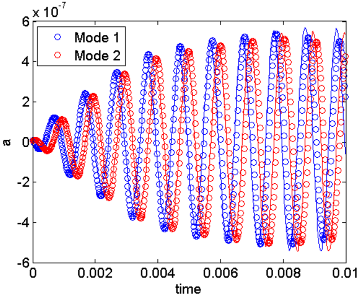

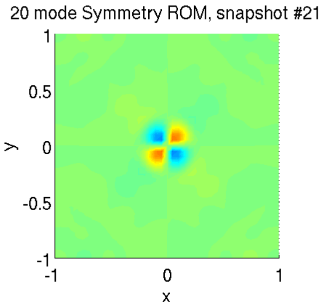

Uncontrolled Symmetry ROM Results

- Figure below shows:
  - ∘: t vs. $a_i(t)$ (ROM coefficients).
  - $-$: t vs. $(\mathbf{q}'_{CFD}(\mathbf{x},t), \boldsymbol{\phi}_i(\mathbf{x}))$ (projection of snapshots onto modes).
- Movie on right shows u-velocity snapshot (top) vs. 20 mode symmetry ROM solution for u (bottom).

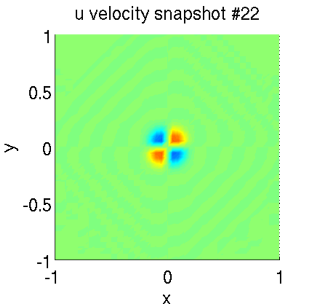

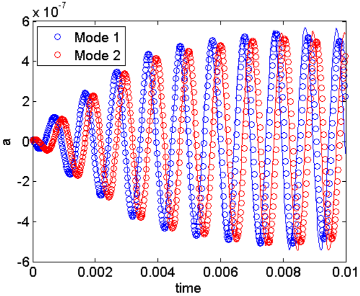

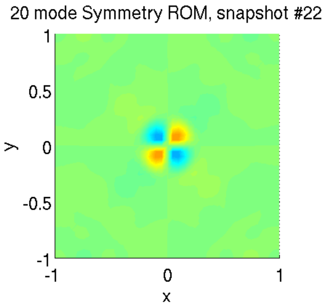

Uncontrolled Symmetry ROM Results

- Figure below shows:
  - ○: t vs. $a_i(t)$ (ROM coefficients).
  - −: t vs. $(\mathbf{q}'_{CFD}(\mathbf{x},t), \boldsymbol{\phi}_i(\mathbf{x}))$ (projection of snapshots onto modes).
- Movie on right shows u-velocity snapshot (top) vs. 20 mode symmetry ROM solution for u (bottom).

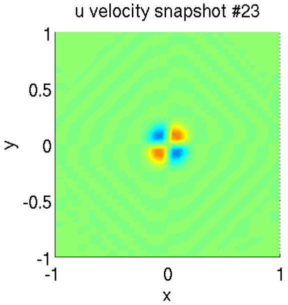

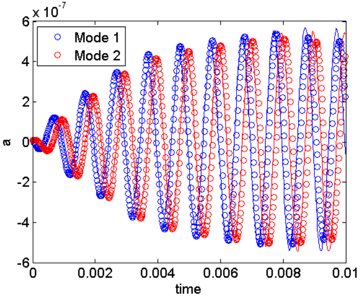

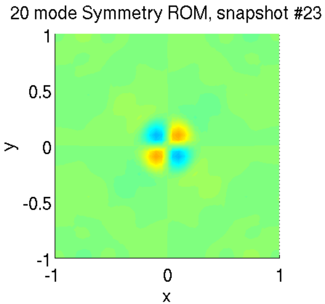

Uncontrolled Symmetry ROM Results

- Figure below shows:
  - $\circ$: t vs. $a_i(t)$ (ROM coefficients).
  - $-$: t vs. $(\mathbf{q}'_{CFD}(\mathbf{x},t), \boldsymbol{\phi}_i(\mathbf{x}))$ (projection of snapshots onto modes).
- Movie on right shows u-velocity snapshot (top) vs. 20 mode symmetry ROM solution for u (bottom).

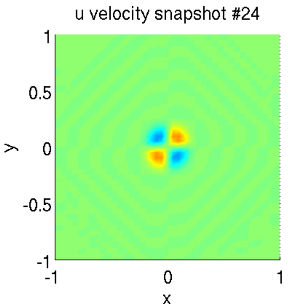

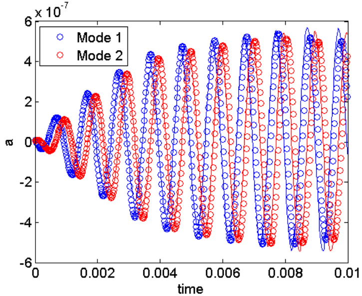

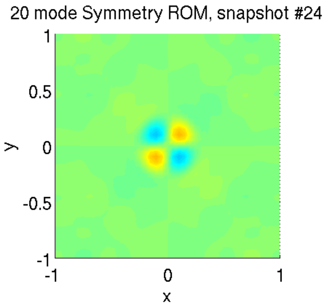

Uncontrolled Symmetry ROM Results

- Figure below shows:
  - $\circ$: t vs. $a_i(t)$ (ROM coefficients).
  - $-$: t vs. $(\mathbf{q}'_{CFD}(\mathbf{x},t), \boldsymbol{\phi}_i(\mathbf{x}))$ (projection of snapshots onto modes).
- Movie on right shows u-velocity snapshot (top) vs. 20 mode symmetry ROM solution for u (bottom).

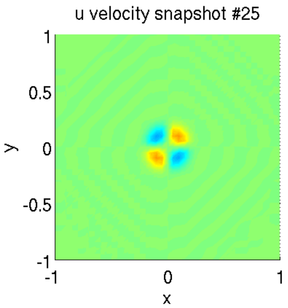

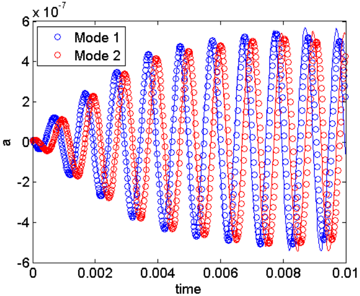

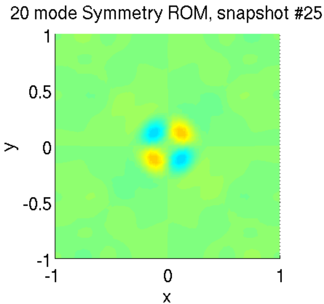

Uncontrolled Symmetry ROM Results

- Figure below shows:
  - $\circ$: t vs. $a_i(t)$ (ROM coefficients).
  - $-$: t vs. $(\mathbf{q}'_{CFD}(\mathbf{x},t), \boldsymbol{\phi}_i(\mathbf{x}))$ (projection of snapshots onto modes).
- Movie on right shows u-velocity snapshot (top) vs. 20 mode symmetry ROM solution for u (bottom).

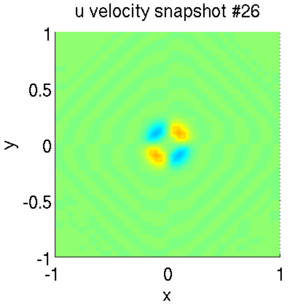

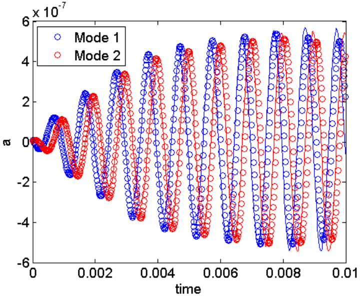

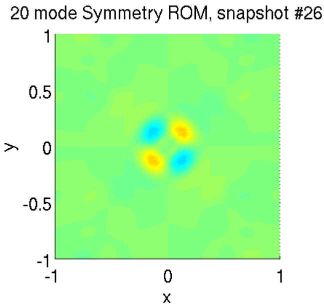

Uncontrolled Symmetry ROM Results

- Figure below shows:
  - $\circ$: t vs. $a_i(t)$ (ROM coefficients).
  - $-$: t vs. $(\mathbf{q}'_{CFD}(\mathbf{x}, t), \boldsymbol{\phi}_i(\mathbf{x}))$ (projection of snapshots onto modes).
- Movie on right shows u-velocity snapshot (top) vs. 20 mode symmetry ROM solution for u (bottom).

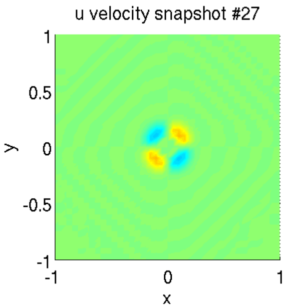

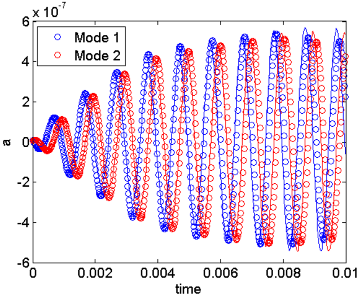

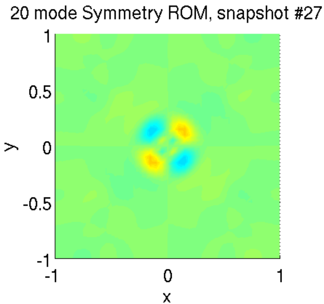

Uncontrolled Symmetry ROM Results

- Figure below shows:
  - $\circ$: t vs. $a_i(t)$ (ROM coefficients).
  - $-$: t vs. $(\mathbf{q}'_{CFD}(\mathbf{x},t), \boldsymbol{\phi}_i(\mathbf{x}))$ (projection of snapshots onto modes).
- Movie on right shows u-velocity snapshot (top) vs. 20 mode symmetry ROM solution for u (bottom).

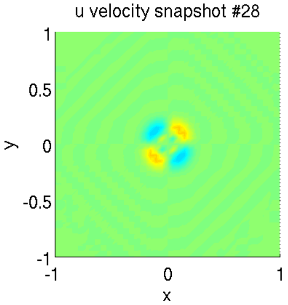

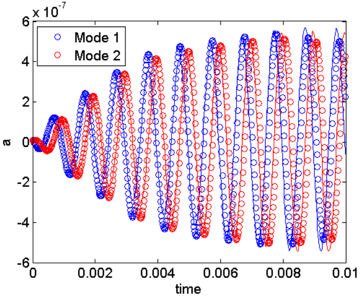

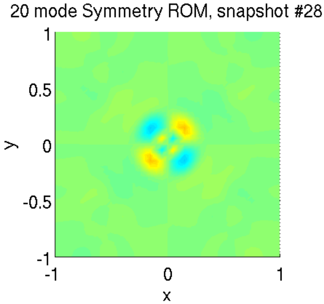

Uncontrolled Symmetry ROM Results

- Figure below shows:
  - $\circ$: t vs. $a_i(t)$ (ROM coefficients).
  - $-$: t vs. $(\mathbf{q}'_{CFD}(\mathbf{x},t), \boldsymbol{\phi}_i(\mathbf{x}))$ (projection of snapshots onto modes).
- Movie on right shows u-velocity snapshot (top) vs. 20 mode symmetry ROM solution for u (bottom).

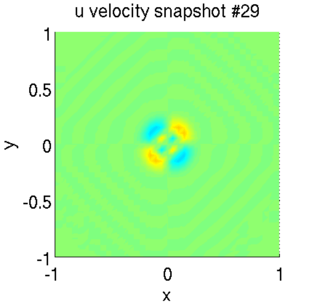

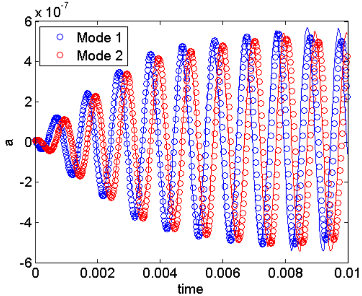

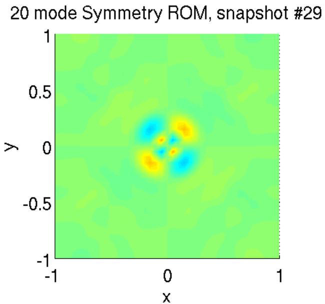

Uncontrolled Symmetry ROM Results

- Figure below shows:
  - $\circ$: t vs. $a_i(t)$ (ROM coefficients).
  - $-$: t vs. $(\mathbf{q}'_{CFD}(\mathbf{x},t), \boldsymbol{\phi}_i(\mathbf{x}))$ (projection of snapshots onto modes).
- Movie on right shows u-velocity snapshot (top) vs. 20 mode symmetry ROM solution for u (bottom).

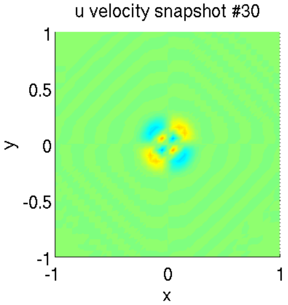

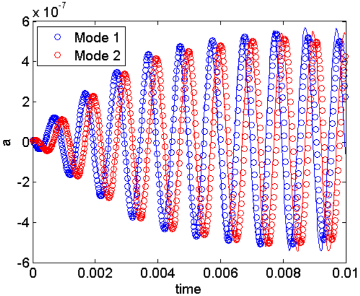

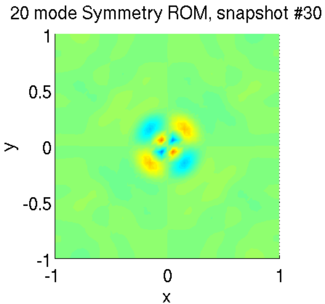

Uncontrolled Symmetry ROM Results

- Figure below shows:
  - $\circ$: t vs. $a_i(t)$ (ROM coefficients).
  - $-$: t vs. $(\mathbf{q}'_{CFD}(\mathbf{x},t), \boldsymbol{\phi}_i(\mathbf{x}))$ (projection of snapshots onto modes).
- Movie on right shows u-velocity snapshot (top) vs. 20 mode symmetry ROM solution for u (bottom).

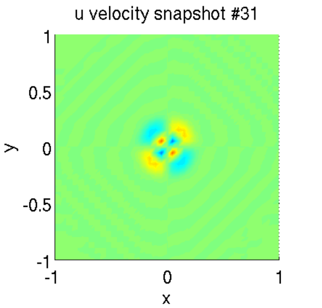

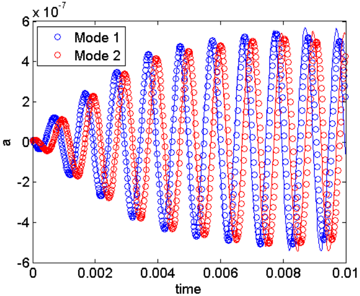

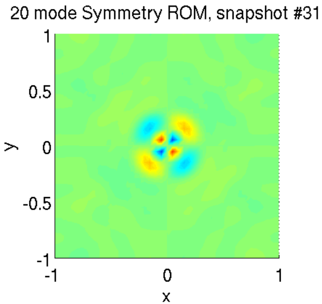

Uncontrolled Symmetry ROM Results

- Figure below shows:
  - $\circ$: t vs. $a_i(t)$ (ROM coefficients).
  - $-$: t vs. $(\mathbf{q}'_{CFD}(\mathbf{x},t), \boldsymbol{\phi}_i(\mathbf{x}))$ (projection of snapshots onto modes).
- Movie on right shows u-velocity snapshot (top) vs. 20 mode symmetry ROM solution for u (bottom).

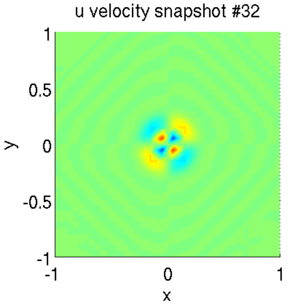

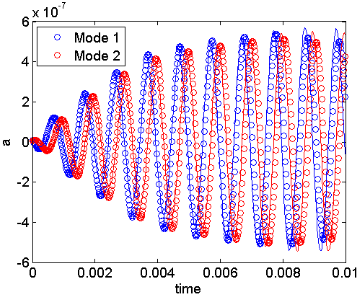

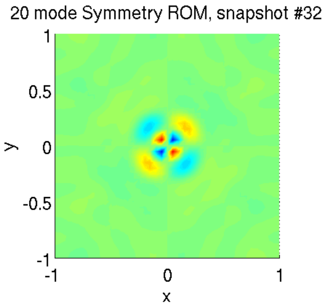

Uncontrolled Symmetry ROM Results

- Figure below shows:
  - $\circ$: t vs. $a_i(t)$ (ROM coefficients).
  - $-$: t vs. $(\mathbf{q}'_{CFD}(\mathbf{x}, t), \boldsymbol{\phi}_i(\mathbf{x}))$ (projection of snapshots onto modes).
- Movie on right shows u-velocity snapshot (top) vs. 20 mode symmetry ROM solution for u (bottom).

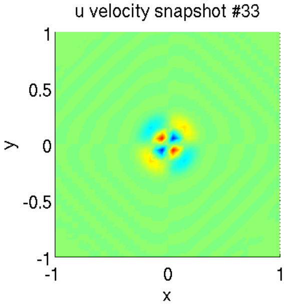

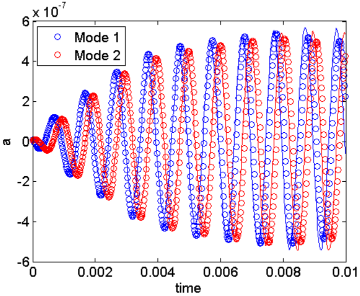

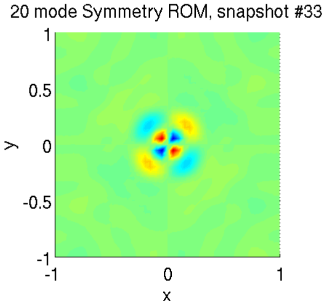

Uncontrolled Symmetry ROM Results

- Figure below shows:
  - $\circ$: t vs. $a_i(t)$ (ROM coefficients).
  - $-$: t vs. $(\mathbf{q}'_{CFD}(\mathbf{x}, t), \boldsymbol{\phi}_i(\mathbf{x}))$ (projection of snapshots onto modes).
- Movie on right shows u-velocity snapshot (top) vs. 20 mode symmetry ROM solution for u (bottom).

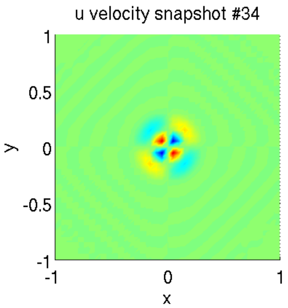

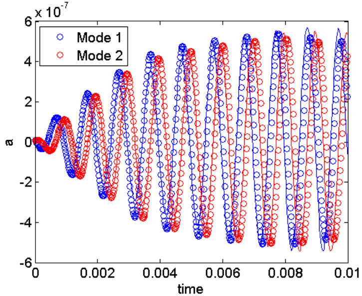

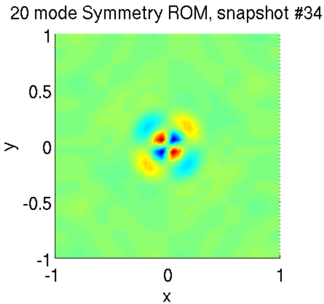

Uncontrolled Symmetry ROM Results

- Figure below shows:
  - $\circ$: t vs. $a_i(t)$ (ROM coefficients).
  - $-$: t vs. $(\mathbf{q}'_{CFD}(\mathbf{x},t), \boldsymbol{\phi}_i(\mathbf{x}))$ (projection of snapshots onto modes).
- Movie on right shows u-velocity snapshot (top) vs. 20 mode symmetry ROM solution for u (bottom).

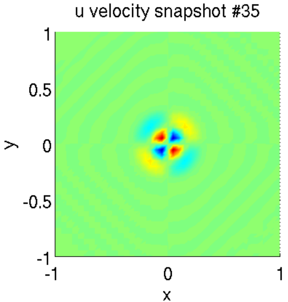

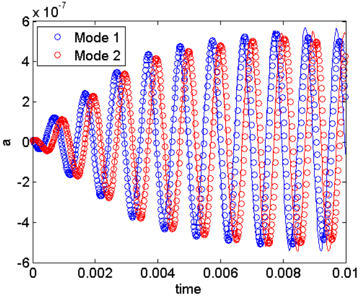

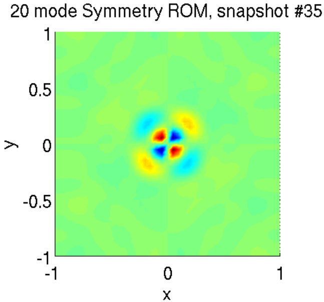

Uncontrolled Symmetry ROM Results

- Figure below shows:
  - ∘: t vs. $a_i(t)$ (ROM coefficients).
  - $-$: t vs. $(\mathbf{q}'_{CFD}(\mathbf{x},t), \boldsymbol{\phi}_i(\mathbf{x}))$ (projection of snapshots onto modes).
- Movie on right shows u-velocity snapshot (top) vs. 20 mode symmetry ROM solution for u (bottom).

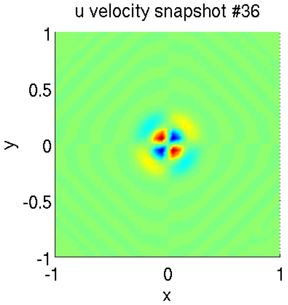

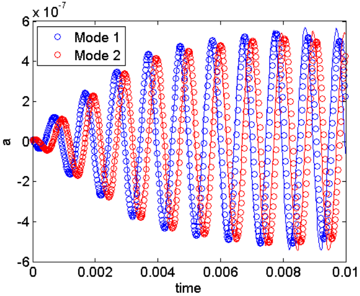

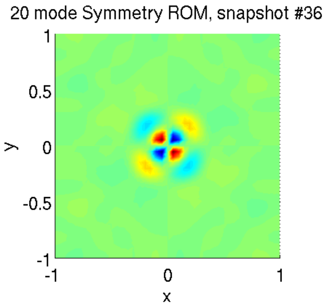

Uncontrolled Symmetry ROM Results

- Figure below shows:
  - $\circ$: t vs. $a_i(t)$ (ROM coefficients).
  - $-$: t vs. $(\mathbf{q}'_{CFD}(\mathbf{x},t), \boldsymbol{\phi}_i(\mathbf{x}))$ (projection of snapshots onto modes).
- Movie on right shows u-velocity snapshot (top) vs. 20 mode symmetry ROM solution for u (bottom).

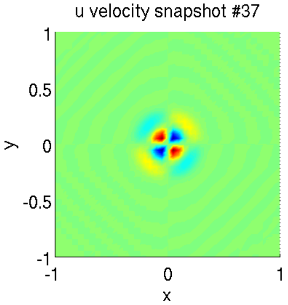

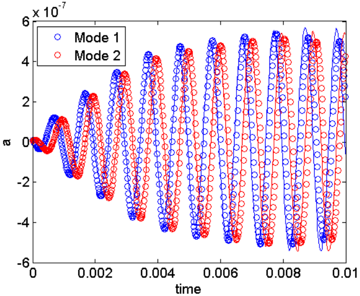

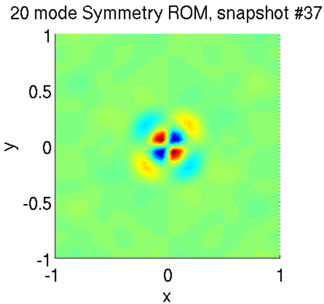

Uncontrolled Symmetry ROM Results

- Figure below shows:
  - $\circ$: t vs. $a_i(t)$ (ROM coefficients).
  - $-$: t vs. $(\mathbf{q}'_{CFD}(\mathbf{x},t), \boldsymbol{\phi}_i(\mathbf{x}))$ (projection of snapshots onto modes).
- Movie on right shows u-velocity snapshot (top) vs. 20 mode symmetry ROM solution for u (bottom).

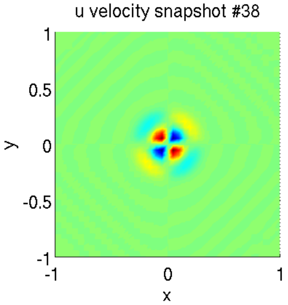

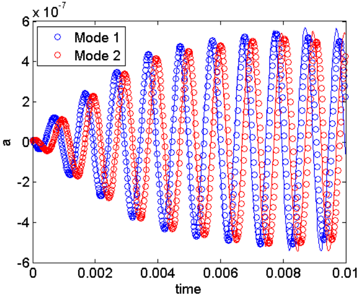

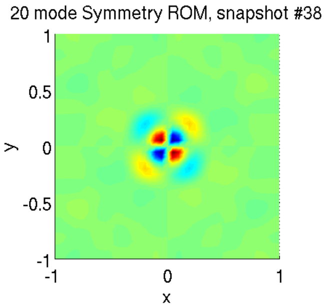

Uncontrolled Symmetry ROM Results

- Figure below shows:
  - $\circ$: t vs. $a_i(t)$ (ROM coefficients).
  - $-$: t vs. $(\mathbf{q}'_{CFD}(\mathbf{x}, t), \boldsymbol{\phi}_i(\mathbf{x}))$ (projection of snapshots onto modes).
- Movie on right shows u-velocity snapshot (top) vs. 20 mode symmetry ROM solution for u (bottom).

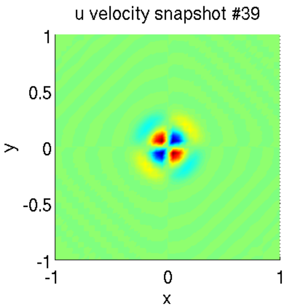

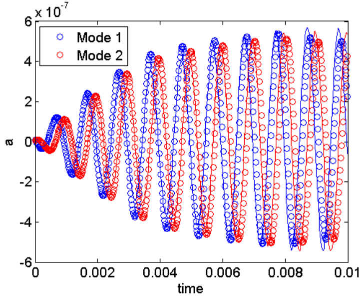

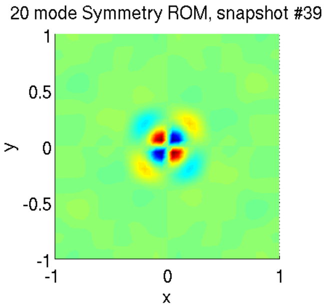

Uncontrolled Symmetry ROM Results

- Figure below shows:
  - $\circ$: t vs. $a_i(t)$ (ROM coefficients).
  - $-$: t vs. $(\mathbf{q}'_{CFD}(\mathbf{x},t), \boldsymbol{\phi}_i(\mathbf{x}))$ (projection of snapshots onto modes).
- Movie on right shows u-velocity snapshot (top) vs. 20 mode symmetry ROM solution for u (bottom).

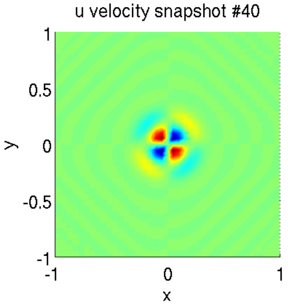

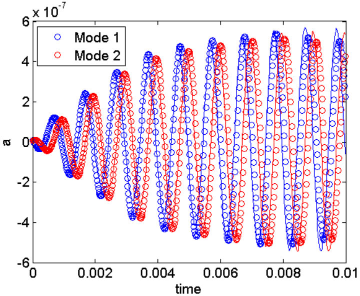

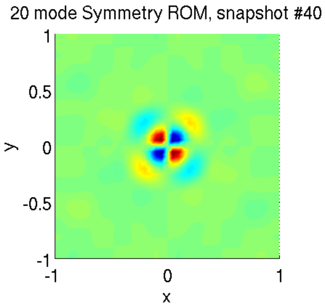

Uncontrolled Symmetry ROM Results

- Figure below shows:
  - $\circ$: t vs. $a_i(t)$ (ROM coefficients).
  - $-$: t vs. $(\mathbf{q}'_{CFD}(\mathbf{x}, t), \boldsymbol{\phi}_i(\mathbf{x}))$ (projection of snapshots onto modes).
- Movie on right shows u-velocity snapshot (top) vs. 20 mode symmetry ROM solution for u (bottom).

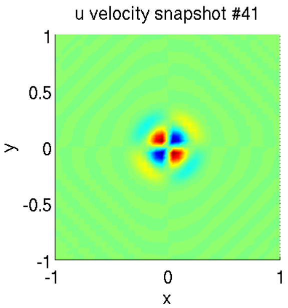

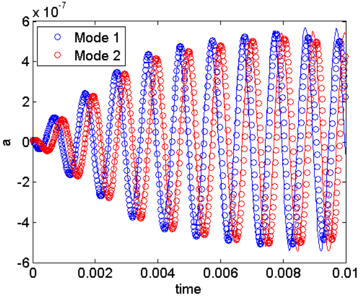

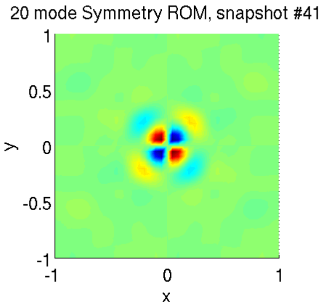

Uncontrolled Symmetry ROM Results

- Figure below shows:
  - $\circ$: t vs. $a_i(t)$ (ROM coefficients).
  - $-$: t vs. $(\mathbf{q}'_{CFD}(\mathbf{x},t), \boldsymbol{\phi}_i(\mathbf{x}))$ (projection of snapshots onto modes).
- Movie on right shows u-velocity snapshot (top) vs. 20 mode symmetry ROM solution for u (bottom).

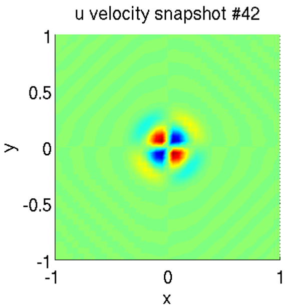

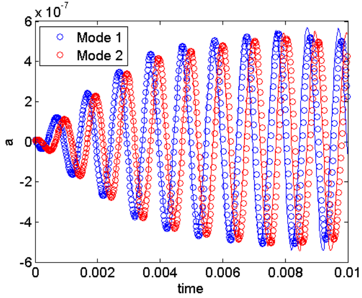

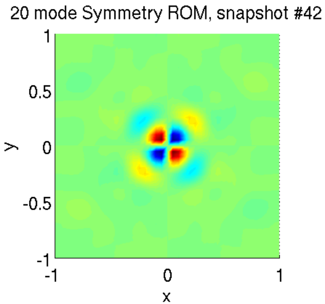

Uncontrolled Symmetry ROM Results

- Figure below shows:
  - $\circ$: t vs. $a_i(t)$ (ROM coefficients).
  - $-$: t vs. $(\mathbf{q}'_{CFD}(\mathbf{x},t), \boldsymbol{\phi}_i(\mathbf{x}))$ (projection of snapshots onto modes).
- Movie on right shows u-velocity snapshot (top) vs. 20 mode symmetry ROM solution for u (bottom).

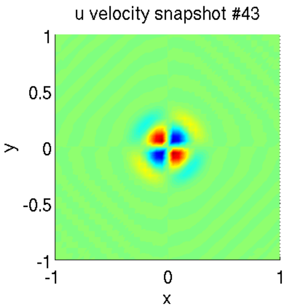

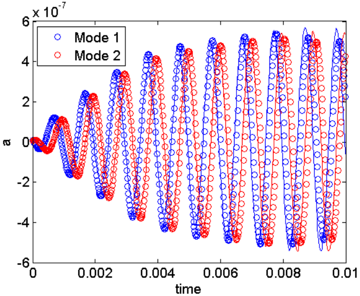

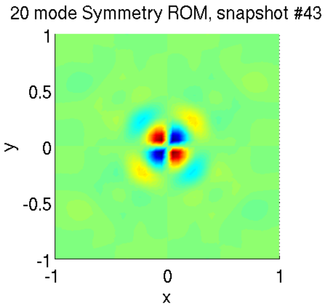

Uncontrolled Symmetry ROM Results

- Figure below shows:
  - $\circ$: t vs. $a_i(t)$ (ROM coefficients).
  - $-$: t vs. $(\mathbf{q}'_{CFD}(\mathbf{x},t), \boldsymbol{\phi}_i(\mathbf{x}))$ (projection of snapshots onto modes).
- Movie on right shows u-velocity snapshot (top) vs. 20 mode symmetry ROM solution for u (bottom).

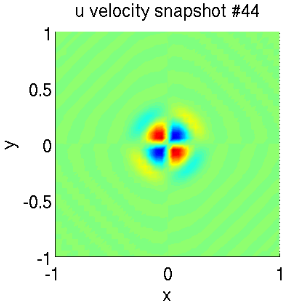

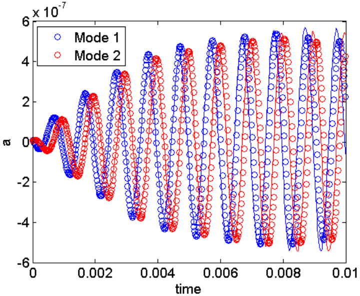

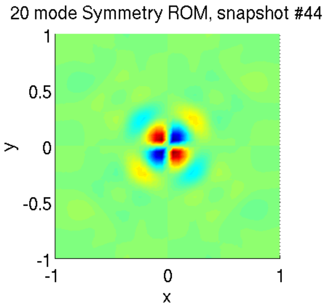

Uncontrolled Symmetry ROM Results

- Figure below shows:
  - $\circ$: t vs. $a_i(t)$ (ROM coefficients).
  - $-$: t vs. $(\mathbf{q}'_{CFD}(\mathbf{x},t), \boldsymbol{\phi}_i(\mathbf{x}))$ (projection of snapshots onto modes).
- Movie on right shows u-velocity snapshot (top) vs. 20 mode symmetry ROM solution for u (bottom).

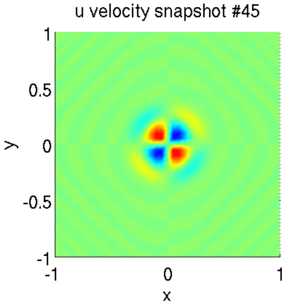

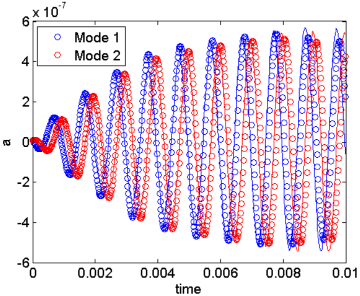

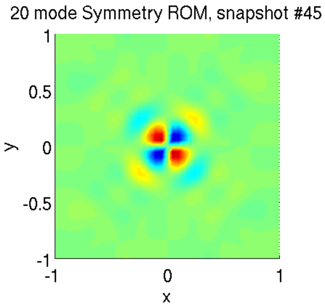

Uncontrolled Symmetry ROM Results

- Figure below shows:
  - $\circ$: t vs. $a_i(t)$ (ROM coefficients).
  - $-$: t vs. $(\mathbf{q}'_{CFD}(\mathbf{x}, t), \boldsymbol{\phi}_i(\mathbf{x}))$ (projection of snapshots onto modes).
- Movie on right shows u-velocity snapshot (top) vs. 20 mode symmetry ROM solution for u (bottom).

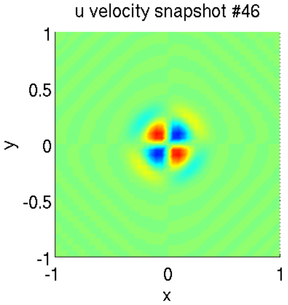

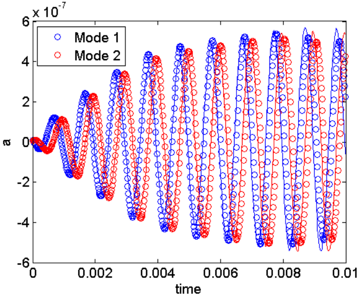

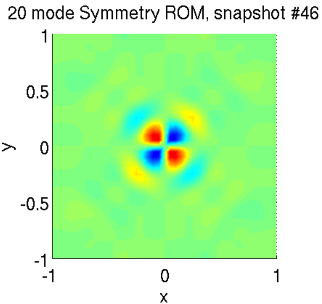

Uncontrolled Symmetry ROM Results

- Figure below shows:
  - ○: t vs. $a_i(t)$ (ROM coefficients).
  - $-$: t vs. $(\mathbf{q}'_{CFD}(\mathbf{x},t), \boldsymbol{\phi}_i(\mathbf{x}))$ (projection of snapshots onto modes).
- Movie on right shows u-velocity snapshot (top) vs. 20 mode symmetry ROM solution for u (bottom).

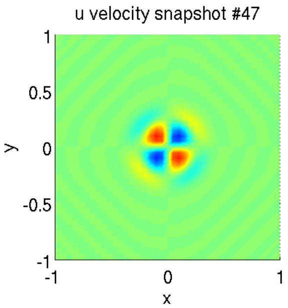

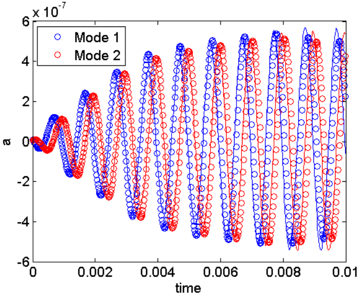

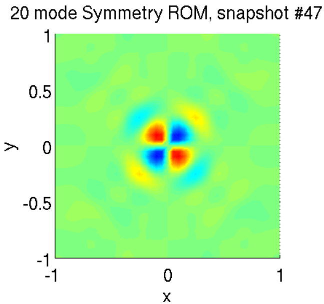

Uncontrolled Symmetry ROM Results

- Figure below shows:
  - ∘: t vs. $a_i(t)$ (ROM coefficients).
  - $-$: t vs. $(\mathbf{q}'_{CFD}(\mathbf{x},t), \boldsymbol{\phi}_i(\mathbf{x}))$ (projection of snapshots onto modes).
- Movie on right shows u-velocity snapshot (top) vs. 20 mode symmetry ROM solution for u (bottom).

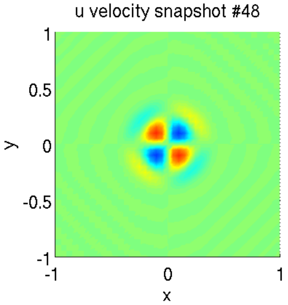

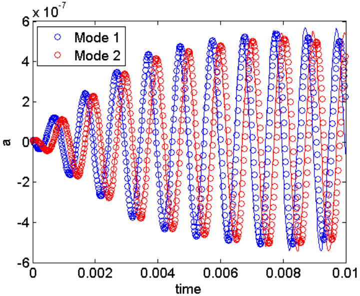

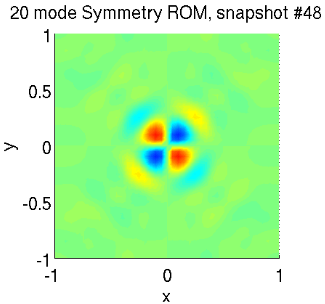

Uncontrolled Symmetry ROM Results

- Figure below shows:
  - ○: t vs. $a_i(t)$ (ROM coefficients).
  - $-$: t vs. $(\mathbf{q}'_{CFD}(\mathbf{x},t), \boldsymbol{\phi}_i(\mathbf{x}))$ (projection of snapshots onto modes).
- Movie on right shows u-velocity snapshot (top) vs. 20 mode symmetry ROM solution for u (bottom).

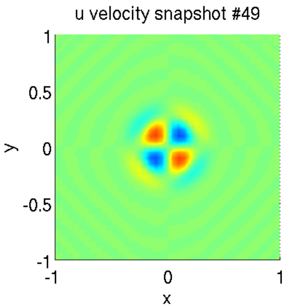

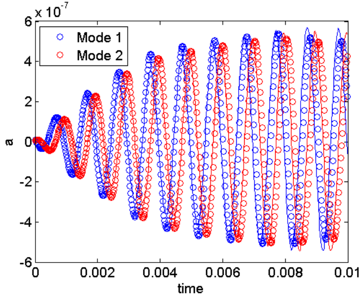

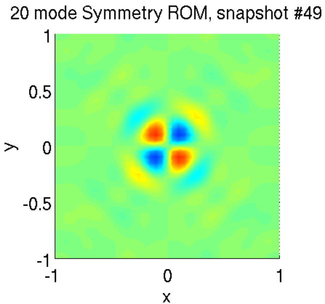

Uncontrolled Symmetry ROM Results

- Figure below shows:
  - ∘: t vs. $a_i(t)$ (ROM coefficients).
  - $-$: t vs. $(\mathbf{q}'_{CFD}(\mathbf{x},t), \boldsymbol{\phi}_i(\mathbf{x}))$ (projection of snapshots onto modes).
- Movie on right shows u-velocity snapshot (top) vs. 20 mode symmetry ROM solution for u (bottom).

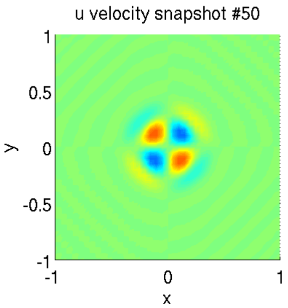

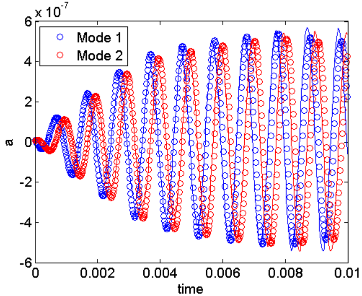

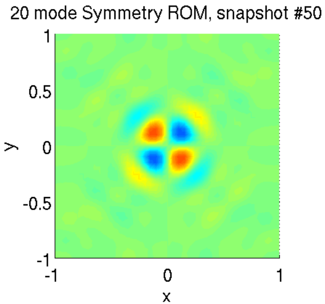

Uncontrolled Symmetry ROM Results

- Figure below shows:
  - $\circ$: t vs. $a_i(t)$ (ROM coefficients).
  - $-$: t vs. $(\mathbf{q}'_{CFD}(\mathbf{x}, t), \boldsymbol{\phi}_i(\mathbf{x}))$ (projection of snapshots onto modes).
- Movie on right shows u-velocity snapshot (top) vs. 20 mode symmetry ROM solution for u (bottom).

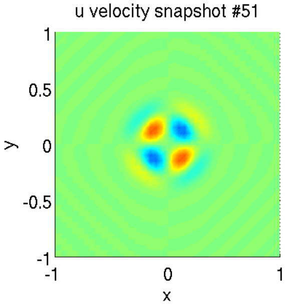

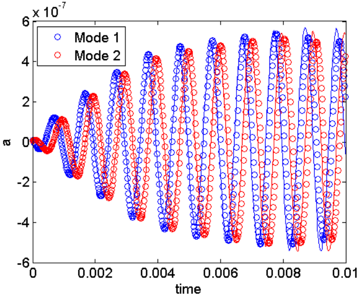

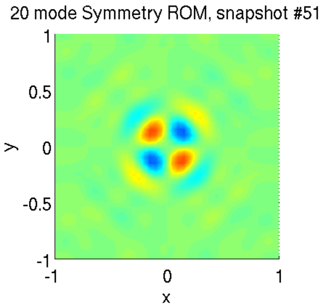

Uncontrolled Symmetry ROM Results

- Figure below shows:
  - $\circ$: t vs. $a_i(t)$ (ROM coefficients).
  - $-$: t vs. $(\mathbf{q}'_{CFD}(\mathbf{x},t), \boldsymbol{\phi}_i(\mathbf{x}))$ (projection of snapshots onto modes).
- Movie on right shows u-velocity snapshot (top) vs. 20 mode symmetry ROM solution for u (bottom).

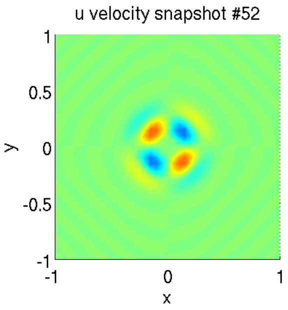

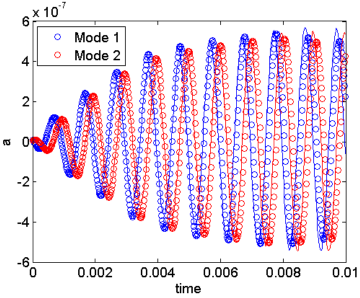

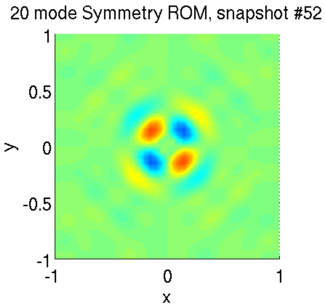

Uncontrolled Symmetry ROM Results

- Figure below shows:
  - $\circ$: t vs. $a_i(t)$ (ROM coefficients).
  - $-$: t vs. $(\mathbf{q}'_{CFD}(\mathbf{x},t), \boldsymbol{\phi}_i(\mathbf{x}))$ (projection of snapshots onto modes).
- Movie on right shows u-velocity snapshot (top) vs. 20 mode symmetry ROM solution for u (bottom).

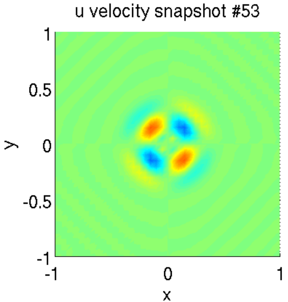

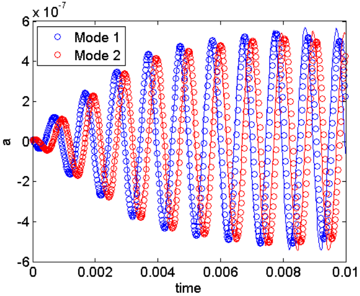

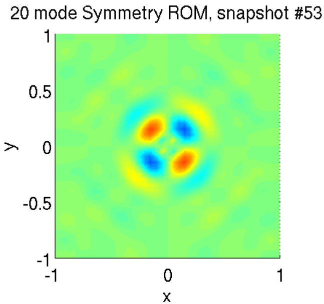

Uncontrolled Symmetry ROM Results

- Figure below shows:
  - $\circ$: t vs. $a_i(t)$ (ROM coefficients).
  - $-$: t vs. $(\mathbf{q}'_{CFD}(\mathbf{x}, t), \boldsymbol{\phi}_i(\mathbf{x}))$ (projection of snapshots onto modes).
- Movie on right shows u-velocity snapshot (top) vs. 20 mode symmetry ROM solution for u (bottom).

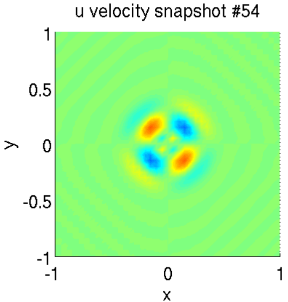

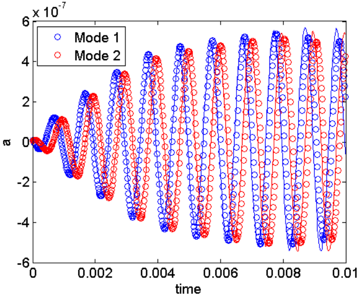

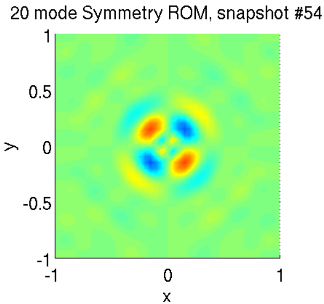

Uncontrolled Symmetry ROM Results

- Figure below shows:
  - $\circ$: t vs. $a_i(t)$ (ROM coefficients).
  - $-$: t vs. $(\mathbf{q}'_{CFD}(\mathbf{x},t), \boldsymbol{\phi}_i(\mathbf{x}))$ (projection of snapshots onto modes).
- Movie on right shows u-velocity snapshot (top) vs. 20 mode symmetry ROM solution for u (bottom).

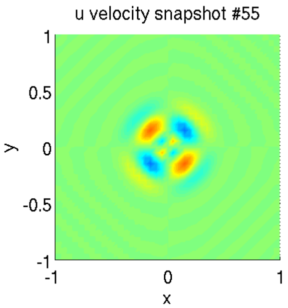

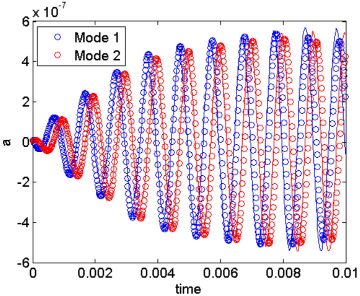

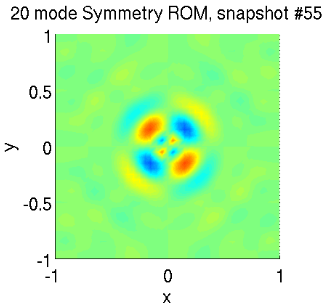

Uncontrolled Symmetry ROM Results

- Figure below shows:
  - $\circ$: t vs. $a_i(t)$ (ROM coefficients).
  - $-$: t vs. $(\mathbf{q}'_{CFD}(\mathbf{x},t), \boldsymbol{\phi}_i(\mathbf{x}))$ (projection of snapshots onto modes).
- Movie on right shows u-velocity snapshot (top) vs. 20 mode symmetry ROM solution for u (bottom).

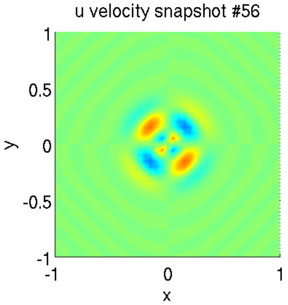

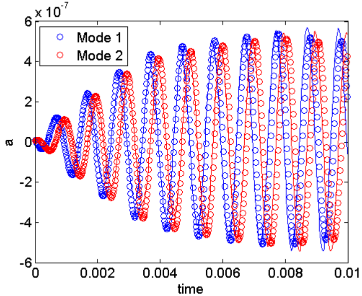

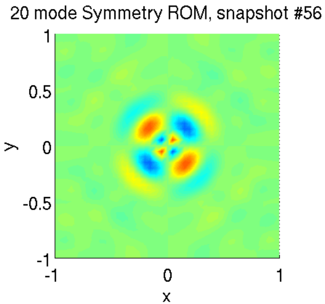

Uncontrolled Symmetry ROM Results

- Figure below shows:
  - $\circ$: t vs. $a_i(t)$ (ROM coefficients).
  - $-$: t vs. $(\mathbf{q}'_{CFD}(\mathbf{x},t), \boldsymbol{\phi}_i(\mathbf{x}))$ (projection of snapshots onto modes).
- Movie on right shows u-velocity snapshot (top) vs. 20 mode symmetry ROM solution for u (bottom).

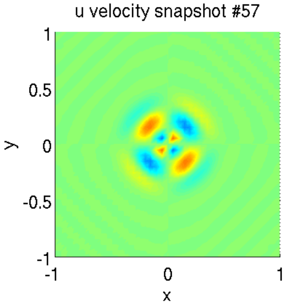

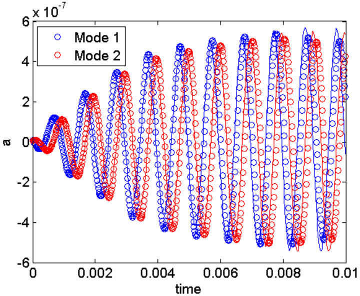

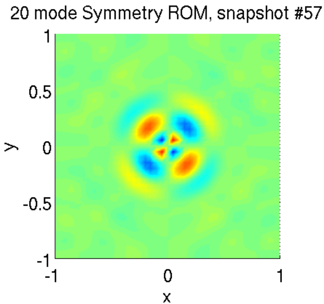

Uncontrolled Symmetry ROM Results

- Figure below shows:
  - $\circ$: t vs. $a_i(t)$ (ROM coefficients).
  - $-$: t vs. $(\mathbf{q}'_{CFD}(\mathbf{x},t), \boldsymbol{\phi}_i(\mathbf{x}))$ (projection of snapshots onto modes).
- Movie on right shows u-velocity snapshot (top) vs. 20 mode symmetry ROM solution for u (bottom).

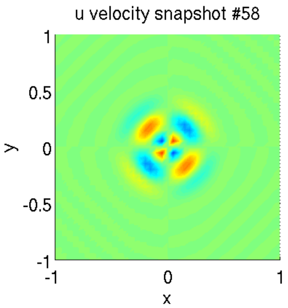

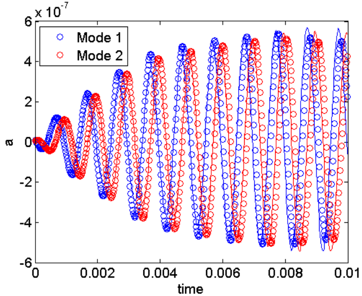

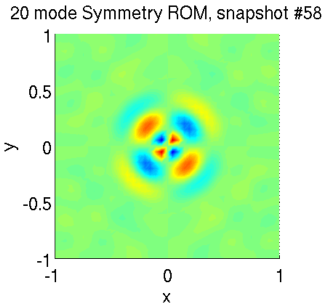

Uncontrolled Symmetry ROM Results

- Figure below shows:
  - $\circ$: t vs. $a_i(t)$ (ROM coefficients).
  - $-$: t vs. $(\mathbf{q}'_{CFD}(\mathbf{x},t), \boldsymbol{\phi}_i(\mathbf{x}))$ (projection of snapshots onto modes).
- Movie on right shows u-velocity snapshot (top) vs. 20 mode symmetry ROM solution for u (bottom).

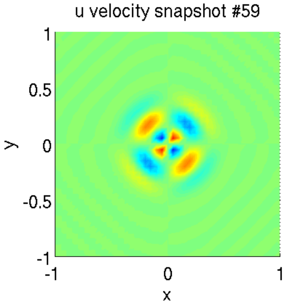

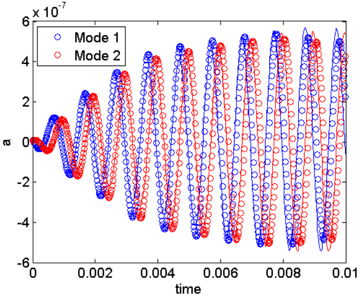

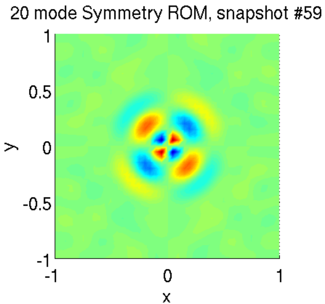

Uncontrolled Symmetry ROM Results

- Figure below shows:
  - $\circ$: t vs. $a_i(t)$ (ROM coefficients).
  - $-$: t vs. $(\mathbf{q}'_{CFD}(\mathbf{x}, t), \boldsymbol{\phi}_i(\mathbf{x}))$ (projection of snapshots onto modes).
- Movie on right shows u-velocity snapshot (top) vs. 20 mode symmetry ROM solution for u (bottom).

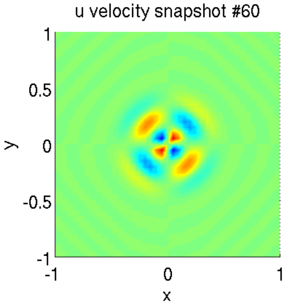

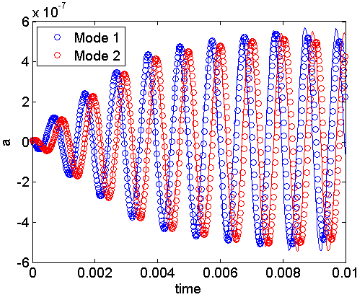

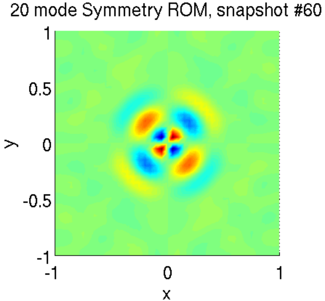

Uncontrolled Symmetry ROM Results

- Figure below shows:
  - ○: t vs. $a_i(t)$ (ROM coefficients).
  - $-$: t vs. $(\mathbf{q}'_{CFD}(\mathbf{x},t), \boldsymbol{\phi}_i(\mathbf{x}))$ (projection of snapshots onto modes).
- Movie on right shows u-velocity snapshot (top) vs. 20 mode symmetry ROM solution for u (bottom).

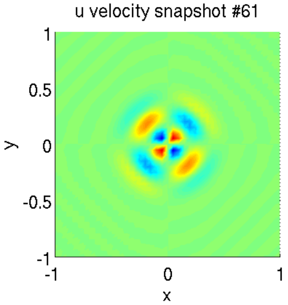

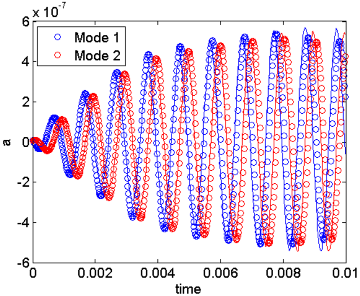

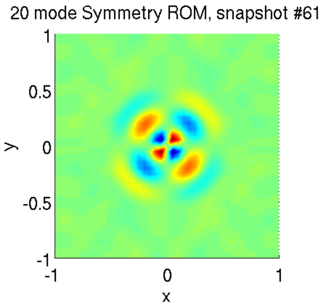

Uncontrolled Symmetry ROM Results

- Figure below shows:
  - ○: t vs. $a_i(t)$ (ROM coefficients).
  - $-$: t vs. $(\mathbf{q}'_{CFD}(\mathbf{x},t), \boldsymbol{\phi}_i(\mathbf{x}))$ (projection of snapshots onto modes).
- Movie on right shows u-velocity snapshot (top) vs. 20 mode symmetry ROM solution for u (bottom).

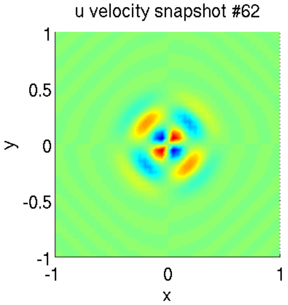

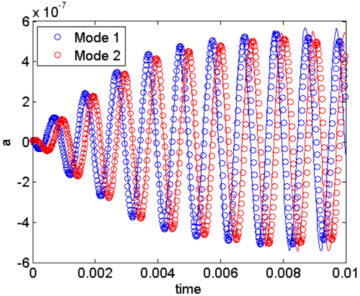

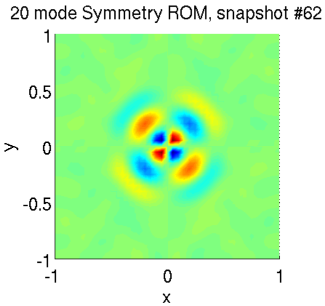

Uncontrolled Symmetry ROM Results

- Figure below shows:
  - $\circ$: t vs. $a_i(t)$ (ROM coefficients).
  - $-$: t vs. $(\mathbf{q}'_{CFD}(\mathbf{x},t), \boldsymbol{\phi}_i(\mathbf{x}))$ (projection of snapshots onto modes).
- Movie on right shows u-velocity snapshot (top) vs. 20 mode symmetry ROM solution for u (bottom).

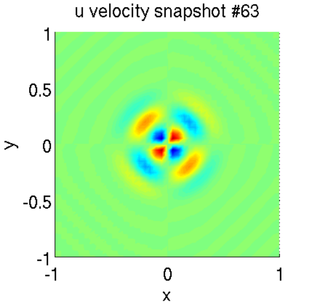

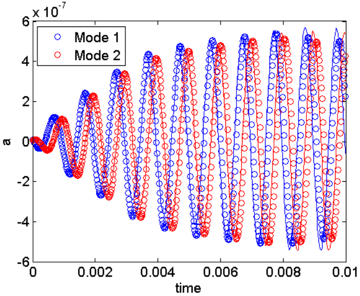

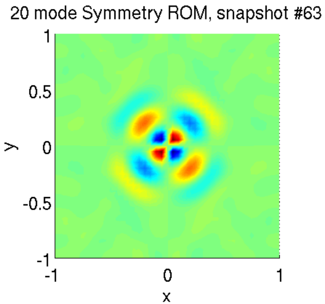

Uncontrolled Symmetry ROM Results

- Figure below shows:
  - ○: t vs. $a_i(t)$ (ROM coefficients).
  - $-$: t vs. $(\mathbf{q}'_{CFD}(\mathbf{x},t), \boldsymbol{\phi}_i(\mathbf{x}))$ (projection of snapshots onto modes).
- Movie on right shows u-velocity snapshot (top) vs. 20 mode symmetry ROM solution for u (bottom).

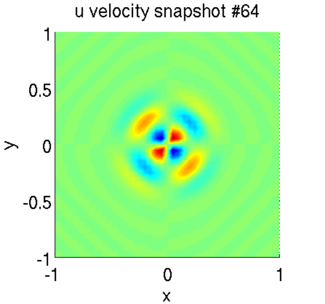

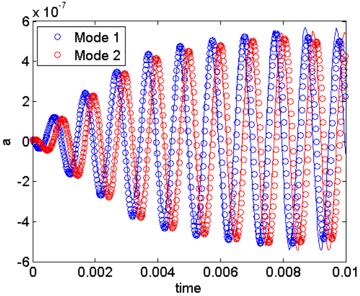

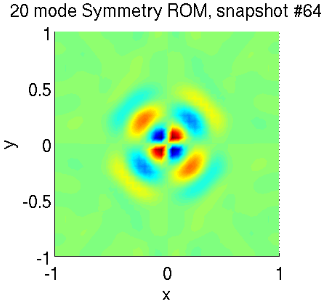

Uncontrolled Symmetry ROM Results

- Figure below shows:
  - $\circ$: t vs. $a_i(t)$ (ROM coefficients).
  - $-$: t vs. $(\mathbf{q}'_{CFD}(\mathbf{x},t), \boldsymbol{\phi}_i(\mathbf{x}))$ (projection of snapshots onto modes).
- Movie on right shows u-velocity snapshot (top) vs. 20 mode symmetry ROM solution for u (bottom).

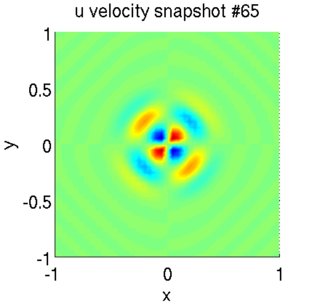

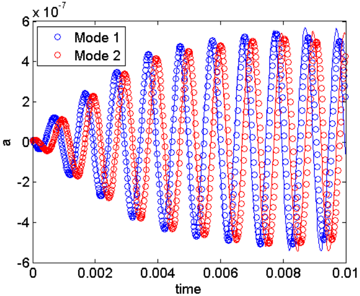

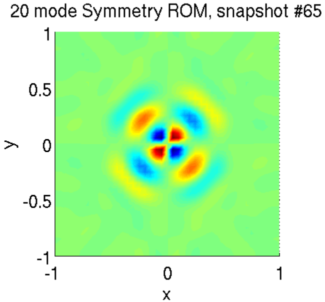

Uncontrolled Symmetry ROM Results

- Figure below shows:
  - $\circ$: t vs. $a_i(t)$ (ROM coefficients).
  - $-$: t vs. $(\mathbf{q}'_{CFD}(\mathbf{x},t), \boldsymbol{\phi}_i(\mathbf{x}))$ (projection of snapshots onto modes).
- Movie on right shows u-velocity snapshot (top) vs. 20 mode symmetry ROM solution for u (bottom).

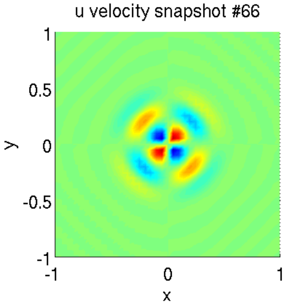

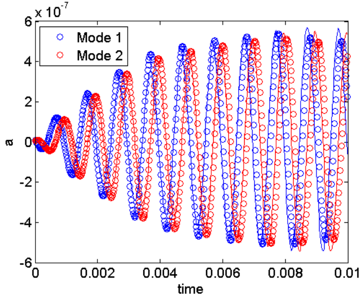

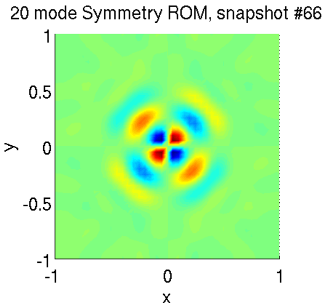

Uncontrolled Symmetry ROM Results

- Figure below shows:
  - $\circ$: t vs. $a_i(t)$ (ROM coefficients).
  - $-$: t vs. $(\mathbf{q}'_{CFD}(\mathbf{x},t), \boldsymbol{\phi}_i(\mathbf{x}))$ (projection of snapshots onto modes).
- Movie on right shows u-velocity snapshot (top) vs. 20 mode symmetry ROM solution for u (bottom).

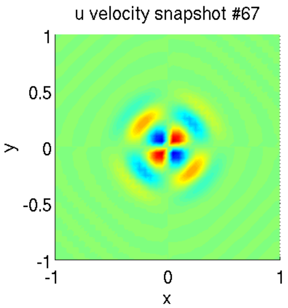

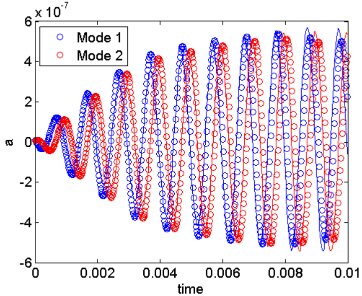

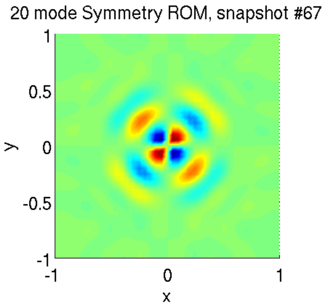

Uncontrolled Symmetry ROM Results

- Figure below shows:
  - $\circ$: t vs. $a_i(t)$ (ROM coefficients).
  - $-$: t vs. $(\mathbf{q}'_{CFD}(\mathbf{x},t), \boldsymbol{\phi}_i(\mathbf{x}))$ (projection of snapshots onto modes).
- Movie on right shows u-velocity snapshot (top) vs. 20 mode symmetry ROM solution for u (bottom).

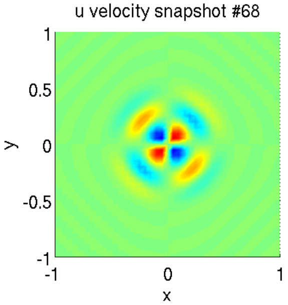

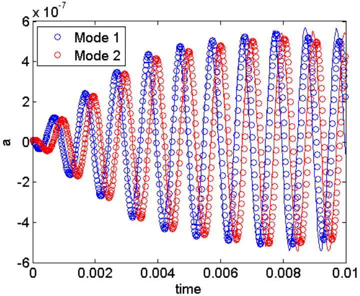

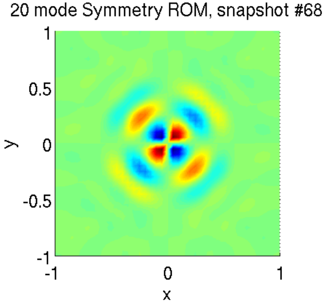

Uncontrolled Symmetry ROM Results

- Figure below shows:
  - $\circ$: t vs. $a_i(t)$ (ROM coefficients).
  - $-$: t vs. $(\mathbf{q}'_{CFD}(\mathbf{x},t), \boldsymbol{\phi}_i(\mathbf{x}))$ (projection of snapshots onto modes).
- Movie on right shows u-velocity snapshot (top) vs. 20 mode symmetry ROM solution for u (bottom).

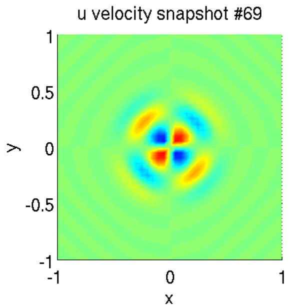

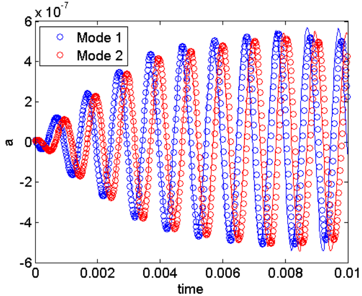

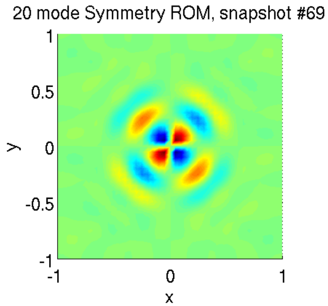

Uncontrolled Symmetry ROM Results

- Figure below shows:
  - $\circ$: t vs. $a_i(t)$ (ROM coefficients).
  - $-$: t vs. $(\mathbf{q}'_{CFD}(\mathbf{x},t), \boldsymbol{\phi}_i(\mathbf{x}))$ (projection of snapshots onto modes).
- Movie on right shows u-velocity snapshot (top) vs. 20 mode symmetry ROM solution for u (bottom).

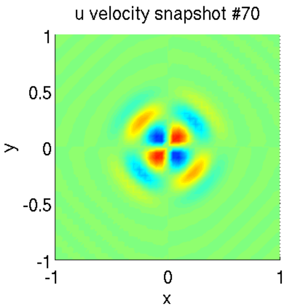

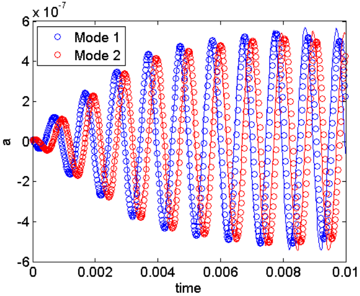

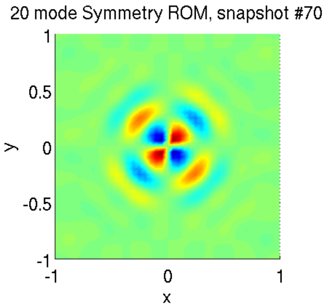

Uncontrolled Symmetry ROM Results

- Figure below shows:
  - ○: t vs. $a_i(t)$ (ROM coefficients).
  - $-$: t vs. $(\mathbf{q}'_{CFD}(\mathbf{x},t), \boldsymbol{\phi}_i(\mathbf{x}))$ (projection of snapshots onto modes).
- Movie on right shows u-velocity snapshot (top) vs. 20 mode symmetry ROM solution for u (bottom).

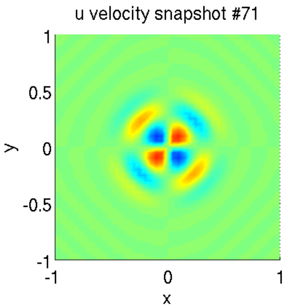

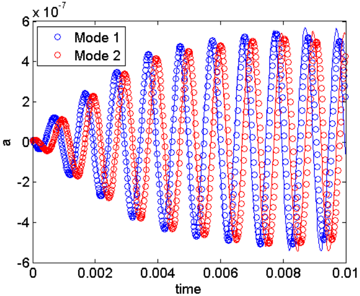

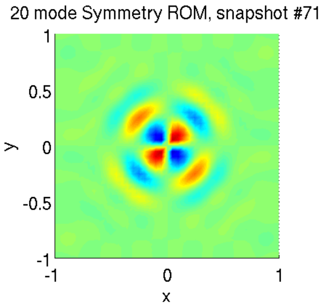

Uncontrolled Symmetry ROM Results

- Figure below shows:
  - $\circ$: t vs. $a_i(t)$ (ROM coefficients).
  - $-$: t vs. $(\mathbf{q}'_{CFD}(\mathbf{x},t), \boldsymbol{\phi}_i(\mathbf{x}))$ (projection of snapshots onto modes).
- Movie on right shows u-velocity snapshot (top) vs. 20 mode symmetry ROM solution for u (bottom).

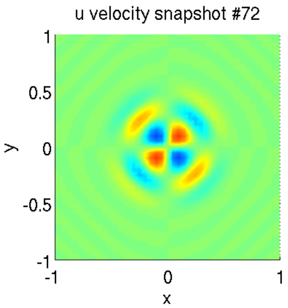

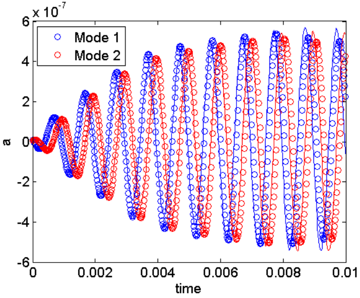

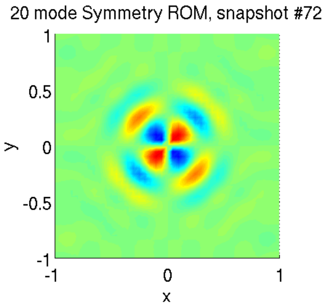

Uncontrolled Symmetry ROM Results

- Figure below shows:
  - $\circ$: t vs. $a_i(t)$ (ROM coefficients).
  - $-$: t vs. $(\mathbf{q}'_{CFD}(\mathbf{x},t), \boldsymbol{\phi}_i(\mathbf{x}))$ (projection of snapshots onto modes).
- Movie on right shows u-velocity snapshot (top) vs. 20 mode symmetry ROM solution for u (bottom).

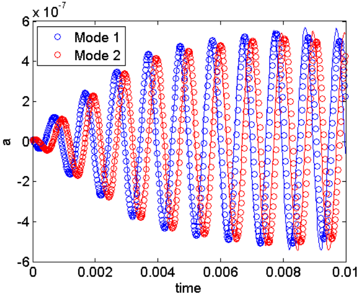

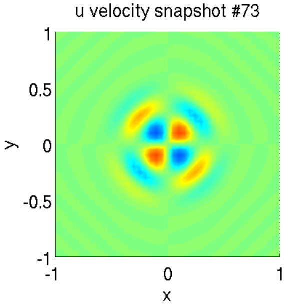

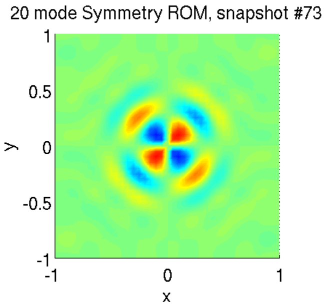

Uncontrolled Symmetry ROM Results

- Figure below shows:
  - $\circ$: t vs. $a_i(t)$ (ROM coefficients).
  - $-$: t vs. $(\mathbf{q}'_{CFD}(\mathbf{x},t), \boldsymbol{\phi}_i(\mathbf{x}))$ (projection of snapshots onto modes).
- Movie on right shows u-velocity snapshot (top) vs. 20 mode symmetry ROM solution for u (bottom).

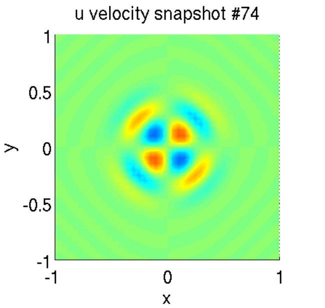

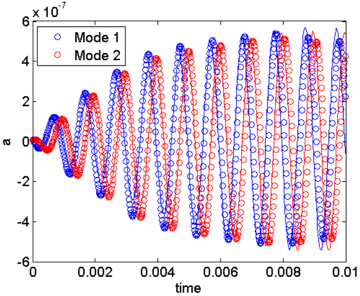

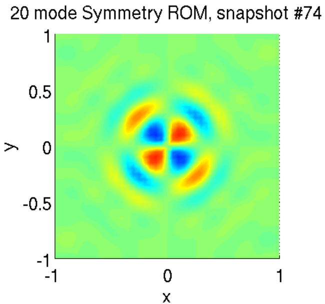

Uncontrolled Symmetry ROM Results

- Figure below shows:
  - ○: t vs. $a_i(t)$ (ROM coefficients).
  - $-$: t vs. $(\mathbf{q}'_{CFD}(\mathbf{x}, t), \boldsymbol{\phi}_i(\mathbf{x}))$ (projection of snapshots onto modes).
- Movie on right shows u-velocity snapshot (top) vs. 20 mode symmetry ROM solution for u (bottom).

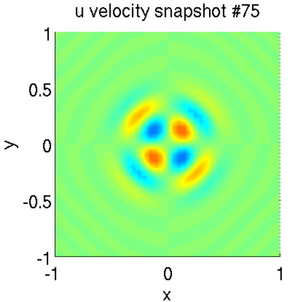

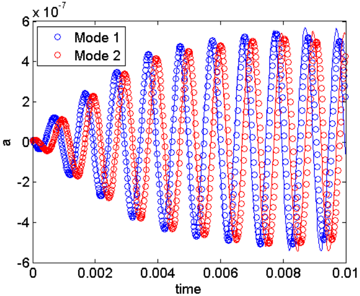

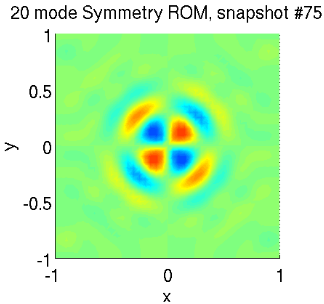

Uncontrolled Symmetry ROM Results

- Figure below shows:
  - $\circ$: t vs. $a_i(t)$ (ROM coefficients).
  - $-$: t vs. $(\mathbf{q}'_{CFD}(\mathbf{x},t), \boldsymbol{\phi}_i(\mathbf{x}))$ (projection of snapshots onto modes).
- Movie on right shows u-velocity snapshot (top) vs. 20 mode symmetry ROM solution for u (bottom).

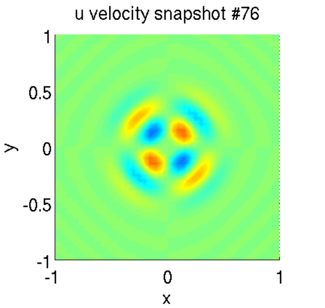

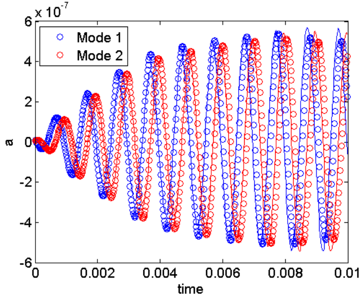

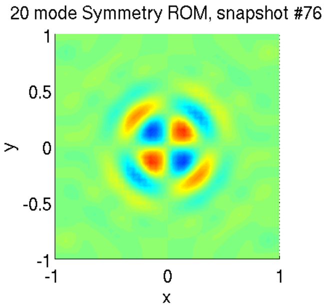

Uncontrolled Symmetry ROM Results

- Figure below shows:
  - $\circ$: t vs. $a_i(t)$ (ROM coefficients).
  - $-$: t vs. $(\mathbf{q}'_{CFD}(\mathbf{x},t), \boldsymbol{\phi}_i(\mathbf{x}))$ (projection of snapshots onto modes).
- Movie on right shows u-velocity snapshot (top) vs. 20 mode symmetry ROM solution for u (bottom).

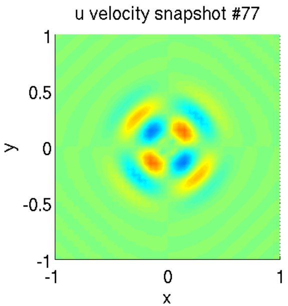

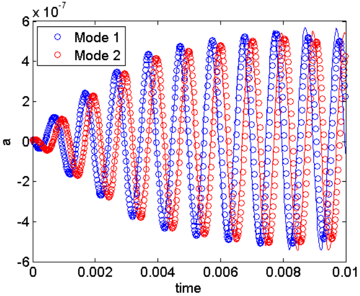

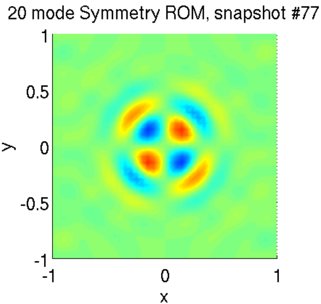

Uncontrolled Symmetry ROM Results

- Figure below shows:
  - $\circ$: t vs. $a_i(t)$ (ROM coefficients).
  - $-$: t vs. $(\mathbf{q}'_{CFD}(\mathbf{x},t), \boldsymbol{\phi}_i(\mathbf{x}))$ (projection of snapshots onto modes).
- Movie on right shows u-velocity snapshot (top) vs. 20 mode symmetry ROM solution for u (bottom).

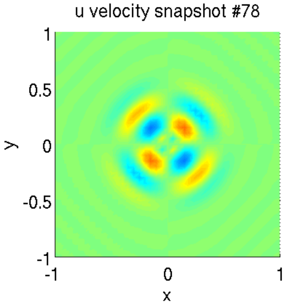

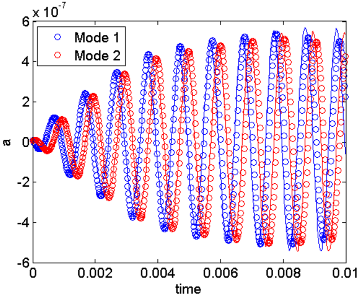

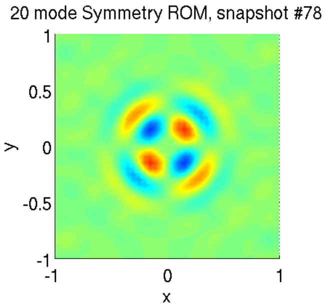

Uncontrolled Symmetry ROM Results

- Figure below shows:
  - ○: t vs. $a_i(t)$ (ROM coefficients).
  - $-$: t vs. $(\mathbf{q}'_{CFD}(\mathbf{x},t), \boldsymbol{\phi}_i(\mathbf{x}))$ (projection of snapshots onto modes).
- Movie on right shows u-velocity snapshot (top) vs. 20 mode symmetry ROM solution for u (bottom).

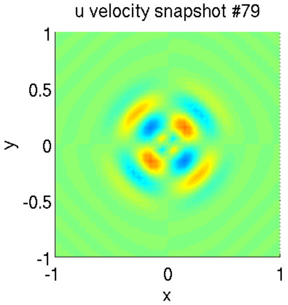

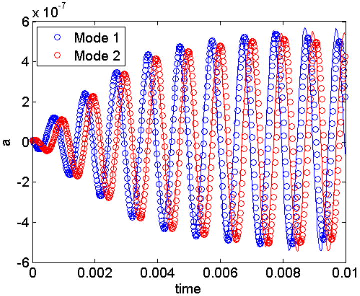

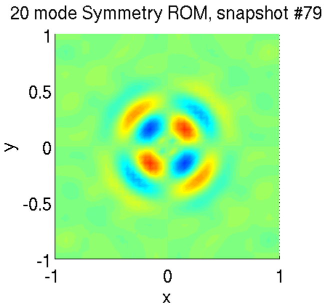

Uncontrolled Symmetry ROM Results

- Figure below shows:
  - ∘: t vs. $a_i(t)$ (ROM coefficients).
  - $-$: t vs. $(\mathbf{q}'_{CFD}(\mathbf{x},t), \boldsymbol{\phi}_i(\mathbf{x}))$ (projection of snapshots onto modes).
- Movie on right shows u-velocity snapshot (top) vs. 20 mode symmetry ROM solution for u (bottom).

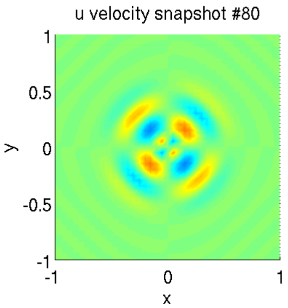

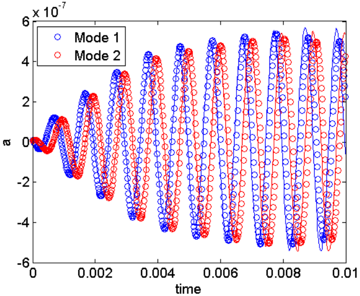

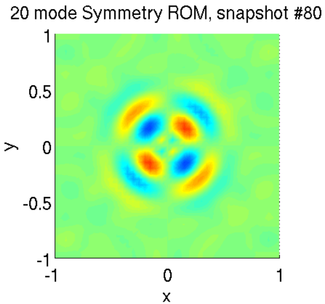

Uncontrolled Symmetry ROM Results

- Figure below shows:
  - ∘: t vs. $a_i(t)$ (ROM coefficients).
  - $-$: t vs. $(\mathbf{q}'_{CFD}(\mathbf{x},t), \boldsymbol{\phi}_i(\mathbf{x}))$ (projection of snapshots onto modes).
- Movie on right shows u-velocity snapshot (top) vs. 20 mode symmetry ROM solution for u (bottom).

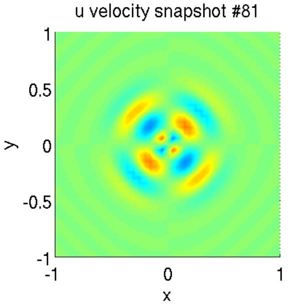

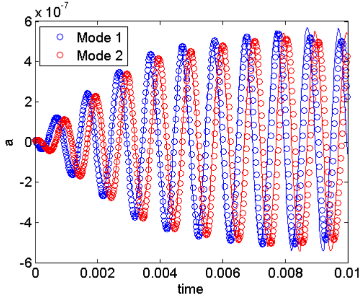

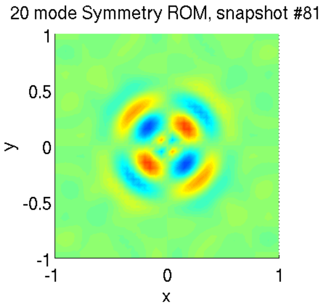

Uncontrolled Symmetry ROM Results

- Figure below shows:
  - ∘: t vs. $a_i(t)$ (ROM coefficients).
  - $-$: t vs. $(\mathbf{q}'_{CFD}(\mathbf{x},t), \boldsymbol{\phi}_i(\mathbf{x}))$ (projection of snapshots onto modes).
- Movie on right shows u-velocity snapshot (top) vs. 20 mode symmetry ROM solution for u (bottom).

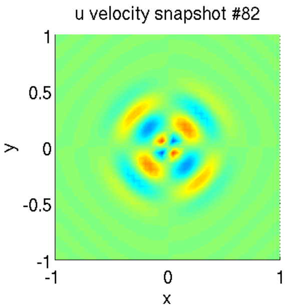

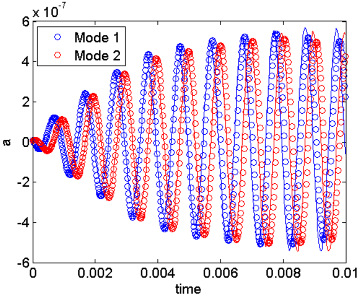

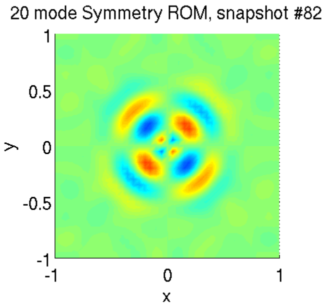

Uncontrolled Symmetry ROM Results

- Figure below shows:
  - $\circ$: t vs. $a_i(t)$ (ROM coefficients).
  - $-$: t vs. $(\mathbf{q}'_{CFD}(\mathbf{x},t), \boldsymbol{\phi}_i(\mathbf{x}))$ (projection of snapshots onto modes).
- Movie on right shows u-velocity snapshot (top) vs. 20 mode symmetry ROM solution for u (bottom).

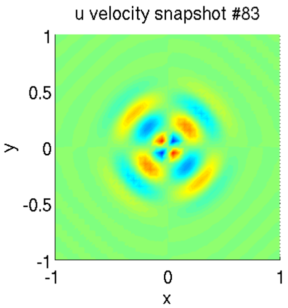

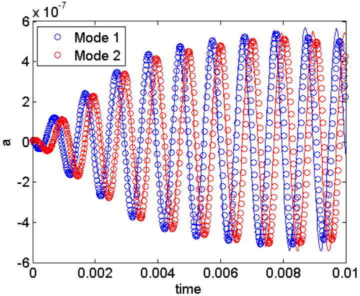

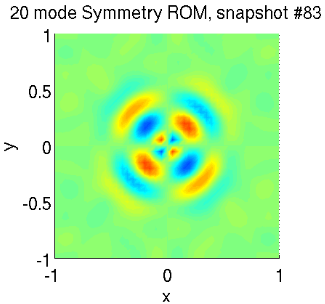

Uncontrolled Symmetry ROM Results

- Figure below shows:
  - $\circ$: t vs. $a_i(t)$ (ROM coefficients).
  - $-$: t vs. $(\mathbf{q}'_{CFD}(\mathbf{x}, t), \boldsymbol{\phi}_i(\mathbf{x}))$ (projection of snapshots onto modes).
- Movie on right shows u-velocity snapshot (top) vs. 20 mode symmetry ROM solution for u (bottom).

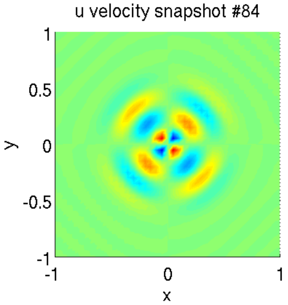

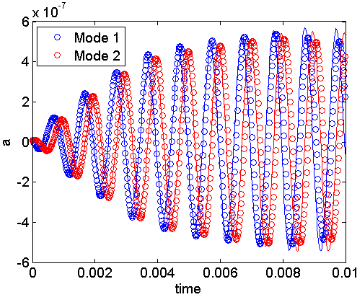

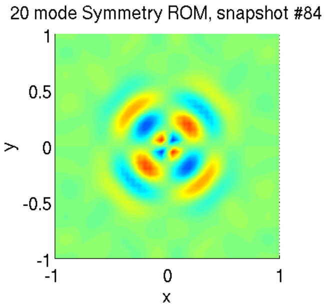

Uncontrolled Symmetry ROM Results

- Figure below shows:
  - $\circ$: t vs. $a_i(t)$ (ROM coefficients).
  - $-$: t vs. $(\mathbf{q}'_{CFD}(\mathbf{x},t), \boldsymbol{\phi}_i(\mathbf{x}))$ (projection of snapshots onto modes).
- Movie on right shows u-velocity snapshot (top) vs. 20 mode symmetry ROM solution for u (bottom).

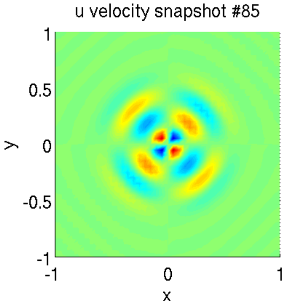

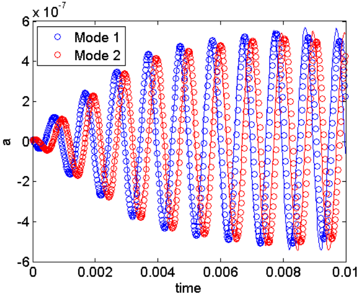

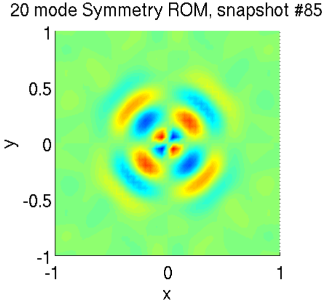

Uncontrolled Symmetry ROM Results

- Figure below shows:
  - ∘: t vs. $a_i(t)$ (ROM coefficients).
  - $-$: t vs. $(\mathbf{q}'_{CFD}(\mathbf{x}, t), \boldsymbol{\phi}_i(\mathbf{x}))$ (projection of snapshots onto modes).
- Movie on right shows u-velocity snapshot (top) vs. 20 mode symmetry ROM solution for u (bottom).

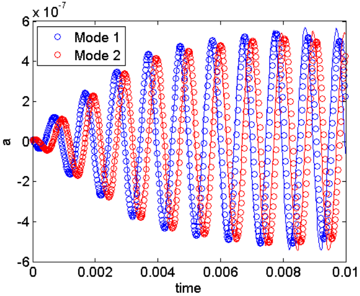

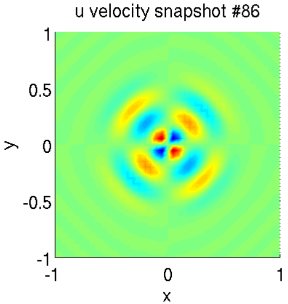

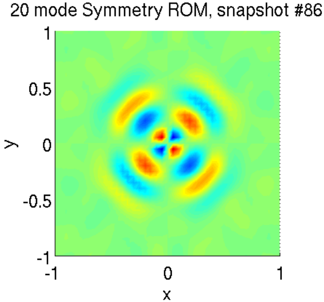

Uncontrolled Symmetry ROM Results

- Figure below shows:
  - $\circ$: t vs. $a_i(t)$ (ROM coefficients).
  - $-$: t vs. $(\mathbf{q}'_{CFD}(\mathbf{x}, t), \boldsymbol{\phi}_i(\mathbf{x}))$ (projection of snapshots onto modes).
- Movie on right shows u-velocity snapshot (top) vs. 20 mode symmetry ROM solution for u (bottom).

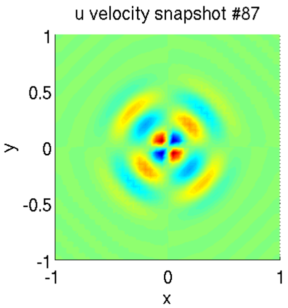

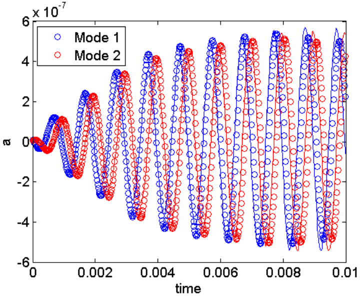

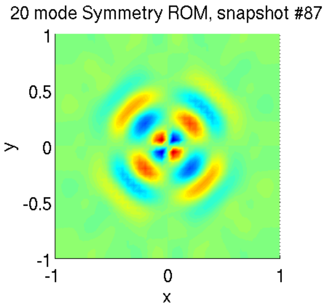

Uncontrolled Symmetry ROM Results

- Figure below shows:
  - $\circ$: t vs. $a_i(t)$ (ROM coefficients).
  - $-$: t vs. $(\mathbf{q}'_{CFD}(\mathbf{x},t), \boldsymbol{\phi}_i(\mathbf{x}))$ (projection of snapshots onto modes).
- Movie on right shows u-velocity snapshot (top) vs. 20 mode symmetry ROM solution for u (bottom).

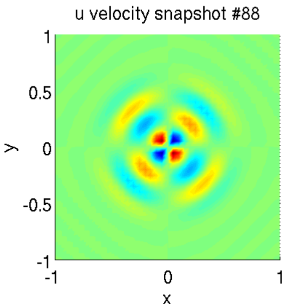

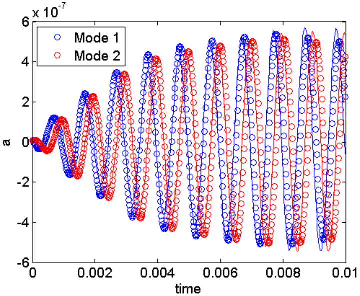

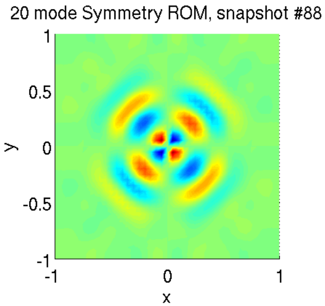

Uncontrolled Symmetry ROM Results

- Figure below shows:
  - $\circ$: t vs. $a_i(t)$ (ROM coefficients).
  - $-$: t vs. $(\mathbf{q}'_{CFD}(\mathbf{x},t), \boldsymbol{\phi}_i(\mathbf{x}))$ (projection of snapshots onto modes).
- Movie on right shows u-velocity snapshot (top) vs. 20 mode symmetry ROM solution for u (bottom).

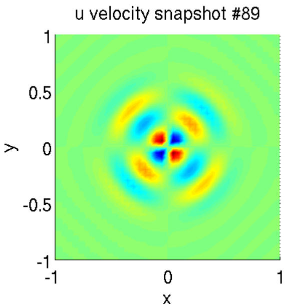

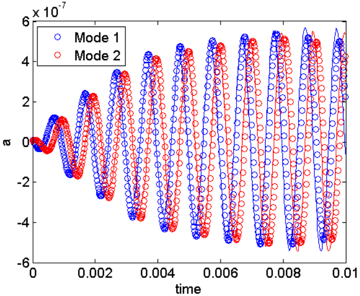

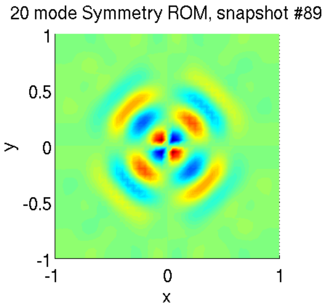

Uncontrolled Symmetry ROM Results

- Figure below shows:
  - $\circ$: t vs. $a_i(t)$ (ROM coefficients).
  - $-$: t vs. $(\mathbf{q}'_{CFD}(\mathbf{x},t), \boldsymbol{\phi}_i(\mathbf{x}))$ (projection of snapshots onto modes).
- Movie on right shows u-velocity snapshot (top) vs. 20 mode symmetry ROM solution for u (bottom).

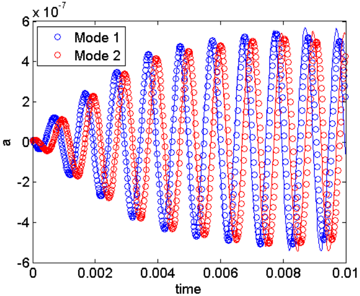

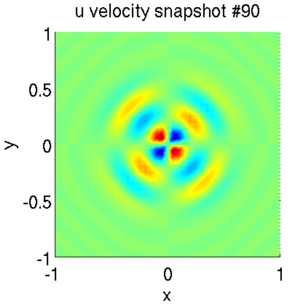

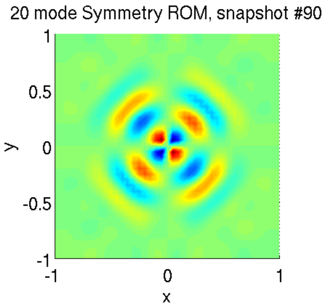

Uncontrolled Symmetry ROM Results

- Figure below shows:
  - ∘: t vs. $a_i(t)$ (ROM coefficients).
  - $-$: t vs. $(\mathbf{q}'_{CFD}(\mathbf{x}, t), \boldsymbol{\phi}_i(\mathbf{x}))$ (projection of snapshots onto modes).
- Movie on right shows u-velocity snapshot (top) vs. 20 mode symmetry ROM solution for u (bottom).

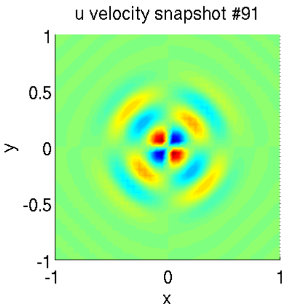

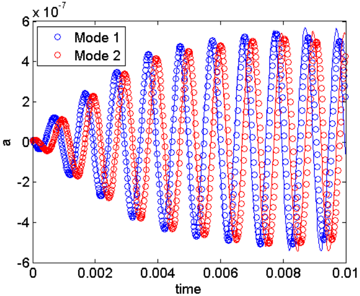

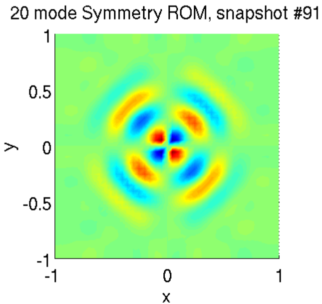

Uncontrolled Symmetry ROM Results

- Figure below shows:
  - $\circ$: t vs. $a_i(t)$ (ROM coefficients).
  - $-$: t vs. $(\mathbf{q}'_{CFD}(\mathbf{x},t), \boldsymbol{\phi}_i(\mathbf{x}))$ (projection of snapshots onto modes).
- Movie on right shows u-velocity snapshot (top) vs. 20 mode symmetry ROM solution for u (bottom).

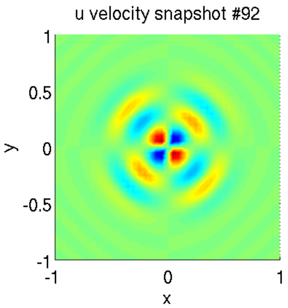

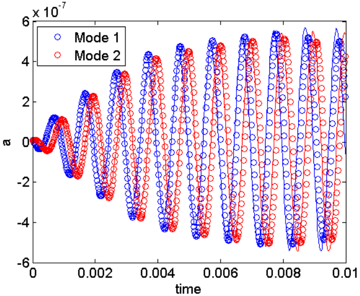

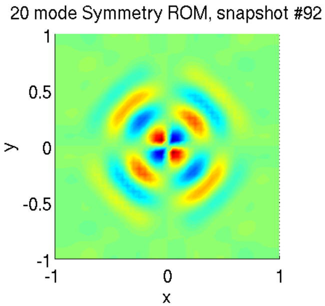

Uncontrolled Symmetry ROM Results

- Figure below shows:
  - ○: t vs. $a_i(t)$ (ROM coefficients).
  - $-$: t vs. $(\mathbf{q}'_{CFD}(\mathbf{x},t), \boldsymbol{\phi}_i(\mathbf{x}))$ (projection of snapshots onto modes).
- Movie on right shows u-velocity snapshot (top) vs. 20 mode symmetry ROM solution for u (bottom).

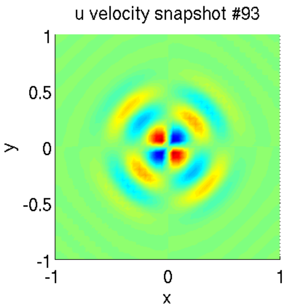

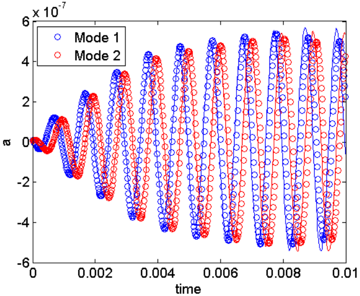

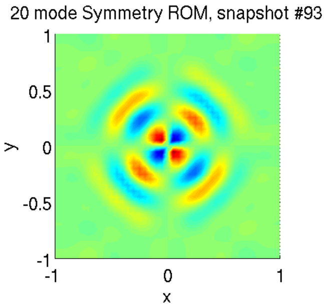

Uncontrolled Symmetry ROM Results

- Figure below shows:
  - $\circ$: t vs. $a_i(t)$ (ROM coefficients).
  - $-$: t vs. $(\mathbf{q}'_{CFD}(\mathbf{x}, t), \boldsymbol{\phi}_i(\mathbf{x}))$ (projection of snapshots onto modes).
- Movie on right shows u-velocity snapshot (top) vs. 20 mode symmetry ROM solution for u (bottom).

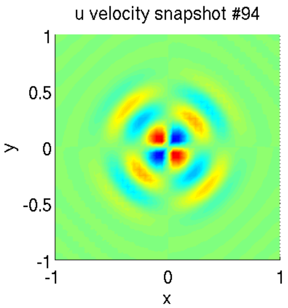

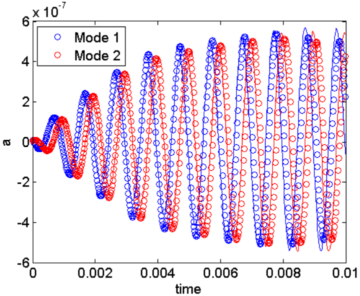

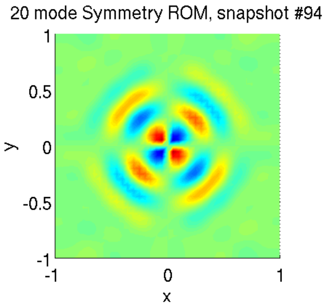

Uncontrolled Symmetry ROM Results

- Figure below shows:
  - $\circ$: t vs. $a_i(t)$ (ROM coefficients).
  - $-$: t vs. $(\mathbf{q}'_{CFD}(\mathbf{x},t), \boldsymbol{\phi}_i(\mathbf{x}))$ (projection of snapshots onto modes).
- Movie on right shows u-velocity snapshot (top) vs. 20 mode symmetry ROM solution for u (bottom).

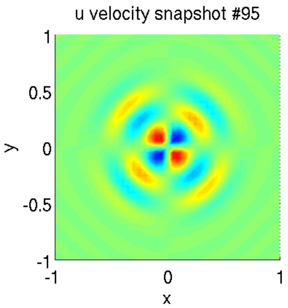

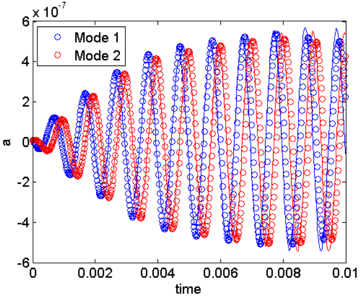

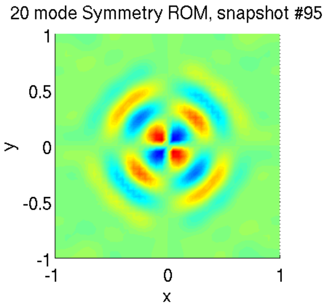

Uncontrolled Symmetry ROM Results

- Figure below shows:
  - ○: t vs. $a_i(t)$ (ROM coefficients).
  - $-$: t vs. $(\mathbf{q}'_{CFD}(\mathbf{x},t), \boldsymbol{\phi}_i(\mathbf{x}))$ (projection of snapshots onto modes).
- Movie on right shows u-velocity snapshot (top) vs. 20 mode symmetry ROM solution for u (bottom).

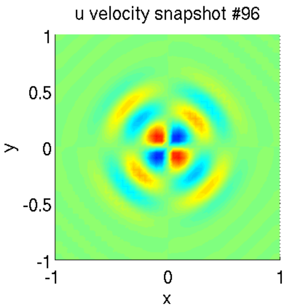

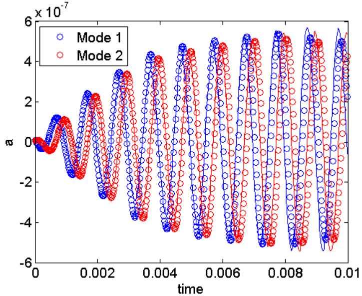

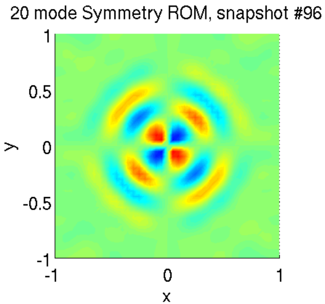

Uncontrolled Symmetry ROM Results

- Figure below shows:
  - $\circ$: t vs. $a_i(t)$ (ROM coefficients).
  - $-$: t vs. $(\mathbf{q}'_{CFD}(\mathbf{x}, t), \boldsymbol{\phi}_i(\mathbf{x}))$ (projection of snapshots onto modes).
- Movie on right shows u-velocity snapshot (top) vs. 20 mode symmetry ROM solution for u (bottom).

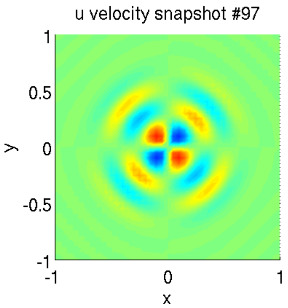

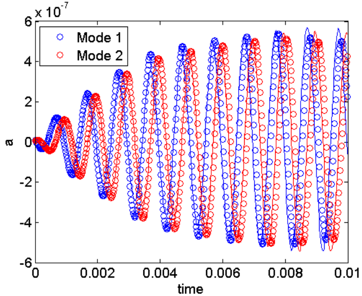

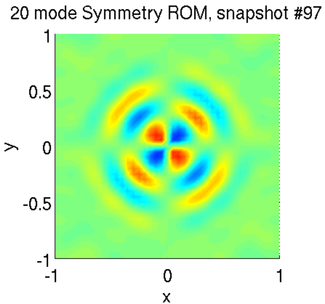

Uncontrolled Symmetry ROM Results

- Figure below shows:
  - $\circ$: t vs. $a_i(t)$ (ROM coefficients).
  - $-$: t vs. $(\mathbf{q}'_{CFD}(\mathbf{x},t), \boldsymbol{\phi}_i(\mathbf{x}))$ (projection of snapshots onto modes).
- Movie on right shows u-velocity snapshot (top) vs. 20 mode symmetry ROM solution for u (bottom).

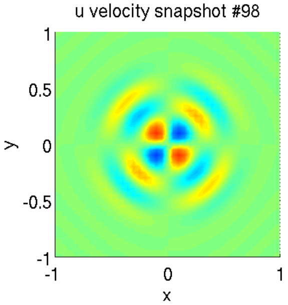

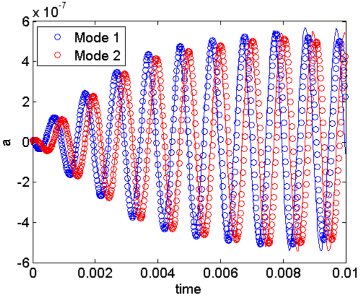

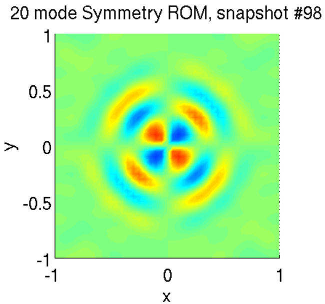

Uncontrolled Symmetry ROM Results

- Figure below shows:
  - $\circ$: t vs. $a_i(t)$ (ROM coefficients).
  - $-$: t vs. $(\mathbf{q}'_{CFD}(\mathbf{x},t), \boldsymbol{\phi}_i(\mathbf{x}))$ (projection of snapshots onto modes).
- Movie on right shows u-velocity snapshot (top) vs. 20 mode symmetry ROM solution for u (bottom).

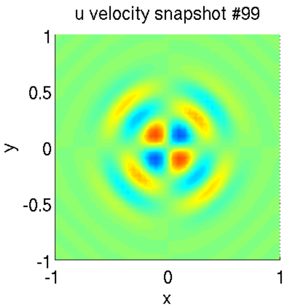

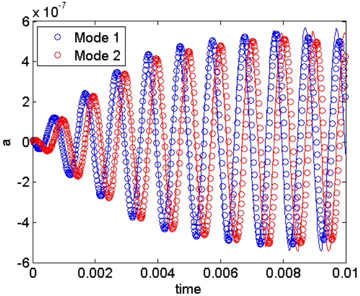

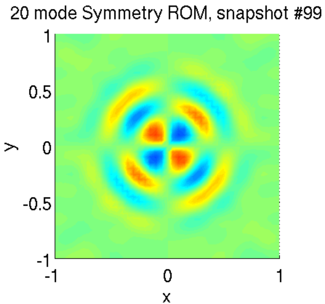

Uncontrolled Symmetry ROM Results

- Figure below shows:
  - $\circ$: t vs. $a_i(t)$ (ROM coefficients).
  - $-$: t vs. $(\mathbf{q}'_{CFD}(\mathbf{x}, t), \boldsymbol{\phi}_i(\mathbf{x}))$ (projection of snapshots onto modes).
- Movie on right shows u-velocity snapshot (top) vs. 20 mode symmetry ROM solution for u (bottom).

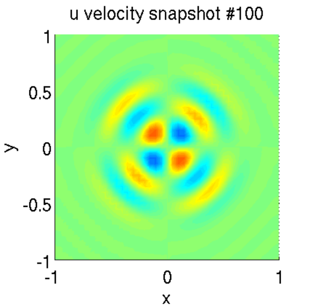

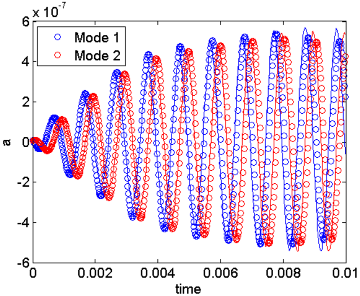

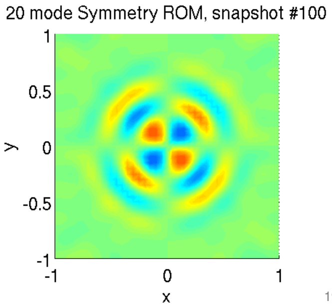

Uncontrolled Symmetry ROM Results

LQR Control of Driven Pulse

- **Control problem:** compute actuation that will minimize p' at $(x, y) = (1, 0)$.
  - Compute **LQR controller** feedback law $u_M = -\mathbf{K}\mathbf{x}_M$ to minimize quadratic cost functional using ROM*:

$$J \equiv \frac{1}{T}\int_0^T [p'^2(1,0;t) + \tau u^2]dt$$

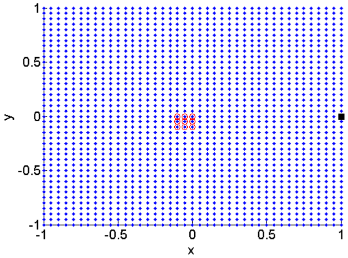

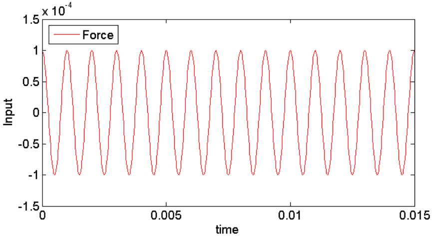

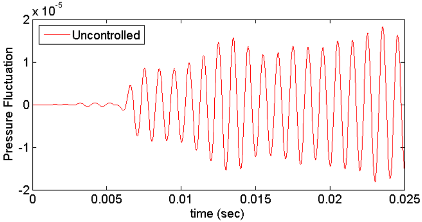

* The computation of $\mathbf{K} = \mathbf{R}^{-1}\mathbf{B}^T\mathbf{X}$ requires solution of algebraic Ricatti equation $\mathbf{A}^T\mathbf{X} + \mathbf{X}\mathbf{A} - \frac{1}{\tau}\mathbf{X}\mathbf{B}\mathbf{B}^T\mathbf{X} + \mathbf{C}^T\mathbf{C} = \mathbf{0}$ [8].

Sandia National Laboratories

LQR Control of Driven Pulse

- **Control problem:** compute actuation that will minimize p' at $(x, y) = (1, 0)$.
  - Compute **LQR controller** feedback law $u_M = -\mathbf{K}\mathbf{x}_M$ to minimize quadratic cost functional using ROM*:

$$J \equiv \frac{1}{T}\int_0^T [p'^2(1, 0; t) + \tau u^2] dt$$

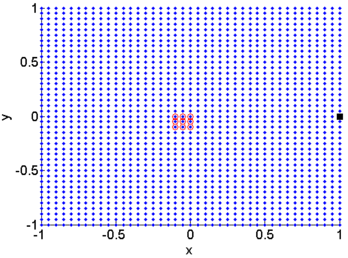

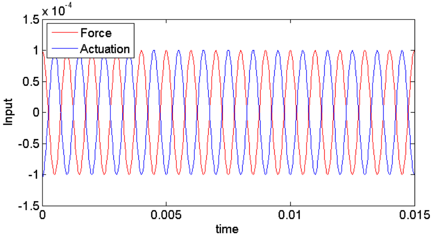

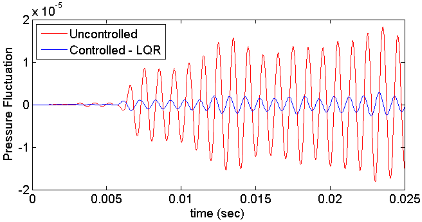

* The computation of $\mathbf{K} = \mathbf{R}^{-1}\mathbf{B}^T\mathbf{X}$ requires solution of algebraic Ricatti equation $\mathbf{A}^T\mathbf{X} + \mathbf{X}\mathbf{A} - \frac{1}{\tau}\mathbf{X}\mathbf{B}\mathbf{B}^T\mathbf{X} + \mathbf{C}^T\mathbf{C} = \mathbf{0}$ [8].

Laminar Viscous Driven Cavity Problem

- Mach = 0.6, Re = 1898 (laminar regime).

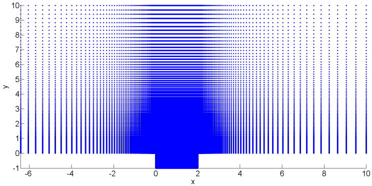

Laminar Viscous Driven Cavity Problem

- Mach = 0.6, Re = 1898 (laminar regime).
- Force for y–momentum equation drives the flow:

$$F_v(\mathbf{x}, t) = \frac{1}{2}\cos(2000\pi t), \qquad \mathbf{x} \in \Omega_c$$

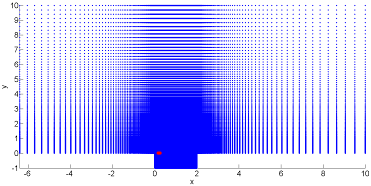

Laminar Viscous Driven Cavity Problem

- Mach = 0.6, Re = 1898 (laminar regime).
- Force for y–momentum equation drives the flow:

$$F_v(\mathbf{x}, t) = \frac{1}{2}\cos(2000\pi t), \qquad \mathbf{x} \in \Omega_c$$

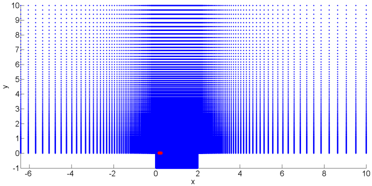

- High-fidelity CFD simulation was run on 343,408 node mesh until time $T = 0.202$ seconds.
- 101 snapshots were saved (every 2×10^{-4} seconds), to construct a 20 mode POD basis.

Laminar Viscous Driven Cavity Problem

- Mach = 0.6, Re = 1898 (laminar regime).
- Force for y–momentum equation drives the flow:

$$F_v(\mathbf{x}, t) = \frac{1}{2}\cos(2000\pi t), \qquad \mathbf{x} \in \Omega_c$$

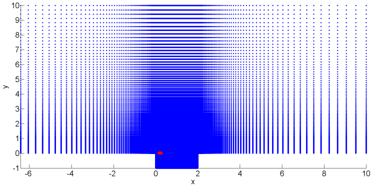

- High-fidelity CFD simulation was run on 343,408 node mesh until time $T = 0.202$ seconds.
- 101 snapshots were saved (every 2×10^{-4} seconds), to construct a 20 mode POD basis.

Inherently non-linear problem!
High-fidelity solution obtained by solving full *non-linear* Navier-Stokes equations.

Expected ROM Performance

ROM based on Navier-Stokes equations *linearized* around snapshot mean.

Expected ROM Performance

ROM based on Navier-Stokes equations
linearized around snapshot mean.

Non-linear dynamics of flow
are captured in
POD reduced basis modes.

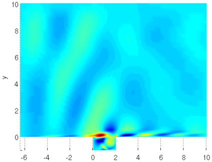

u mode 1
(24.9% energy)

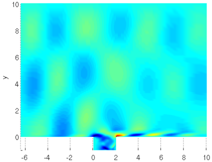

u mode 2
(23.7% energy)

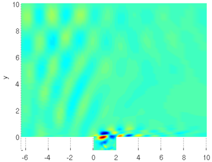

u mode 3
(6.93% energy)

Expected ROM Performance

ROM based on Navier-Stokes equations
linearized around snapshot mean.

Non-linear dynamics of flow
are captured in
POD reduced basis modes.

Non-linear dynamics of the flow
are *not* fully captured in equations
projected onto POD modes.

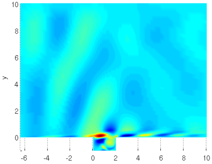

u mode 1
(24.9% energy)

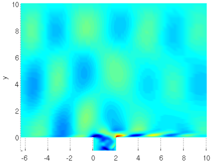

u mode 2
(23.7% energy)

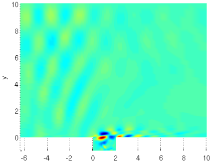

u mode 3
(6.93% energy)

ROM based on Linearized Navier-Stokes Neglecting $\nabla\bar{\mathbf{q}}$ Terms

$$\mathbf{q}'_{,t} + \mathbf{A}_i(\bar{\mathbf{q}})\mathbf{q}'_{,i} - [\mathbf{K}_{ij}(\bar{\mathbf{q}})\mathbf{q}'_{,j}]_{,i} = \mathbf{F}$$

- Figure below shows:
  - $\circ$: t vs. $a_i(t)$ (ROM coefficients).
  - $-$: t vs. $(\mathbf{q}'_{CFD}(\mathbf{x}, t), \boldsymbol{\phi}_i(\mathbf{x}))$ (projection of snapshots onto modes).
- Movie on right shows v-velocity snapshot (top) vs. 20 mode symmetry ROM solution v (bottom).

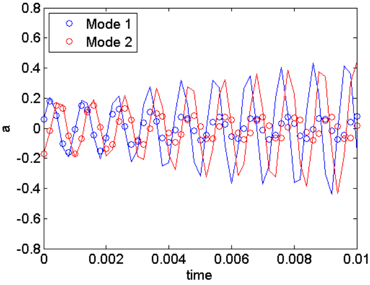

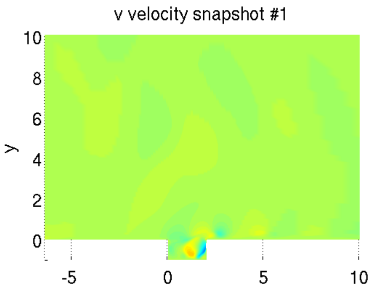

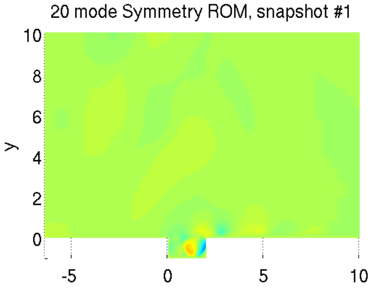

ROM based on Linearized Navier-Stokes Neglecting $\nabla\bar{\mathbf{q}}$ Terms

$$\mathbf{q}'_{,t} + \mathbf{A}_i(\bar{\mathbf{q}})\mathbf{q}'_{,i} - [\mathbf{K}_{ij}(\bar{\mathbf{q}})\mathbf{q}'_{,j}]_{,i} = \mathbf{F}$$

- Figure below shows:
  - $\circ$: t vs. $a_i(t)$ (ROM coefficients).
  - $-$: t vs. $(\mathbf{q}'_{CFD}(\mathbf{x}, t), \boldsymbol{\phi}_i(\mathbf{x}))$ (projection of snapshots onto modes).
- Movie on right shows v-velocity snapshot (top) vs. 20 mode symmetry ROM solution v (bottom).

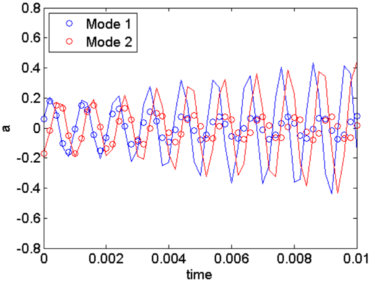

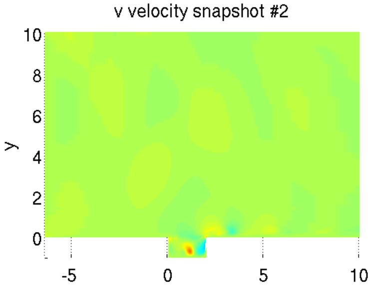

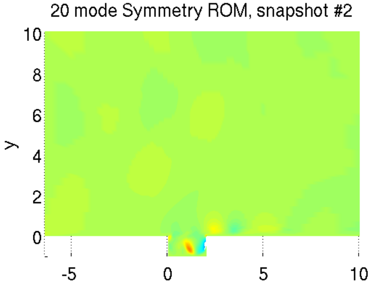

ROM based on Linearized Navier-Stokes Neglecting $\nabla\bar{\mathbf{q}}$ Terms

$$\mathbf{q}'_{,t} + \mathbf{A}_i(\bar{\mathbf{q}})\mathbf{q}'_{,i} - [\mathbf{K}_{ij}(\bar{\mathbf{q}})\mathbf{q}'_{,j}]_{,i} = \mathbf{F}$$

- Figure below shows:
  - ∘: t vs. $a_i(t)$ (ROM coefficients).
  - $-$: t vs. $(\mathbf{q}'_{CFD}(\mathbf{x}, t), \boldsymbol{\phi}_i(\mathbf{x}))$ (projection of snapshots onto modes).
- Movie on right shows v-velocity snapshot (top) vs. 20 mode symmetry ROM solution v (bottom).

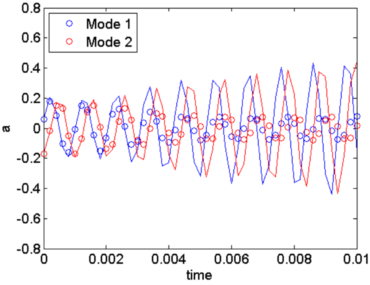

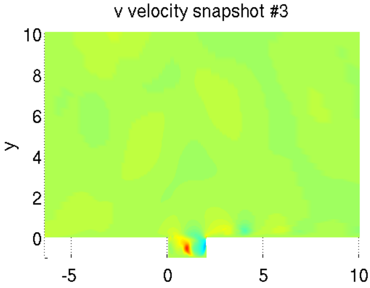

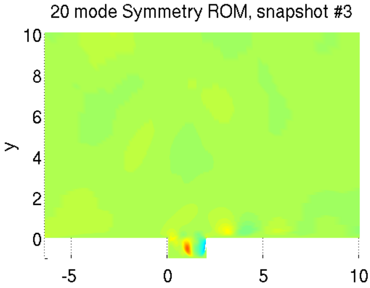

ROM based on Linearized Navier-Stokes Neglecting $\nabla\bar{\mathrm{q}}$ Terms

$$\mathbf{q}'_{,t} + \mathbf{A}_i(\bar{\mathbf{q}})\mathbf{q}'_{,i} - [\mathbf{K}_{ij}(\bar{\mathbf{q}})\mathbf{q}'_{,j}]_{,i} = \mathbf{F}$$

- Figure below shows:
  - $\circ$: t vs. $a_i(t)$ (ROM coefficients).
  - $-$: t vs. $(\mathbf{q}'_{CFD}(\mathbf{x}, t), \boldsymbol{\phi}_i(\mathbf{x}))$ (projection of snapshots onto modes).
- Movie on right shows v-velocity snapshot (top) vs. 20 mode symmetry ROM solution v (bottom).

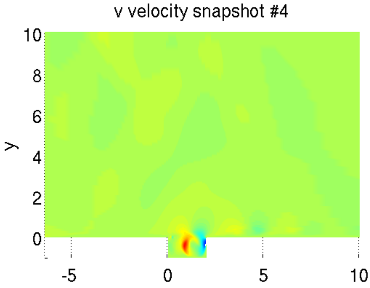

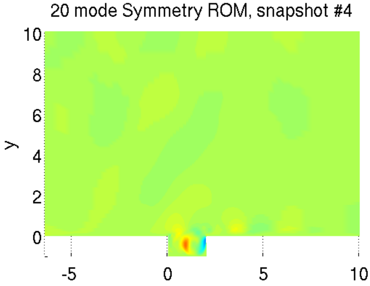

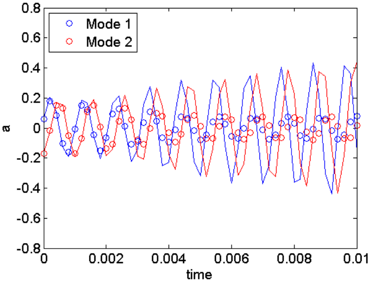

ROM based on Linearized Navier-Stokes Neglecting $\nabla\bar{\mathbf{q}}$ Terms

$$\mathbf{q}'_{,t} + \mathbf{A}_i(\bar{\mathbf{q}})\mathbf{q}'_{,i} - [\mathbf{K}_{ij}(\bar{\mathbf{q}})\mathbf{q}'_{,j}]_{,i} = \mathbf{F}$$

- Figure below shows:
  - $\circ$: t vs. $a_i(t)$ (ROM coefficients).
  - $-$: t vs. $(\mathbf{q}'_{CFD}(\mathbf{x},t), \boldsymbol{\phi}_i(\mathbf{x}))$ (projection of snapshots onto modes).
- Movie on right shows v-velocity snapshot (top) vs. 20 mode symmetry ROM solution v (bottom).

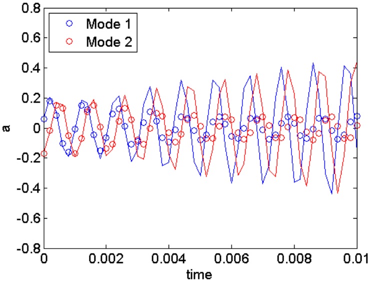

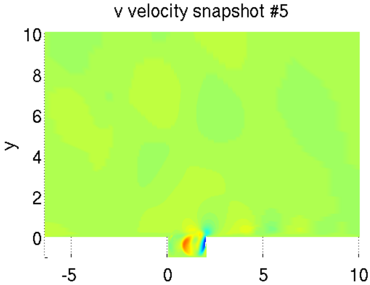

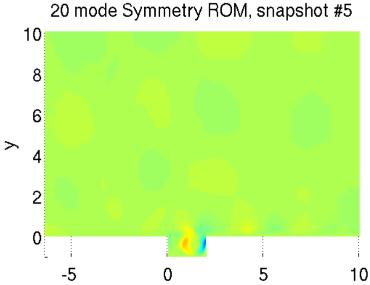

ROM based on Linearized Navier-Stokes Neglecting $\nabla\bar{\mathbf{q}}$ Terms

$$\mathbf{q}'_{,t} + \mathbf{A}_i(\bar{\mathbf{q}})\mathbf{q}'_{,i} - [\mathbf{K}_{ij}(\bar{\mathbf{q}})\mathbf{q}'_{,j}]_{,i} = \mathbf{F}$$

- Figure below shows:
  - $\circ$: t vs. $a_i(t)$ (ROM coefficients).
  - $-$: t vs. $(\mathbf{q}'_{CFD}(\mathbf{x},t), \boldsymbol{\phi}_i(\mathbf{x}))$ (projection of snapshots onto modes).
- Movie on right shows v-velocity snapshot (top) vs. 20 mode symmetry ROM solution v (bottom).

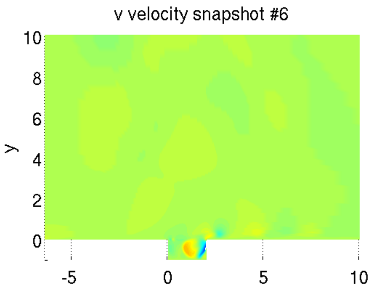

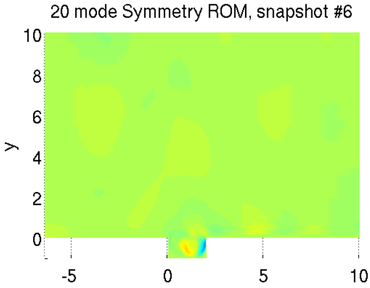

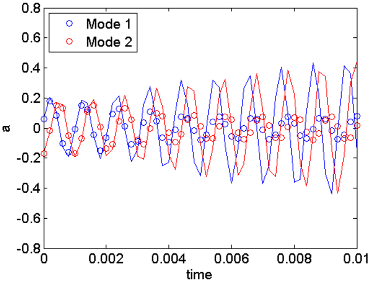

ROM based on Linearized Navier-Stokes Neglecting $\nabla\bar{\mathrm{q}}$ Terms

$$\mathbf{q}'_{,t} + \mathbf{A}_i(\bar{\mathbf{q}})\mathbf{q}'_{,i} - [\mathbf{K}_{ij}(\bar{\mathbf{q}})\mathbf{q}'_{,j}]_{,i} = \mathbf{F}$$

- Figure below shows:
  - $\circ$: t vs. $a_i(t)$ (ROM coefficients).
  - $-$: t vs. $(\mathbf{q}'_{CFD}(\mathbf{x},t), \boldsymbol{\phi}_i(\mathbf{x}))$ (projection of snapshots onto modes).
- Movie on right shows v-velocity snapshot (top) vs. 20 mode symmetry ROM solution v (bottom).

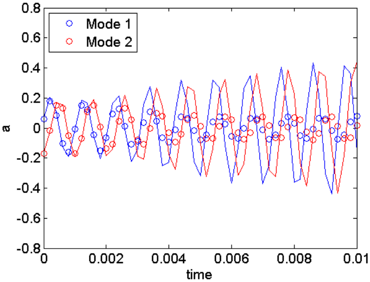

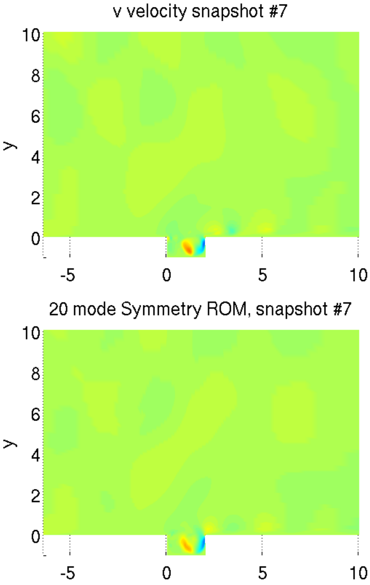

ROM based on Linearized Navier-Stokes Neglecting $\nabla\bar{\mathbf{q}}$ Terms

$$\mathbf{q}'_{,t} + \mathbf{A}_i(\bar{\mathbf{q}})\mathbf{q}'_{,i} - [\mathbf{K}_{ij}(\bar{\mathbf{q}})\mathbf{q}'_{,j}]_{,i} = \mathbf{F}$$

- Figure below shows:
  - ○: t vs. $a_i(t)$ (ROM coefficients).
  - $-$: t vs. $(\mathbf{q}'_{CFD}(\mathbf{x}, t), \boldsymbol{\phi}_i(\mathbf{x}))$ (projection of snapshots onto modes).
- Movie on right shows v-velocity snapshot (top) vs. 20 mode symmetry ROM solution v (bottom).

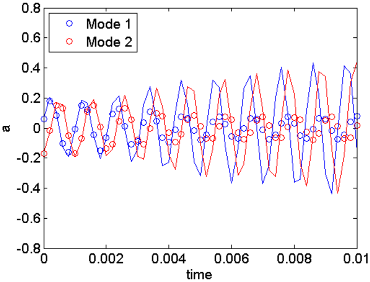

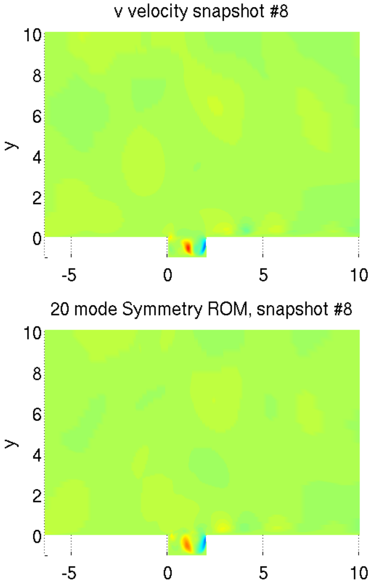

ROM based on Linearized Navier-Stokes Neglecting $\nabla\bar{\mathrm{q}}$ Terms

$$\mathbf{q}'_{,t} + \mathbf{A}_i(\bar{\mathbf{q}})\mathbf{q}'_{,i} - [\mathbf{K}_{ij}(\bar{\mathbf{q}})\mathbf{q}'_{,j}]_{,i} = \mathbf{F}$$

- Figure below shows:
  - $\circ$: t vs. $a_i(t)$ (ROM coefficients).
  - $-$: t vs. $(\mathbf{q}'_{CFD}(\mathbf{x}, t), \boldsymbol{\phi}_i(\mathbf{x}))$ (projection of snapshots onto modes).
- Movie on right shows v-velocity snapshot (top) vs. 20 mode symmetry ROM solution v (bottom).

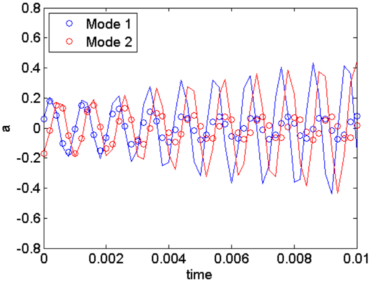

v velocity snapshot #9

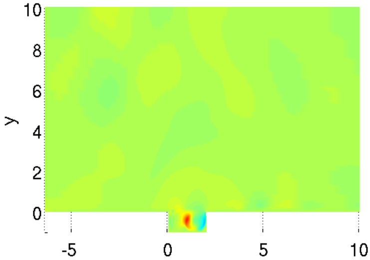

20 mode Symmetry ROM, snapshot #9

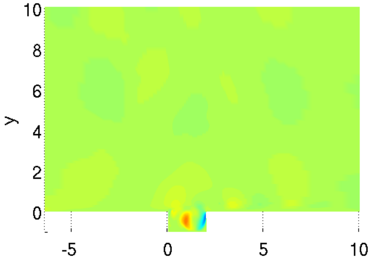

ROM based on Linearized Navier-Stokes Neglecting $\nabla\bar{\mathbf{q}}$ Terms

$$\mathbf{q}'_{,t} + \mathbf{A}_i(\bar{\mathbf{q}})\mathbf{q}'_{,i} - [\mathbf{K}_{ij}(\bar{\mathbf{q}})\mathbf{q}'_{,j}]_{,i} = \mathbf{F}$$

- Figure below shows:
  - $\circ$: t vs. $a_i(t)$ (ROM coefficients).
  - $-$: t vs. $(\mathbf{q}'_{CFD}(\mathbf{x},t), \boldsymbol{\phi}_i(\mathbf{x}))$ (projection of snapshots onto modes).
- Movie on right shows v-velocity snapshot (top) vs. 20 mode symmetry ROM solution v (bottom).

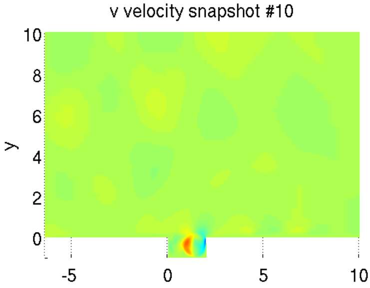

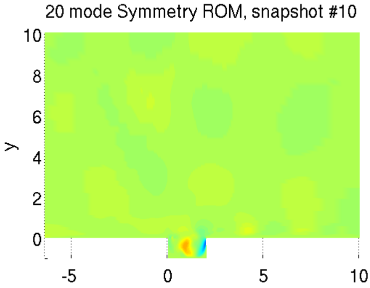

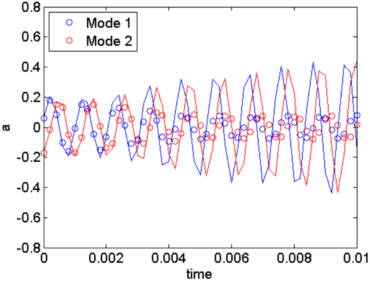

ROM based on Linearized Navier-Stokes Neglecting $\nabla\bar{\mathbf{q}}$ Terms

$$\mathbf{q}'_{,t} + \mathbf{A}_i(\bar{\mathbf{q}})\mathbf{q}'_{,i} - [\mathbf{K}_{ij}(\bar{\mathbf{q}})\mathbf{q}'_{,j}]_{,i} = \mathbf{F}$$

- Figure below shows:
  - $\circ$: t vs. $a_i(t)$ (ROM coefficients).
  - $-$: t vs. $(\mathbf{q}'_{CFD}(\mathbf{x},t), \boldsymbol{\phi}_i(\mathbf{x}))$ (projection of snapshots onto modes).
- Movie on right shows v-velocity snapshot (top) vs. 20 mode symmetry ROM solution v (bottom).

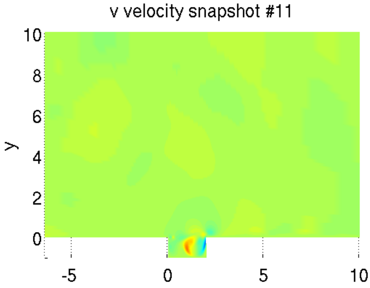

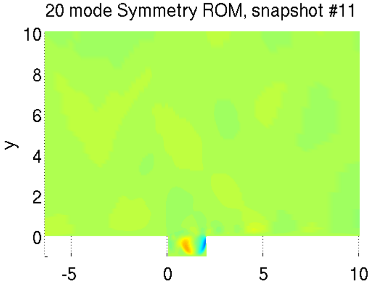

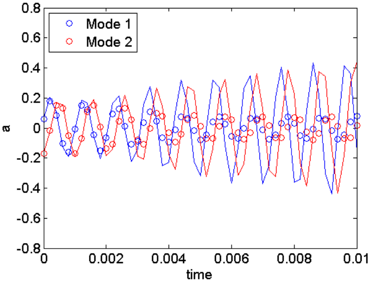

ROM based on Linearized Navier-Stokes Neglecting $\nabla\bar{\mathbf{q}}$ Terms

$$\mathbf{q}'_{,t} + \mathbf{A}_i(\bar{\mathbf{q}})\mathbf{q}'_{,i} - [\mathbf{K}_{ij}(\bar{\mathbf{q}})\mathbf{q}'_{,j}]_{,i} = \mathbf{F}$$

- Figure below shows:
  - ○: t vs. $a_i(t)$ (ROM coefficients).
  - $-$: t vs. $(\mathbf{q}'_{CFD}(\mathbf{x},t), \boldsymbol{\phi}_i(\mathbf{x}))$ (projection of snapshots onto modes).
- Movie on right shows v-velocity snapshot (top) vs. 20 mode symmetry ROM solution v (bottom).

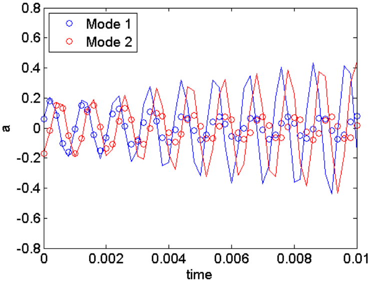

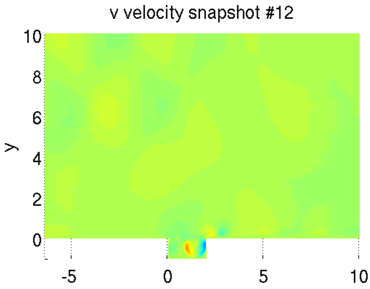

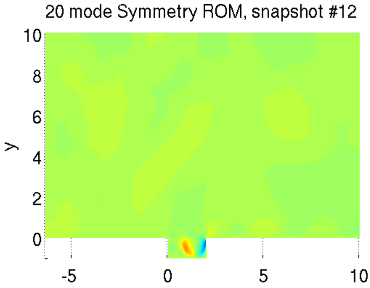

ROM based on Linearized Navier-Stokes Neglecting $\nabla\bar{\mathrm{q}}$ Terms

$$\mathbf{q}'_{,t} + \mathbf{A}_i(\bar{\mathbf{q}})\mathbf{q}'_{,i} - [\mathbf{K}_{ij}(\bar{\mathbf{q}})\mathbf{q}'_{,j}]_{,i} = \mathbf{F}$$

- Figure below shows:
  - ○: t vs. $a_i(t)$ (ROM coefficients).
  - $-$: t vs. $(\mathbf{q}'_{CFD}(\mathbf{x},t), \boldsymbol{\phi}_i(\mathbf{x}))$ (projection of snapshots onto modes).
- Movie on right shows v-velocity snapshot (top) vs. 20 mode symmetry ROM solution v (bottom).

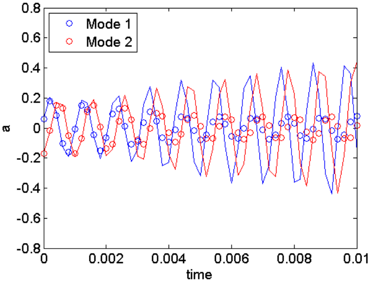

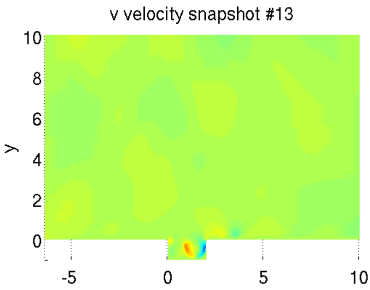

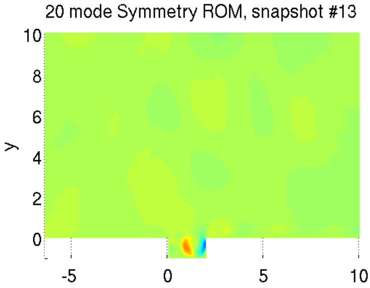

ROM based on Linearized Navier-Stokes Neglecting $\nabla\bar{\mathbf{q}}$ Terms

$$\mathbf{q}'_{,t} + \mathbf{A}_i(\bar{\mathbf{q}})\mathbf{q}'_{,i} - [\mathbf{K}_{ij}(\bar{\mathbf{q}})\mathbf{q}'_{,j}]_{,i} = \mathbf{F}$$

- Figure below shows:
  - ○: t vs. $a_i(t)$ (ROM coefficients).
  - $-$: t vs. $(\mathbf{q}'_{CFD}(\mathbf{x},t), \boldsymbol{\phi}_i(\mathbf{x}))$ (projection of snapshots onto modes).
- Movie on right shows v-velocity snapshot (top) vs. 20 mode symmetry ROM solution v (bottom).

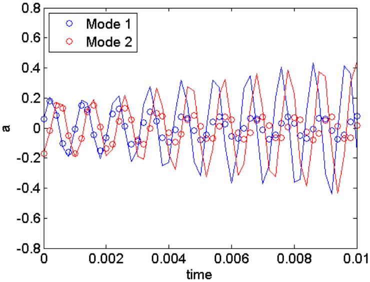

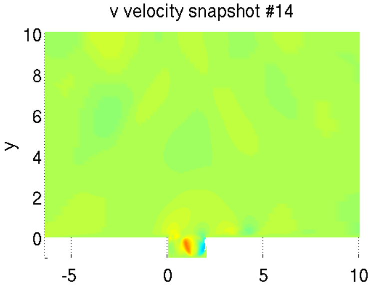

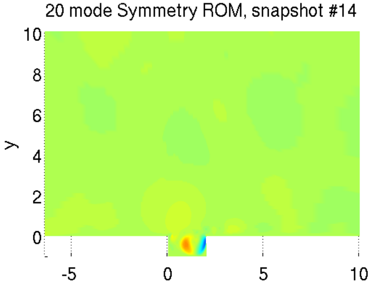

ROM based on Linearized Navier-Stokes Neglecting $\nabla\bar{\mathrm{q}}$ Terms

$$\mathbf{q}'_{,t} + \mathbf{A}_i(\bar{\mathbf{q}})\mathbf{q}'_{,i} - [\mathbf{K}_{ij}(\bar{\mathbf{q}})\mathbf{q}'_{,j}]_{,i} = \mathbf{F}$$

- Figure below shows:
  - $\circ$: t vs. $a_i(t)$ (ROM coefficients).
  - $-$: t vs. $(\mathbf{q}'_{CFD}(\mathbf{x},t), \boldsymbol{\phi}_i(\mathbf{x}))$ (projection of snapshots onto modes).
- Movie on right shows v-velocity snapshot (top) vs. 20 mode symmetry ROM solution v (bottom).

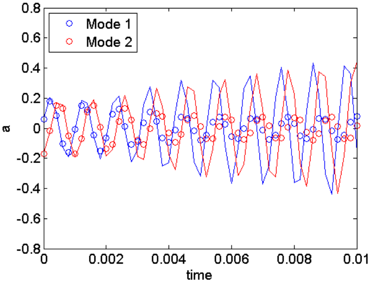

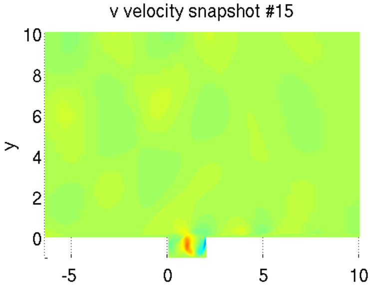

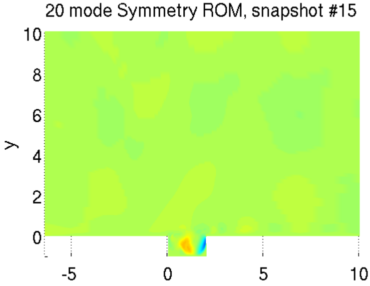

ROM based on Linearized Navier-Stokes Neglecting $\nabla\bar{\mathbf{q}}$ Terms

$$\mathbf{q}'_{,t} + \mathbf{A}_i(\bar{\mathbf{q}})\mathbf{q}'_{,i} - [\mathbf{K}_{ij}(\bar{\mathbf{q}})\mathbf{q}'_{,j}]_{,i} = \mathbf{F}$$

- Figure below shows:
  - $\circ$: t vs. $a_i(t)$ (ROM coefficients).
  - $-$: t vs. $(\mathbf{q}'_{CFD}(\mathbf{x},t), \boldsymbol{\phi}_i(\mathbf{x}))$ (projection of snapshots onto modes).
- Movie on right shows v-velocity snapshot (top) vs. 20 mode symmetry ROM solution v (bottom).

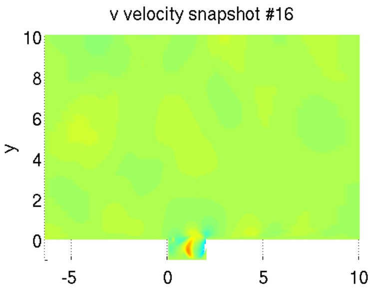

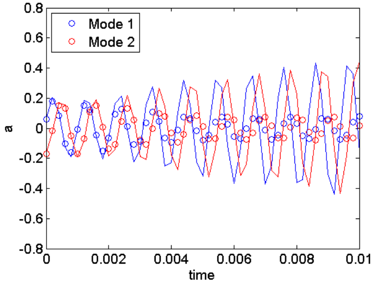

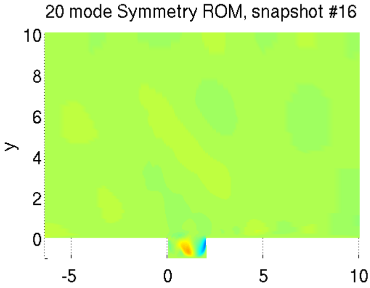

ROM based on Linearized Navier-Stokes Neglecting $\nabla\bar{\mathbf{q}}$ Terms

$$\mathbf{q}'_{,t} + \mathbf{A}_i(\bar{\mathbf{q}})\mathbf{q}'_{,i} - [\mathbf{K}_{ij}(\bar{\mathbf{q}})\mathbf{q}'_{,j}]_{,i} = \mathbf{F}$$

- Figure below shows:
  - ○: t vs. $a_i(t)$ (ROM coefficients).
  - $-$: t vs. $(\mathbf{q}'_{CFD}(\mathbf{x},t), \boldsymbol{\phi}_i(\mathbf{x}))$ (projection of snapshots onto modes).
- Movie on right shows v-velocity snapshot (top) vs. 20 mode symmetry ROM solution v (bottom).

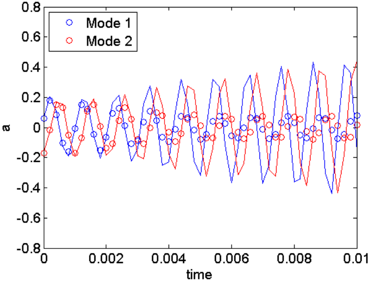

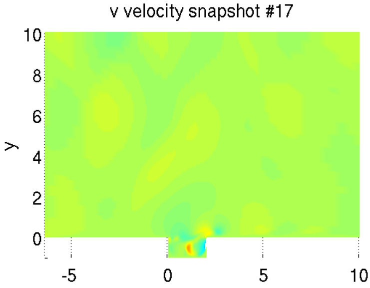

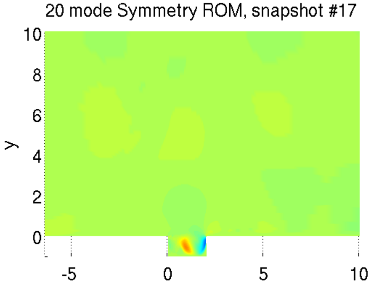

ROM based on Linearized Navier-Stokes Neglecting $\nabla \bar{\mathbf{q}}$ Terms

$$\mathbf{q}'_{,t} + \mathbf{A}_i(\bar{\mathbf{q}})\mathbf{q}'_{,i} - [\mathbf{K}_{ij}(\bar{\mathbf{q}})\mathbf{q}'_{,j}]_{,i} = \mathbf{F}$$

- Figure below shows:
  - ○: t vs. $a_i(t)$ (ROM coefficients).
  - $-$: t vs. $(\mathbf{q}'_{CFD}(\mathbf{x},t), \boldsymbol{\phi}_i(\mathbf{x}))$ (projection of snapshots onto modes).
- Movie on right shows v-velocity snapshot (top) vs. 20 mode symmetry ROM solution v (bottom).

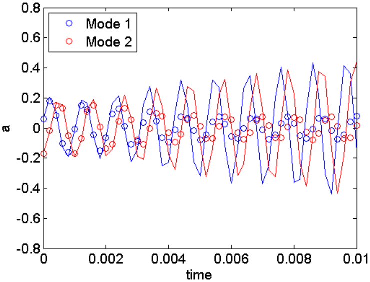

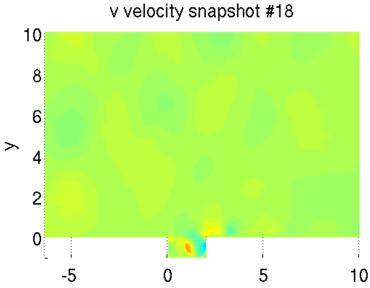

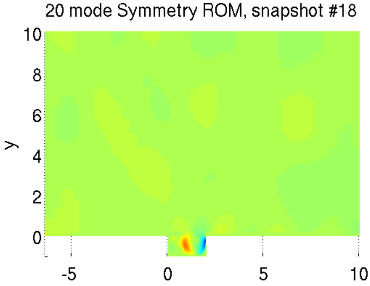

ROM based on Linearized Navier-Stokes Neglecting $\nabla\bar{\mathbf{q}}$ Terms

$$\mathbf{q}'_{,t} + \mathbf{A}_i(\bar{\mathbf{q}})\mathbf{q}'_{,i} - [\mathbf{K}_{ij}(\bar{\mathbf{q}})\mathbf{q}'_{,j}]_{,i} = \mathbf{F}$$

- Figure below shows:
  - ∘: t vs. $a_i(t)$ (ROM coefficients).
  - $-$: t vs. $(\mathbf{q}'_{CFD}(\mathbf{x},t), \boldsymbol{\phi}_i(\mathbf{x}))$ (projection of snapshots onto modes).
- Movie on right shows v-velocity snapshot (top) vs. 20 mode symmetry ROM solution v (bottom).

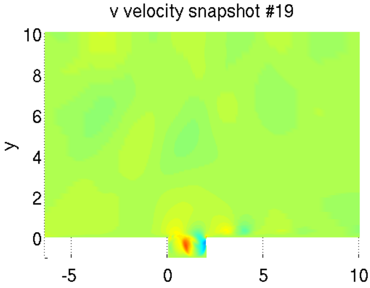

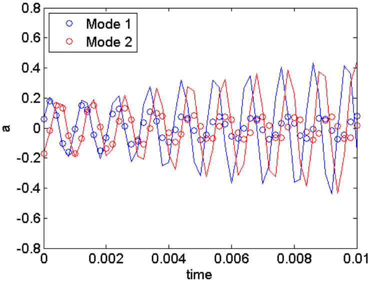

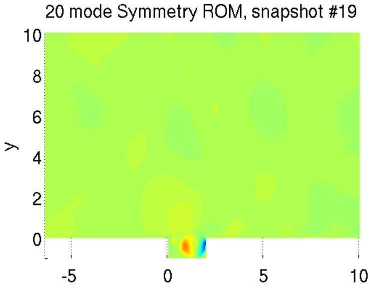

ROM based on Linearized Navier-Stokes Neglecting $\nabla\bar{\mathbf{q}}$ Terms

$$\mathbf{q}'_{,t} + \mathbf{A}_i(\bar{\mathbf{q}})\mathbf{q}'_{,i} - [\mathbf{K}_{ij}(\bar{\mathbf{q}})\mathbf{q}'_{,j}]_{,i} = \mathbf{F}$$

- Figure below shows:
  - $\circ$: t vs. $a_i(t)$ (ROM coefficients).
  - $-$: t vs. $(\mathbf{q}'_{CFD}(\mathbf{x}, t), \boldsymbol{\phi}_i(\mathbf{x}))$ (projection of snapshots onto modes).
- Movie on right shows v-velocity snapshot (top) vs. 20 mode symmetry ROM solution v (bottom).

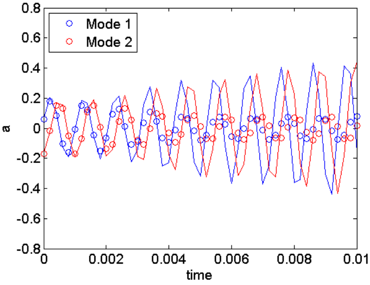

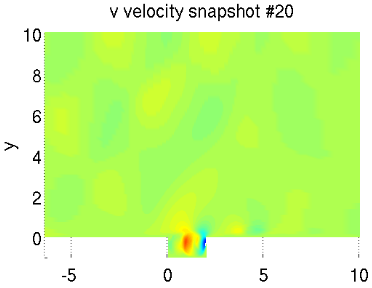

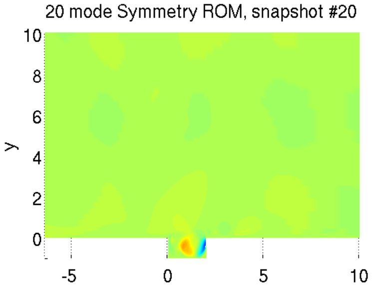

ROM based on Linearized Navier-Stokes Neglecting $\nabla\bar{\mathbf{q}}$ Terms

$$\mathbf{q}'_{,t} + \mathbf{A}_i(\bar{\mathbf{q}})\mathbf{q}'_{,i} - [\mathbf{K}_{ij}(\bar{\mathbf{q}})\mathbf{q}'_{,j}]_{,i} = \mathbf{F}$$

- Figure below shows:
  - $\circ$: t vs. $a_i(t)$ (ROM coefficients).
  - $-$: t vs. $(\mathbf{q}'_{CFD}(\mathbf{x},t), \boldsymbol{\phi}_i(\mathbf{x}))$ (projection of snapshots onto modes).
- Movie on right shows v-velocity snapshot (top) vs. 20 mode symmetry ROM solution v (bottom).

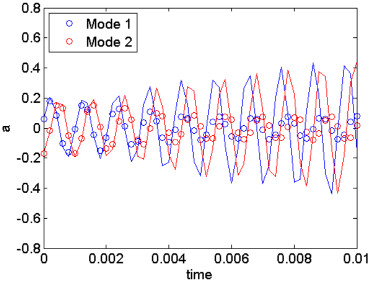

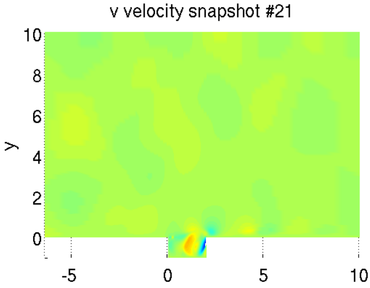

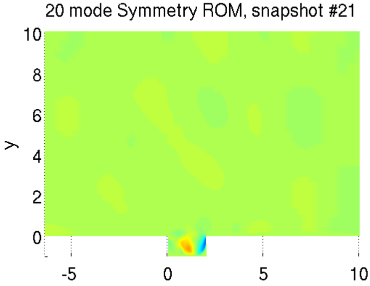

ROM based on Linearized Navier-Stokes Neglecting $\nabla\bar{\mathbf{q}}$ Terms

$$\mathbf{q}'_{,t} + \mathbf{A}_i(\bar{\mathbf{q}})\mathbf{q}'_{,i} - [\mathbf{K}_{ij}(\bar{\mathbf{q}})\mathbf{q}'_{,j}]_{,i} = \mathbf{F}$$

- Figure below shows:
  - ○: t vs. $a_i(t)$ (ROM coefficients).
  - $-$: t vs. $(\mathbf{q}'_{CFD}(\mathbf{x}, t), \boldsymbol{\phi}_i(\mathbf{x}))$ (projection of snapshots onto modes).
- Movie on right shows v-velocity snapshot (top) vs. 20 mode symmetry ROM solution v (bottom).

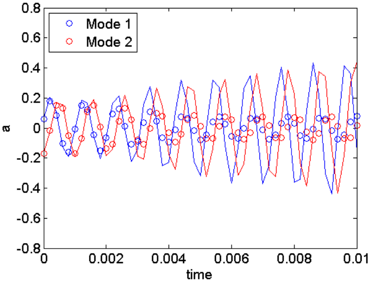

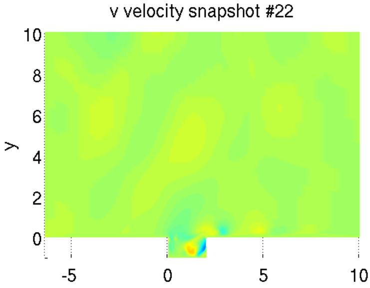

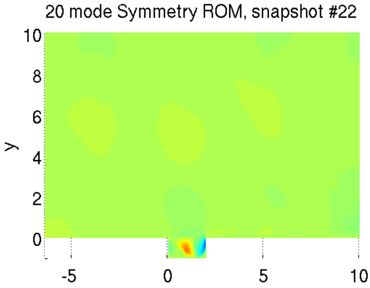

ROM based on Linearized Navier-Stokes Neglecting $\nabla\bar{\mathbf{q}}$ Terms

$$\mathbf{q}'_{,t} + \mathbf{A}_i(\bar{\mathbf{q}})\mathbf{q}'_{,i} - [\mathbf{K}_{ij}(\bar{\mathbf{q}})\mathbf{q}'_{,j}]_{,i} = \mathbf{F}$$

- Figure below shows:
  - $\circ$: t vs. $a_i(t)$ (ROM coefficients).
  - $-$: t vs. $(\mathbf{q}'_{CFD}(\mathbf{x},t), \boldsymbol{\phi}_i(\mathbf{x}))$ (projection of snapshots onto modes).
- Movie on right shows v-velocity snapshot (top) vs. 20 mode symmetry ROM solution v (bottom).

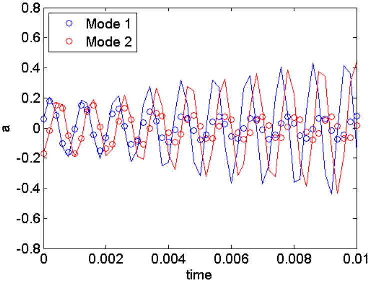

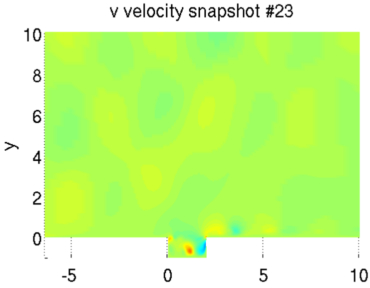

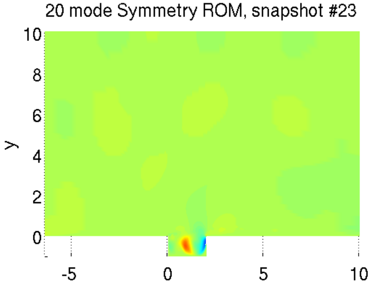

ROM based on Linearized Navier-Stokes Neglecting $\nabla\bar{\mathbf{q}}$ Terms

$$\mathbf{q}'_{,t} + \mathbf{A}_i(\bar{\mathbf{q}})\mathbf{q}'_{,i} - [\mathbf{K}_{ij}(\bar{\mathbf{q}})\mathbf{q}'_{,j}]_{,i} = \mathbf{F}$$

- Figure below shows:
  - $\circ$: t vs. $a_i(t)$ (ROM coefficients).
  - $-$: t vs. $(\mathbf{q}'_{CFD}(\mathbf{x},t), \boldsymbol{\phi}_i(\mathbf{x}))$ (projection of snapshots onto modes).
- Movie on right shows v-velocity snapshot (top) vs. 20 mode symmetry ROM solution v (bottom).

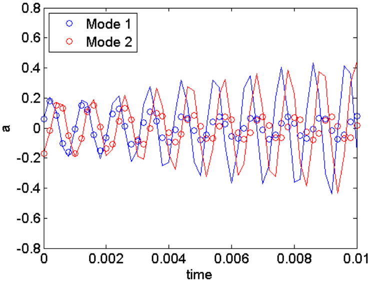

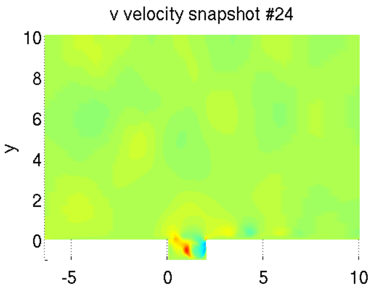

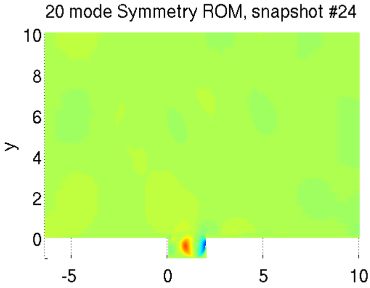

ROM based on Linearized Navier-Stokes Neglecting $\nabla\bar{\mathrm{q}}$ Terms

$$\mathbf{q}'_{,t} + \mathbf{A}_i(\bar{\mathbf{q}})\mathbf{q}'_{,i} - [\mathbf{K}_{ij}(\bar{\mathbf{q}})\mathbf{q}'_{,j}]_{,i} = \mathbf{F}$$

- Figure below shows:
  - $\circ$: t vs. $a_i(t)$ (ROM coefficients).
  - $-$: t vs. $(\mathbf{q}'_{CFD}(\mathbf{x},t), \boldsymbol{\phi}_i(\mathbf{x}))$ (projection of snapshots onto modes).
- Movie on right shows v-velocity snapshot (top) vs. 20 mode symmetry ROM solution v (bottom).

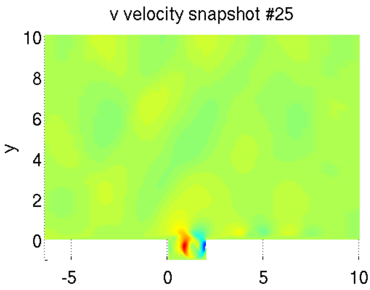

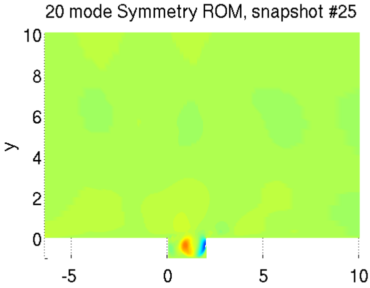

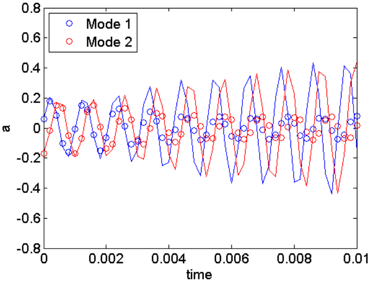

ROM based on Linearized Navier-Stokes Neglecting $\nabla\bar{\mathbf{q}}$ Terms

$$\mathbf{q}'_{,t} + \mathbf{A}_i(\bar{\mathbf{q}})\mathbf{q}'_{,i} - [\mathbf{K}_{ij}(\bar{\mathbf{q}})\mathbf{q}'_{,j}]_{,i} = \mathbf{F}$$

- Figure below shows:
  - $\circ$: t vs. $a_i(t)$ (ROM coefficients).
  - $-$: t vs. $(\mathbf{q}'_{CFD}(\mathbf{x},t), \boldsymbol{\phi}_i(\mathbf{x}))$ (projection of snapshots onto modes).
- Movie on right shows v-velocity snapshot (top) vs. 20 mode symmetry ROM solution v (bottom).

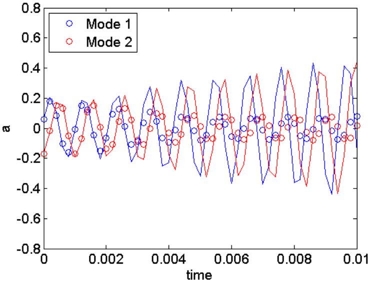

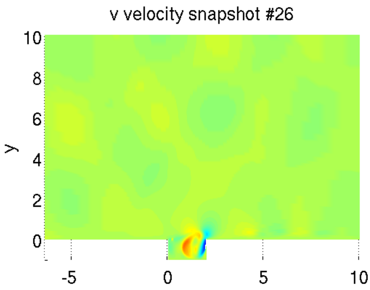

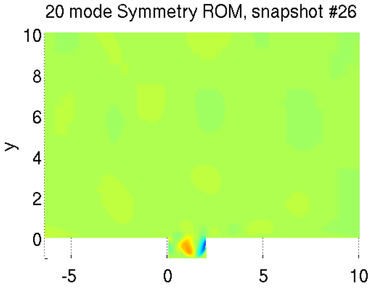

ROM based on Linearized Navier-Stokes Neglecting $\nabla\bar{\mathbf{q}}$ Terms

$$\mathbf{q}'_{,t} + \mathbf{A}_i(\bar{\mathbf{q}})\mathbf{q}'_{,i} - [\mathbf{K}_{ij}(\bar{\mathbf{q}})\mathbf{q}'_{,j}]_{,i} = \mathbf{F}$$

- Figure below shows:
  - $\circ$: t vs. $a_i(t)$ (ROM coefficients).
  - $-$: t vs. $(\mathbf{q}'_{CFD}(\mathbf{x},t), \boldsymbol{\phi}_i(\mathbf{x}))$ (projection of snapshots onto modes).
- Movie on right shows v-velocity snapshot (top) vs. 20 mode symmetry ROM solution v (bottom).

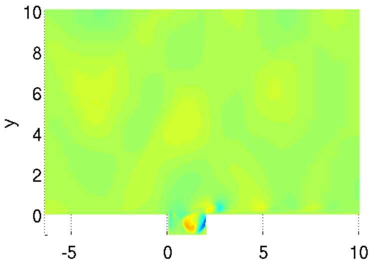

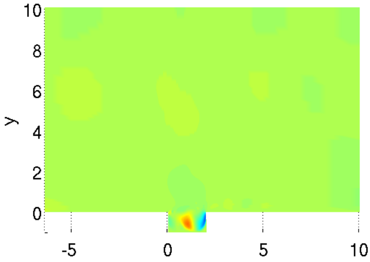

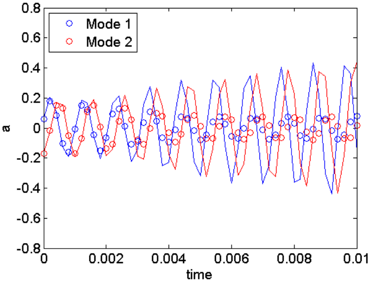

ROM based on Linearized Navier-Stokes Neglecting $\nabla\bar{\mathbf{q}}$ Terms

$$\mathbf{q}'_{,t} + \mathbf{A}_i(\bar{\mathbf{q}})\mathbf{q}'_{,i} - [\mathbf{K}_{ij}(\bar{\mathbf{q}})\mathbf{q}'_{,j}]_{,i} = \mathbf{F}$$

- Figure below shows:
  - $\circ$: t vs. $a_i(t)$ (ROM coefficients).
  - $-$: t vs. $(\mathbf{q}'_{CFD}(\mathbf{x}, t), \boldsymbol{\phi}_i(\mathbf{x}))$ (projection of snapshots onto modes).
- Movie on right shows v-velocity snapshot (top) vs. 20 mode symmetry ROM solution v (bottom).

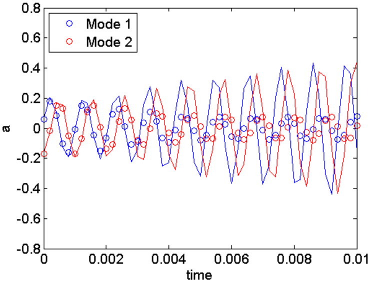

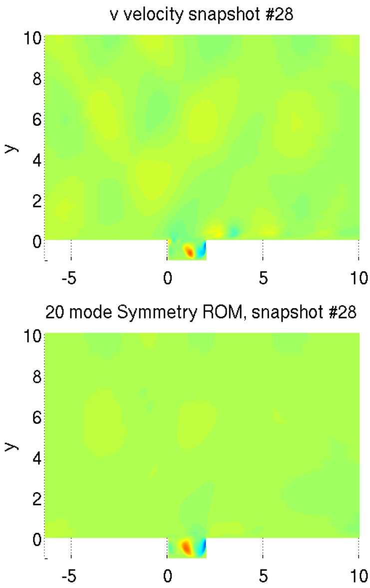

ROM based on Linearized Navier-Stokes Neglecting $\nabla\bar{\mathbf{q}}$ Terms

$$\mathbf{q}'_{,t} + \mathbf{A}_i(\bar{\mathbf{q}})\mathbf{q}'_{,i} - [\mathbf{K}_{ij}(\bar{\mathbf{q}})\mathbf{q}'_{,j}]_{,i} = \mathbf{F}$$

- Figure below shows:
  - $\circ$: t vs. $a_i(t)$ (ROM coefficients).
  - $-$: t vs. $(\mathbf{q}'_{CFD}(\mathbf{x},t), \boldsymbol{\phi}_i(\mathbf{x}))$ (projection of snapshots onto modes).
- Movie on right shows v-velocity snapshot (top) vs. 20 mode symmetry ROM solution v (bottom).

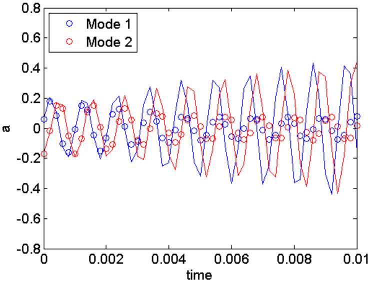

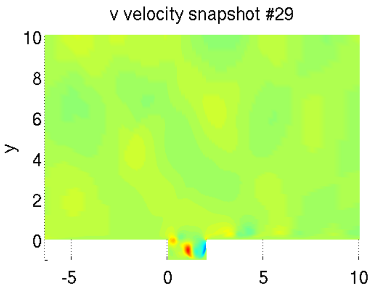

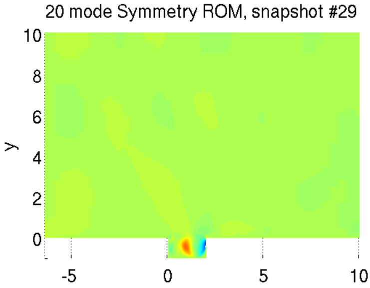

ROM based on Linearized Navier-Stokes Neglecting $\nabla\bar{\mathrm{q}}$ Terms

$$\mathbf{q}'_{,t} + \mathbf{A}_i(\bar{\mathbf{q}})\mathbf{q}'_{,i} - [\mathbf{K}_{ij}(\bar{\mathbf{q}})\mathbf{q}'_{,j}]_{,i} = \mathbf{F}$$

- Figure below shows:
  - $\circ$: t vs. $a_i(t)$ (ROM coefficients).
  - $-$: t vs. $(\mathbf{q}'_{CFD}(\mathbf{x}, t), \boldsymbol{\phi}_i(\mathbf{x}))$ (projection of snapshots onto modes).
- Movie on right shows v-velocity snapshot (top) vs. 20 mode symmetry ROM solution v (bottom).

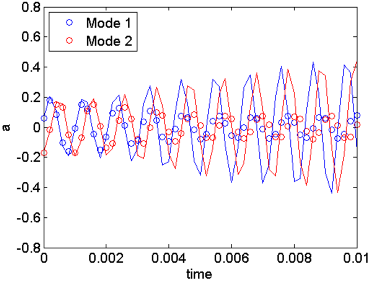

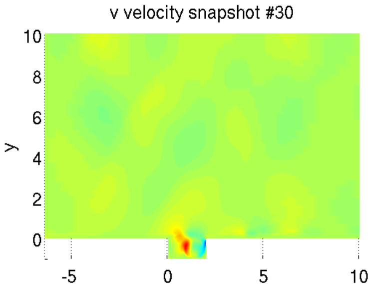

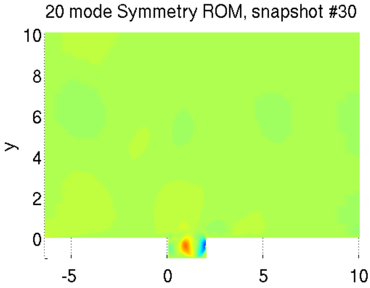

ROM based on Linearized Navier-Stokes Neglecting $\nabla\bar{\mathbf{q}}$ Terms

$$\mathbf{q}'_{,t} + \mathbf{A}_i(\bar{\mathbf{q}})\mathbf{q}'_{,i} - [\mathbf{K}_{ij}(\bar{\mathbf{q}})\mathbf{q}'_{,j}]_{,i} = \mathbf{F}$$

- Figure below shows:
  - $\circ$: t vs. $a_i(t)$ (ROM coefficients).
  - $-$: t vs. $(\mathbf{q}'_{CFD}(\mathbf{x},t), \boldsymbol{\phi}_i(\mathbf{x}))$ (projection of snapshots onto modes).
- Movie on right shows v-velocity snapshot (top) vs. 20 mode symmetry ROM solution v (bottom).

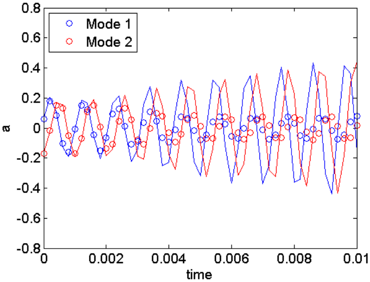

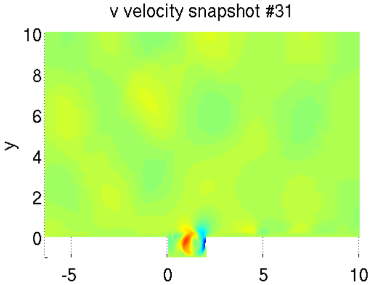

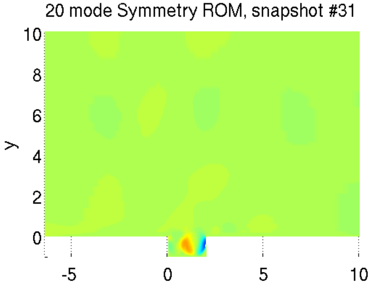

ROM based on Linearized Navier-Stokes Neglecting $\nabla\bar{\mathbf{q}}$ Terms

$$\mathbf{q}'_{,t} + \mathbf{A}_i(\bar{\mathbf{q}})\mathbf{q}'_{,i} - [\mathbf{K}_{ij}(\bar{\mathbf{q}})\mathbf{q}'_{,j}]_{,i} = \mathbf{F}$$

- Figure below shows:
  - $\circ$: t vs. $a_i(t)$ (ROM coefficients).
  - $-$: t vs. $(\mathbf{q}'_{CFD}(\mathbf{x},t), \boldsymbol{\phi}_i(\mathbf{x}))$ (projection of snapshots onto modes).
- Movie on right shows v-velocity snapshot (top) vs. 20 mode symmetry ROM solution v (bottom).

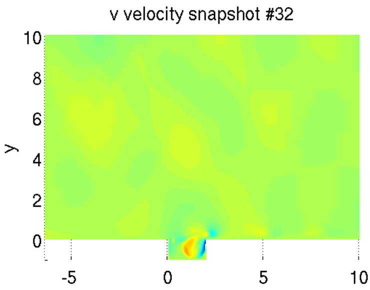

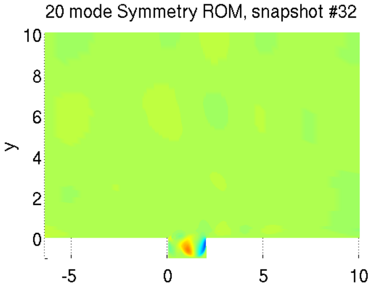

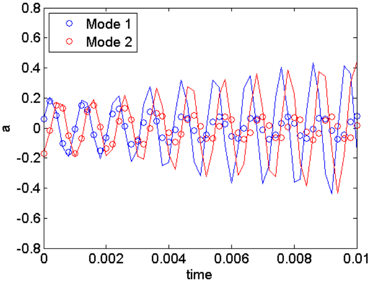

ROM based on Linearized Navier-Stokes Neglecting $\nabla\bar{\mathbf{q}}$ Terms

$$\mathbf{q}'_{,t} + \mathbf{A}_i(\bar{\mathbf{q}})\mathbf{q}'_{,i} - [\mathbf{K}_{ij}(\bar{\mathbf{q}})\mathbf{q}'_{,j}]_{,i} = \mathbf{F}$$

- Figure below shows:
  - ○: t vs. $a_i(t)$ (ROM coefficients).
  - $-$: t vs. $(\mathbf{q}'_{CFD}(\mathbf{x},t), \boldsymbol{\phi}_i(\mathbf{x}))$ (projection of snapshots onto modes).
- Movie on right shows v-velocity snapshot (top) vs. 20 mode symmetry ROM solution v (bottom).

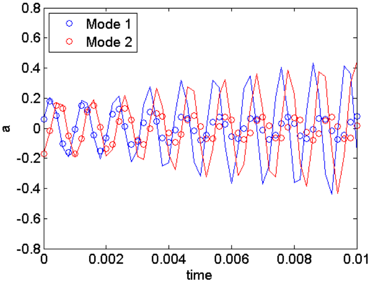

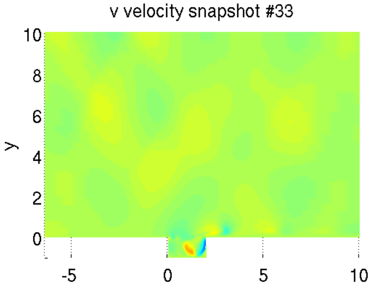

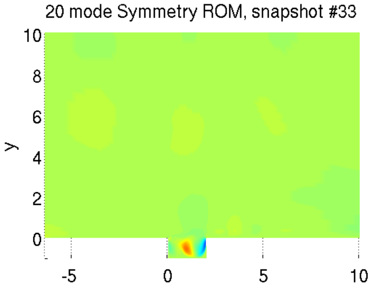

ROM based on Linearized Navier-Stokes Neglecting $\nabla\bar{\mathbf{q}}$ Terms

$$\mathbf{q}'_{,t} + \mathbf{A}_i(\bar{\mathbf{q}})\mathbf{q}'_{,i} - [\mathbf{K}_{ij}(\bar{\mathbf{q}})\mathbf{q}'_{,j}]_{,i} = \mathbf{F}$$

- Figure below shows:
  - ○: t vs. $a_i(t)$ (ROM coefficients).
  - $-$: t vs. $(\mathbf{q}'_{CFD}(\mathbf{x}, t), \boldsymbol{\phi}_i(\mathbf{x}))$ (projection of snapshots onto modes).
- Movie on right shows v-velocity snapshot (top) vs. 20 mode symmetry ROM solution v (bottom).

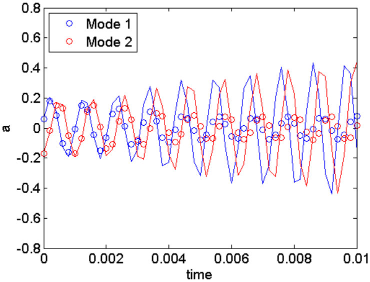

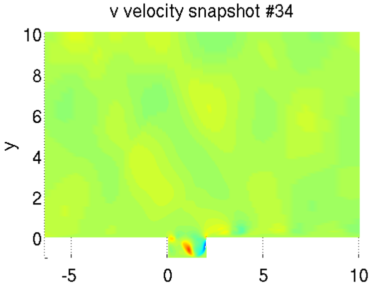

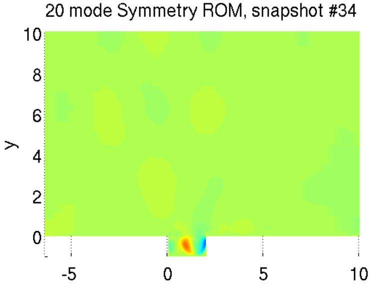

ROM based on Linearized Navier-Stokes Neglecting $\nabla\bar{\mathbf{q}}$ Terms

$$\mathbf{q}'_{,t} + \mathbf{A}_i(\bar{\mathbf{q}})\mathbf{q}'_{,i} - [\mathbf{K}_{ij}(\bar{\mathbf{q}})\mathbf{q}'_{,j}]_{,i} = \mathbf{F}$$

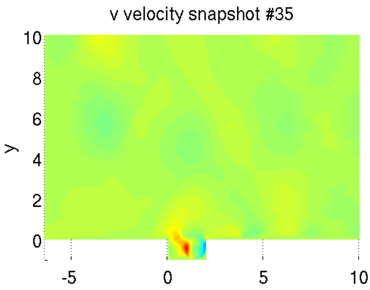

- Figure below shows:
  - $\circ$: t vs. $a_i(t)$ (ROM coefficients).
  - $-$: t vs. $(\mathbf{q}'_{CFD}(\mathbf{x}, t), \boldsymbol{\phi}_i(\mathbf{x}))$ (projection of snapshots onto modes).
- Movie on right shows v-velocity snapshot (top) vs. 20 mode symmetry ROM solution v (bottom).

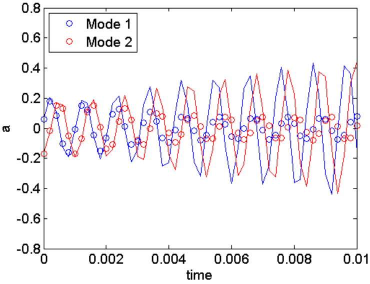

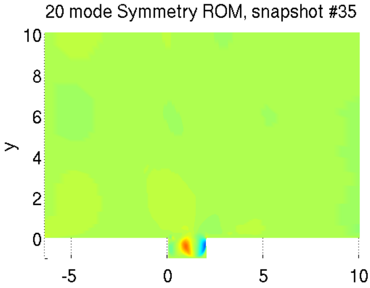

ROM based on Linearized Navier-Stokes Neglecting $\nabla\bar{\mathbf{q}}$ Terms

$$\mathbf{q}'_{,t} + \mathbf{A}_i(\bar{\mathbf{q}})\mathbf{q}'_{,i} - [\mathbf{K}_{ij}(\bar{\mathbf{q}})\mathbf{q}'_{,j}]_{,i} = \mathbf{F}$$

- Figure below shows:
  - ○: t vs. $a_i(t)$ (ROM coefficients).
  - $-$: t vs. $(\mathbf{q}'_{CFD}(\mathbf{x},t), \boldsymbol{\phi}_i(\mathbf{x}))$ (projection of snapshots onto modes).
- Movie on right shows v-velocity snapshot (top) vs. 20 mode symmetry ROM solution v (bottom).

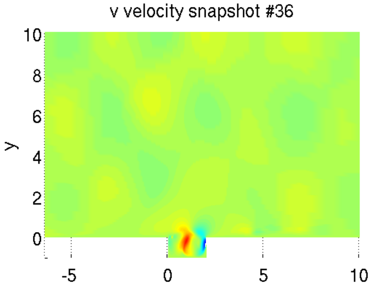

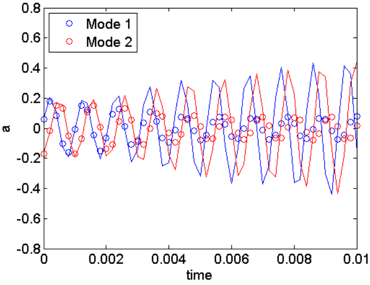

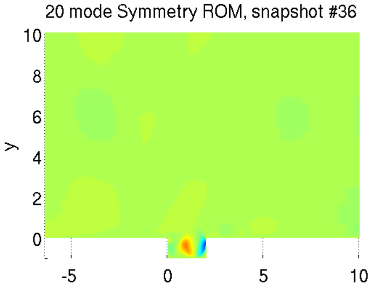

ROM based on Linearized Navier-Stokes Neglecting $\nabla\bar{\mathbf{q}}$ Terms

$$\mathbf{q}'_{,t} + \mathbf{A}_i(\bar{\mathbf{q}})\mathbf{q}'_{,i} - [\mathbf{K}_{ij}(\bar{\mathbf{q}})\mathbf{q}'_{,j}]_{,i} = \mathbf{F}$$

- Figure below shows:
  - $\circ$: t vs. $a_i(t)$ (ROM coefficients).
  - $-$: t vs. $(\mathbf{q}'_{CFD}(\mathbf{x},t), \boldsymbol{\phi}_i(\mathbf{x}))$ (projection of snapshots onto modes).
- Movie on right shows v-velocity snapshot (top) vs. 20 mode symmetry ROM solution v (bottom).

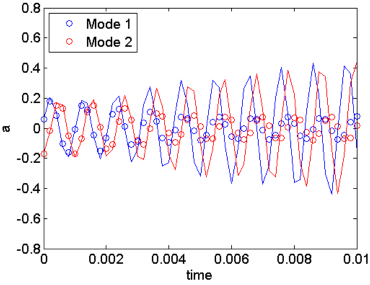

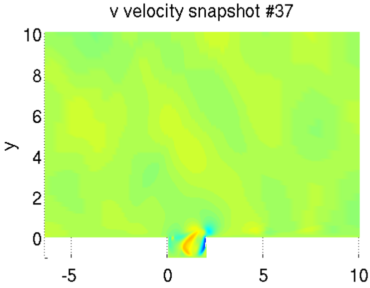

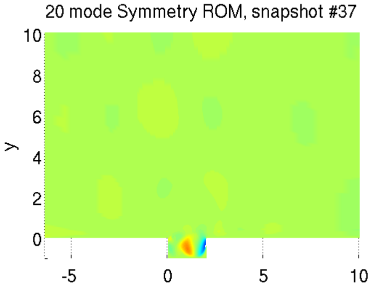

ROM based on Linearized Navier-Stokes Neglecting $\nabla\bar{\mathbf{q}}$ Terms

$$\mathbf{q}'_{,t} + \mathbf{A}_i(\bar{\mathbf{q}})\mathbf{q}'_{,i} - [\mathbf{K}_{ij}(\bar{\mathbf{q}})\mathbf{q}'_{,j}]_{,i} = \mathbf{F}$$

- Figure below shows:
  - $\circ$: t vs. $a_i(t)$ (ROM coefficients).
  - $-$: t vs. $(\mathbf{q}'_{CFD}(\mathbf{x},t), \boldsymbol{\phi}_i(\mathbf{x}))$ (projection of snapshots onto modes).
- Movie on right shows v-velocity snapshot (top) vs. 20 mode symmetry ROM solution v (bottom).

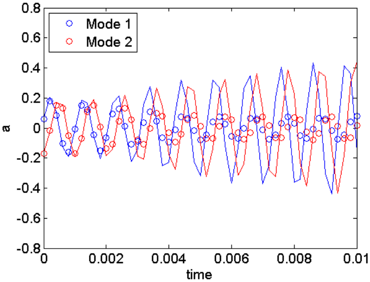

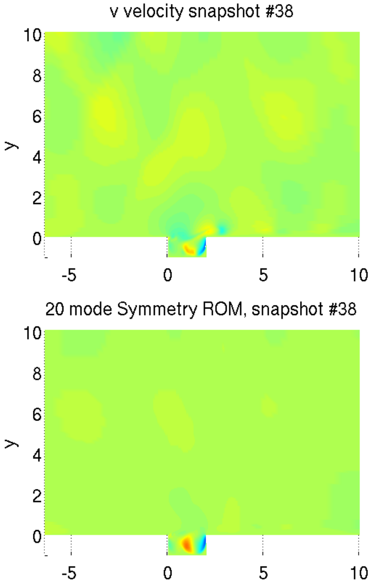

ROM based on Linearized Navier-Stokes Neglecting $\nabla\bar{\mathrm{q}}$ Terms

$$\mathbf{q}'_{,t} + \mathbf{A}_i(\bar{\mathbf{q}})\mathbf{q}'_{,i} - [\mathbf{K}_{ij}(\bar{\mathbf{q}})\mathbf{q}'_{,j}]_{,i} = \mathbf{F}$$

- Figure below shows:
  - $\circ$: t vs. $a_i(t)$ (ROM coefficients).
  - $-$: t vs. $(\mathbf{q}'_{CFD}(\mathbf{x},t), \boldsymbol{\phi}_i(\mathbf{x}))$ (projection of snapshots onto modes).
- Movie on right shows v-velocity snapshot (top) vs. 20 mode symmetry ROM solution v (bottom).

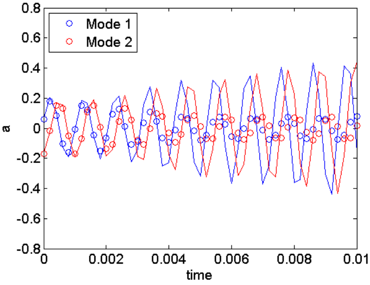

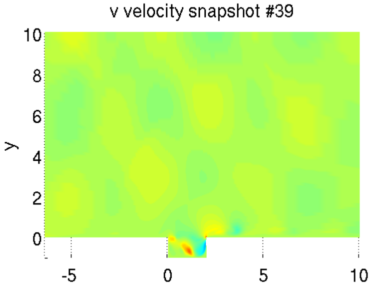

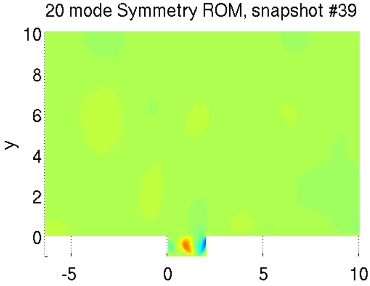

ROM based on Linearized Navier-Stokes Neglecting $\nabla\bar{\mathbf{q}}$ Terms

$$\mathbf{q}'_{,t} + \mathbf{A}_i(\bar{\mathbf{q}})\mathbf{q}'_{,i} - [\mathbf{K}_{ij}(\bar{\mathbf{q}})\mathbf{q}'_{,j}]_{,i} = \mathbf{F}$$

- Figure below shows:
  - ○: t vs. $a_i(t)$ (ROM coefficients).
  - $-$: t vs. $(\mathbf{q}'_{CFD}(\mathbf{x},t), \boldsymbol{\phi}_i(\mathbf{x}))$ (projection of snapshots onto modes).
- Movie on right shows v-velocity snapshot (top) vs. 20 mode symmetry ROM solution v (bottom).

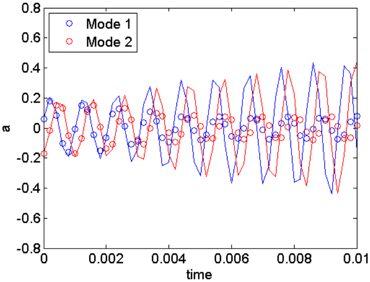

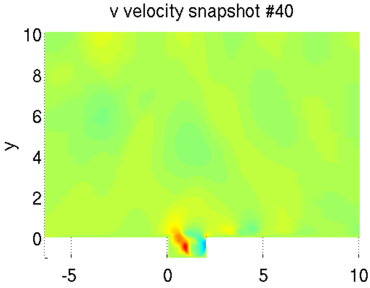

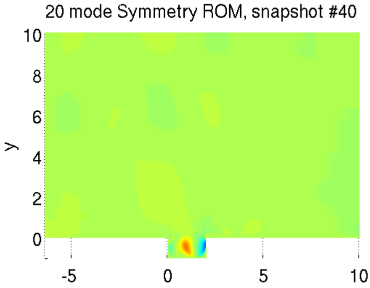

ROM based on Linearized Navier-Stokes Neglecting $\nabla\bar{\mathrm{q}}$ Terms

$$\mathbf{q}'_{,t} + \mathbf{A}_i(\bar{\mathbf{q}})\mathbf{q}'_{,i} - [\mathbf{K}_{ij}(\bar{\mathbf{q}})\mathbf{q}'_{,j}]_{,i} = \mathbf{F}$$

- Figure below shows:
  - $\circ$: t vs. $a_i(t)$ (ROM coefficients).
  - $-$: t vs. $(\mathbf{q}'_{CFD}(\mathbf{x},t), \boldsymbol{\phi}_i(\mathbf{x}))$ (projection of snapshots onto modes).
- Movie on right shows v-velocity snapshot (top) vs. 20 mode symmetry ROM solution v (bottom).

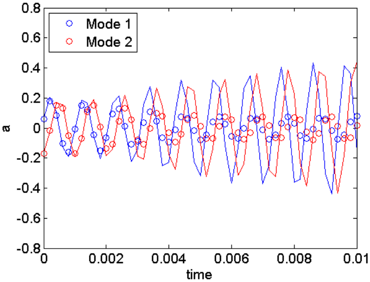

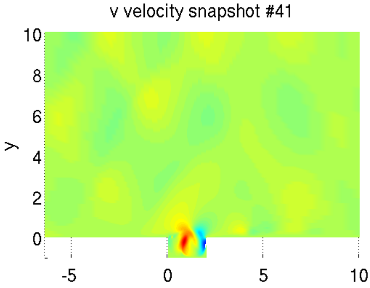

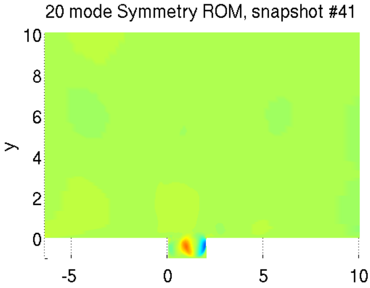

ROM based on Linearized Navier-Stokes Neglecting $\nabla\bar{\mathrm{q}}$ Terms

$$\mathbf{q}'_{,t} + \mathbf{A}_i(\bar{\mathbf{q}})\mathbf{q}'_{,i} - [\mathbf{K}_{ij}(\bar{\mathbf{q}})\mathbf{q}'_{,j}]_{,i} = \mathbf{F}$$

- Figure below shows:
  - $\circ$: t vs. $a_i(t)$ (ROM coefficients).
  - $-$: t vs. $(\mathbf{q}'_{CFD}(\mathbf{x},t), \boldsymbol{\phi}_i(\mathbf{x}))$ (projection of snapshots onto modes).
- Movie on right shows v-velocity snapshot (top) vs. 20 mode symmetry ROM solution v (bottom).

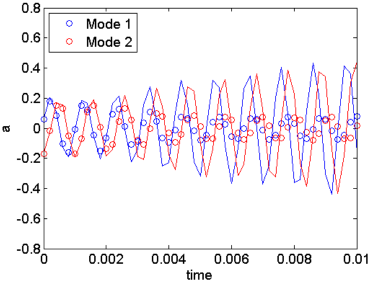

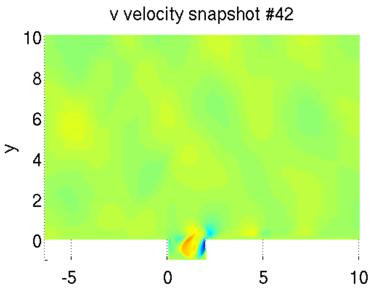

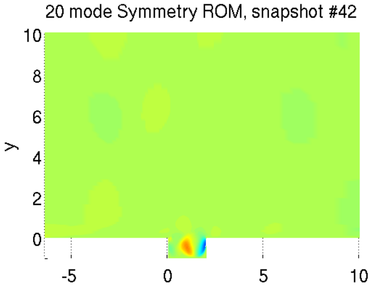

ROM based on Linearized Navier-Stokes Neglecting $\nabla\bar{\mathrm{q}}$ Terms

$$\mathbf{q}'_{,t} + \mathbf{A}_i(\bar{\mathbf{q}})\mathbf{q}'_{,i} - [\mathbf{K}_{ij}(\bar{\mathbf{q}})\mathbf{q}'_{,j}]_{,i} = \mathbf{F}$$

- Figure below shows:
  - $\circ$: t vs. $a_i(t)$ (ROM coefficients).
  - $-$: t vs. $(\mathbf{q}'_{CFD}(\mathbf{x},t), \boldsymbol{\phi}_i(\mathbf{x}))$ (projection of snapshots onto modes).
- Movie on right shows v-velocity snapshot (top) vs. 20 mode symmetry ROM solution v (bottom).

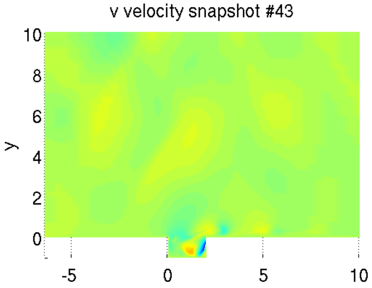

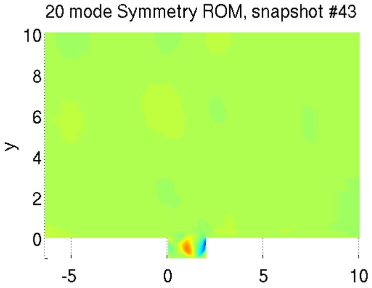

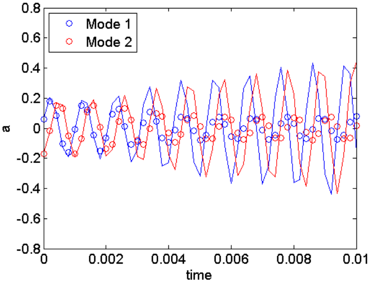

ROM based on Linearized Navier-Stokes Neglecting $\nabla\bar{\mathbf{q}}$ Terms

$$\mathbf{q}'_{,t} + \mathbf{A}_i(\bar{\mathbf{q}})\mathbf{q}'_{,i} - [\mathbf{K}_{ij}(\bar{\mathbf{q}})\mathbf{q}'_{,j}]_{,i} = \mathbf{F}$$

- Figure below shows:
  - $\circ$: t vs. $a_i(t)$ (ROM coefficients).
  - $-$: t vs. $(\mathbf{q}'_{CFD}(\mathbf{x},t), \boldsymbol{\phi}_i(\mathbf{x}))$ (projection of snapshots onto modes).
- Movie on right shows v-velocity snapshot (top) vs. 20 mode symmetry ROM solution v (bottom).

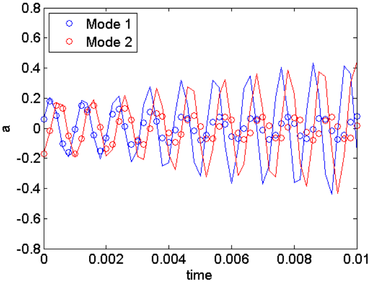

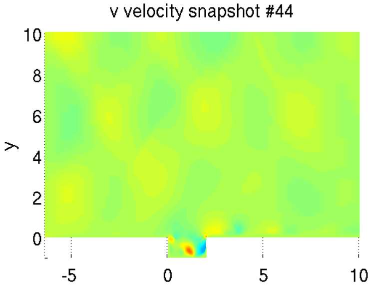

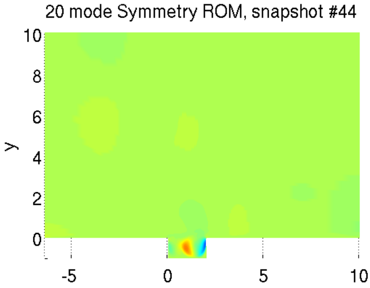

ROM based on Linearized Navier-Stokes Neglecting $\nabla\bar{\mathbf{q}}$ Terms

$$\mathbf{q}'_{,t} + \mathbf{A}_i(\bar{\mathbf{q}})\mathbf{q}'_{,i} - [\mathbf{K}_{ij}(\bar{\mathbf{q}})\mathbf{q}'_{,j}]_{,i} = \mathbf{F}$$

- Figure below shows:
  - $\circ$: t vs. $a_i(t)$ (ROM coefficients).
  - $-$: t vs. $(\mathbf{q}'_{CFD}(\mathbf{x},t), \boldsymbol{\phi}_i(\mathbf{x}))$ (projection of snapshots onto modes).
- Movie on right shows v-velocity snapshot (top) vs. 20 mode symmetry ROM solution v (bottom).

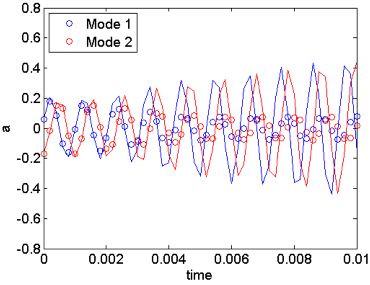

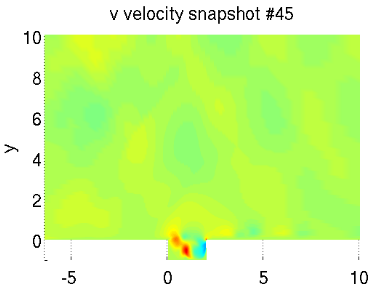

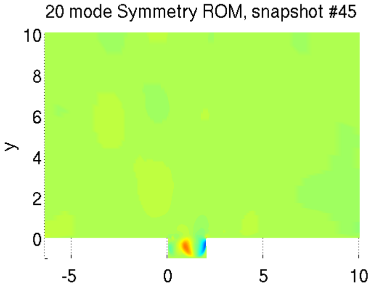

ROM based on Linearized Navier-Stokes Neglecting $\nabla\bar{\mathrm{q}}$ Terms

$$\mathbf{q}'_{,t} + \mathbf{A}_i(\bar{\mathbf{q}})\mathbf{q}'_{,i} - [\mathbf{K}_{ij}(\bar{\mathbf{q}})\mathbf{q}'_{,j}]_{,i} = \mathbf{F}$$

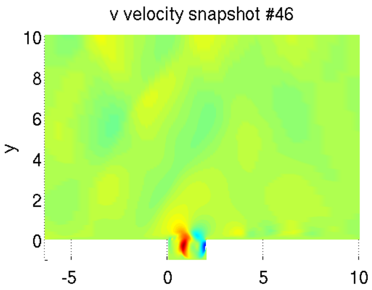

- Figure below shows:
  - $\circ$: t vs. $a_i(t)$ (ROM coefficients).
  - $-$: t vs. $(\mathbf{q}'_{CFD}(\mathbf{x},t), \boldsymbol{\phi}_i(\mathbf{x}))$ (projection of snapshots onto modes).
- Movie on right shows v-velocity snapshot (top) vs. 20 mode symmetry ROM solution v (bottom).

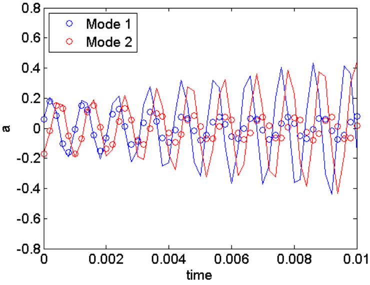

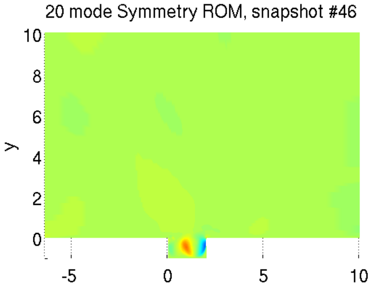

ROM based on Linearized Navier-Stokes Neglecting $\nabla\bar{\mathbf{q}}$ Terms

$$\mathbf{q}'_{,t} + \mathbf{A}_i(\bar{\mathbf{q}})\mathbf{q}'_{,i} - [\mathbf{K}_{ij}(\bar{\mathbf{q}})\mathbf{q}'_{,j}]_{,i} = \mathbf{F}$$

- Figure below shows:
  - ○: t vs. $a_i(t)$ (ROM coefficients).
  - −: t vs. $(\mathbf{q}'_{CFD}(\mathbf{x},t), \boldsymbol{\phi}_i(\mathbf{x}))$ (projection of snapshots onto modes).
- Movie on right shows v-velocity snapshot (top) vs. 20 mode symmetry ROM solution v (bottom).

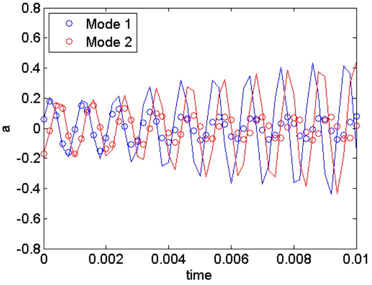

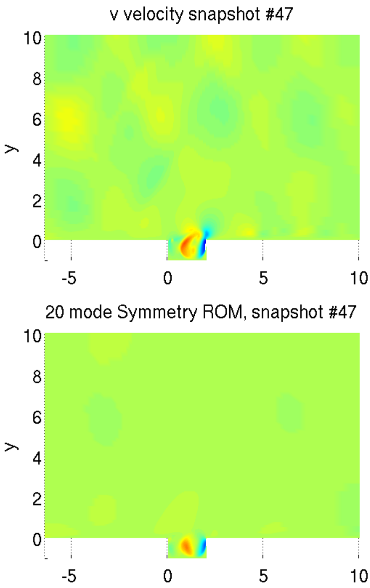

ROM based on Linearized Navier-Stokes Neglecting $\nabla\bar{\mathrm{q}}$ Terms

$$\mathbf{q}'_{,t} + \mathbf{A}_i(\bar{\mathbf{q}})\mathbf{q}'_{,i} - [\mathbf{K}_{ij}(\bar{\mathbf{q}})\mathbf{q}'_{,j}]_{,i} = \mathbf{F}$$

- Figure below shows:
  - ○: t vs. $a_i(t)$ (ROM coefficients).
  - $-$: t vs. $(\mathbf{q}'_{CFD}(\mathbf{x},t), \boldsymbol{\phi}_i(\mathbf{x}))$ (projection of snapshots onto modes).
- Movie on right shows v-velocity snapshot (top) vs. 20 mode symmetry ROM solution v (bottom).

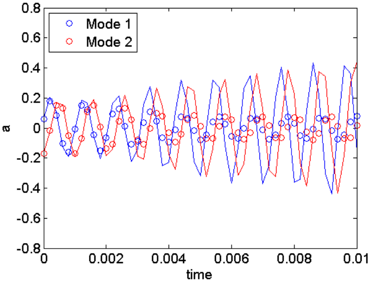

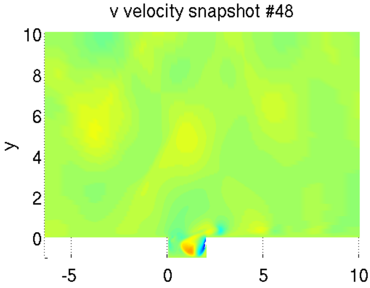

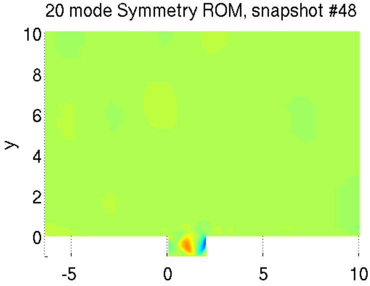

ROM based on Linearized Navier-Stokes Neglecting $\nabla\bar{\mathrm{q}}$ Terms

$$\mathbf{q}'_{,t} + \mathbf{A}_i(\bar{\mathbf{q}})\mathbf{q}'_{,i} - [\mathbf{K}_{ij}(\bar{\mathbf{q}})\mathbf{q}'_{,j}]_{,i} = \mathbf{F}$$

- Figure below shows:
  - $\circ$: t vs. $a_i(t)$ (ROM coefficients).
  - $-$: t vs. $(\mathbf{q}'_{CFD}(\mathbf{x},t), \boldsymbol{\phi}_i(\mathbf{x}))$ (projection of snapshots onto modes).
- Movie on right shows v-velocity snapshot (top) vs. 20 mode symmetry ROM solution v (bottom).

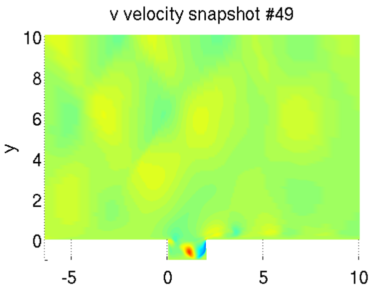

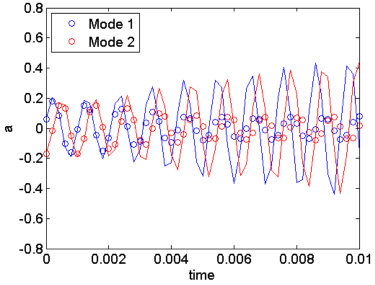

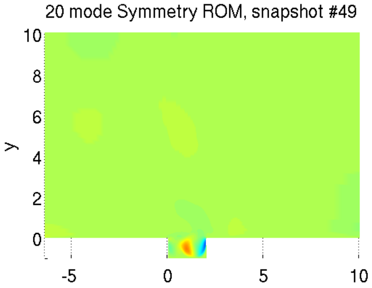

ROM based on Linearized Navier-Stokes Neglecting $\nabla\bar{\mathbf{q}}$ Terms

$$\mathbf{q}'_{,t} + \mathbf{A}_i(\bar{\mathbf{q}})\mathbf{q}'_{,i} - [\mathbf{K}_{ij}(\bar{\mathbf{q}})\mathbf{q}'_{,j}]_{,i} = \mathbf{F}$$

- Figure below shows:
  - $\circ$: t vs. $a_i(t)$ (ROM coefficients).
  - $-$: t vs. $(\mathbf{q}'_{CFD}(\mathbf{x},t), \boldsymbol{\phi}_i(\mathbf{x}))$ (projection of snapshots onto modes).
- Movie on right shows v-velocity snapshot (top) vs. 20 mode symmetry ROM solution v (bottom).

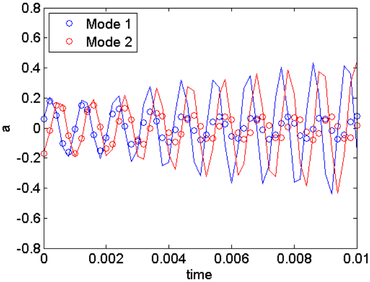

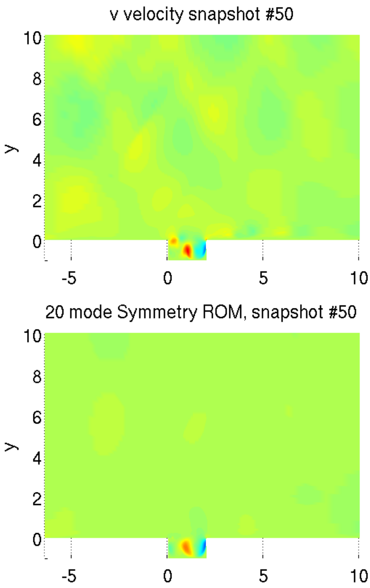

ROM based on Linearized Navier-Stokes Neglecting $\nabla \bar{\mathrm{q}}$ Terms

ROM based on Linearized Navier-Stokes Retaining $\nabla\bar{\mathbf{q}}$ Terms

$$\mathbf{q}'_{,t} + [\mathbf{A}_i(\bar{\mathbf{q}}) - \mathbf{K}_i^{vw}(\nabla\bar{\mathbf{q}})]\mathbf{q}'_{,i} - [\mathbf{K}_{ij}(\bar{\mathbf{q}})\mathbf{q}'_{,j}]_{,i}$$
$$+\mathbf{C}(\nabla\bar{\mathbf{q}})\mathbf{q}' = \mathbf{F}$$

- Figure below shows:
  - $\circ$: t vs. $a_i(t)$ (ROM coefficients).
  - $-$: t vs. $(\mathbf{q}'_{CFD}(\mathbf{x}, t), \boldsymbol{\phi}_i(\mathbf{x}))$ (projection of snapshots onto modes).
- Movie on right shows v-velocity snapshot (top) vs. 20 mode symmetry ROM solution v (bottom).

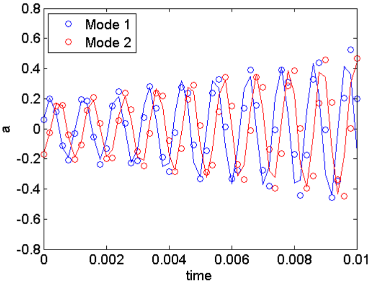

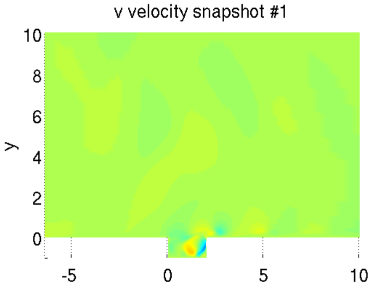

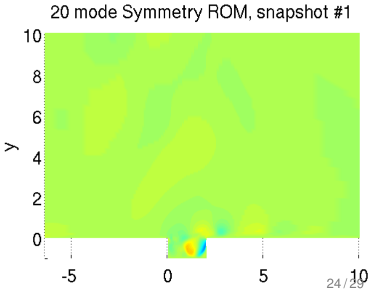

ROM based on Linearized Navier-Stokes Retaining $\nabla\bar{\mathbf{q}}$ Terms

$$\mathbf{q}'_{,t} + [\mathbf{A}_i(\bar{\mathbf{q}}) - \mathbf{K}_i^{vw}(\nabla\bar{\mathbf{q}})]\mathbf{q}'_{,i} - [\mathbf{K}_{ij}(\bar{\mathbf{q}})\mathbf{q}'_{,j}]_{,i}$$
$$+\mathbf{C}(\nabla\bar{\mathbf{q}})\mathbf{q}' = \mathbf{F}$$

- Figure below shows:
  - ○: t vs. $a_i(t)$ (ROM coefficients).
  - $-$: t vs. $(\mathbf{q}'_{CFD}(\mathbf{x}, t), \boldsymbol{\phi}_i(\mathbf{x}))$ (projection of snapshots onto modes).
- Movie on right shows v-velocity snapshot (top) vs. 20 mode symmetry ROM solution v (bottom).

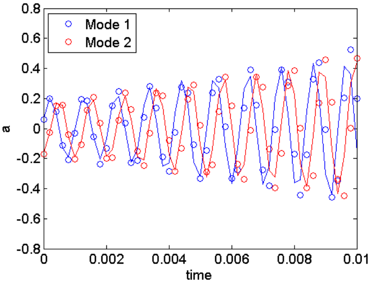

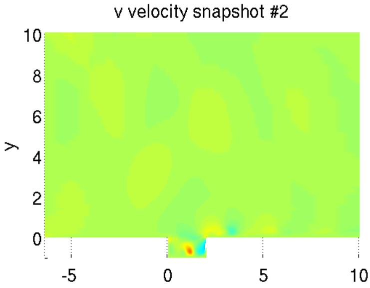

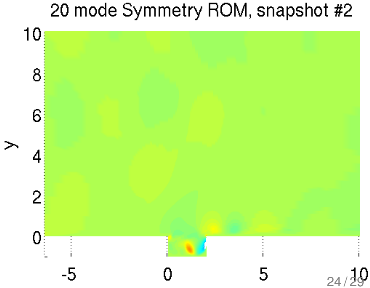

ROM based on Linearized Navier-Stokes Retaining $\nabla\bar{\mathbf{q}}$ Terms

$$\mathbf{q}'_{,t} + [\mathbf{A}_i(\bar{\mathbf{q}}) - \mathbf{K}_i^{vw}(\nabla\bar{\mathbf{q}})]\mathbf{q}'_{,i} - [\mathbf{K}_{ij}(\bar{\mathbf{q}})\mathbf{q}'_{,j}]_{,i} + \mathbf{C}(\nabla\bar{\mathbf{q}})\mathbf{q}' = \mathbf{F}$$

- Figure below shows:
  - $\circ$: t vs. $a_i(t)$ (ROM coefficients).
  - $-$: t vs. $(\mathbf{q}'_{CFD}(\mathbf{x},t), \boldsymbol{\phi}_i(\mathbf{x}))$ (projection of snapshots onto modes).
- Movie on right shows v-velocity snapshot (top) vs. 20 mode symmetry ROM solution v (bottom).

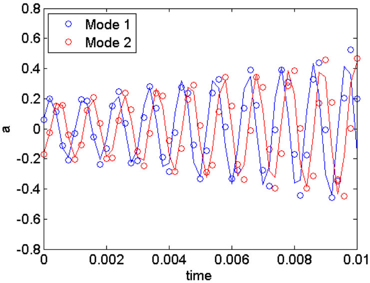

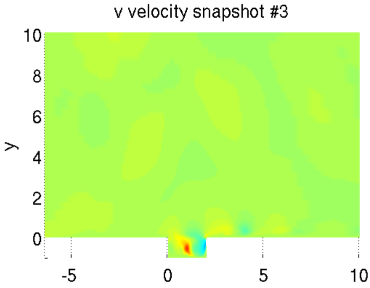

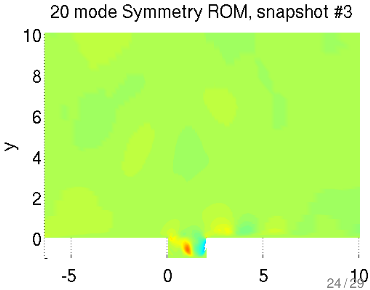

ROM based on Linearized Navier-Stokes Retaining $\nabla\bar{\mathbf{q}}$ Terms

$$\mathbf{q}'_{,t} + [\mathbf{A}_i(\bar{\mathbf{q}}) - \mathbf{K}_i^{vw}(\nabla\bar{\mathbf{q}})]\mathbf{q}'_{,i} - [\mathbf{K}_{ij}(\bar{\mathbf{q}})\mathbf{q}'_{,j}]_{,i} + \mathbf{C}(\nabla\bar{\mathbf{q}})\mathbf{q}' = \mathbf{F}$$

- Figure below shows:
  - $\circ$: t vs. $a_i(t)$ (ROM coefficients).
  - $-$: t vs. $(\mathbf{q}'_{CFD}(\mathbf{x},t), \boldsymbol{\phi}_i(\mathbf{x}))$ (projection of snapshots onto modes).
- Movie on right shows v-velocity snapshot (top) vs. 20 mode symmetry ROM solution v (bottom).

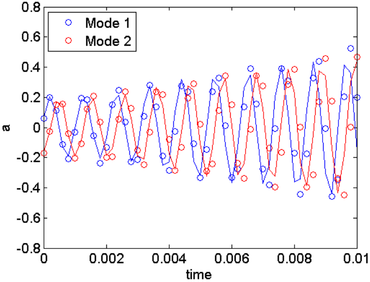

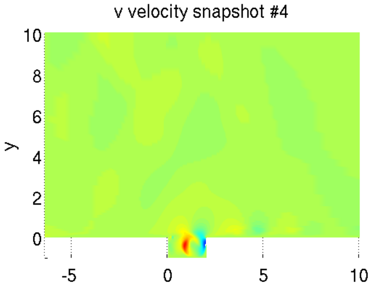

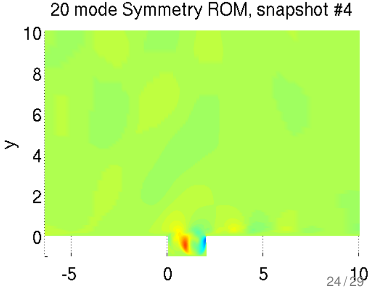

ROM based on Linearized Navier-Stokes Retaining $\nabla\bar{\mathbf{q}}$ Terms

$$\mathbf{q}'_{,t} + [\mathbf{A}_i(\bar{\mathbf{q}}) - \mathbf{K}_i^{vw}(\nabla\bar{\mathbf{q}})]\mathbf{q}'_{,i} - [\mathbf{K}_{ij}(\bar{\mathbf{q}})\mathbf{q}'_{,j}]_{,i}$$
$$+\mathbf{C}(\nabla\bar{\mathbf{q}})\mathbf{q}' = \mathbf{F}$$

- Figure below shows:
  - $\circ$: t vs. $a_i(t)$ (ROM coefficients).
  - $-$: t vs. $(\mathbf{q}'_{CFD}(\mathbf{x}, t), \boldsymbol{\phi}_i(\mathbf{x}))$ (projection of snapshots onto modes).
- Movie on right shows v-velocity snapshot (top) vs. 20 mode symmetry ROM solution v (bottom).

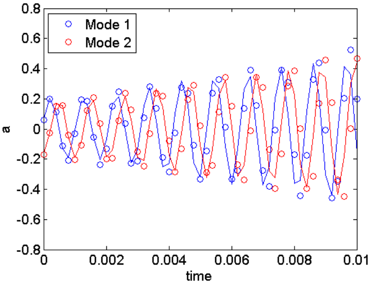

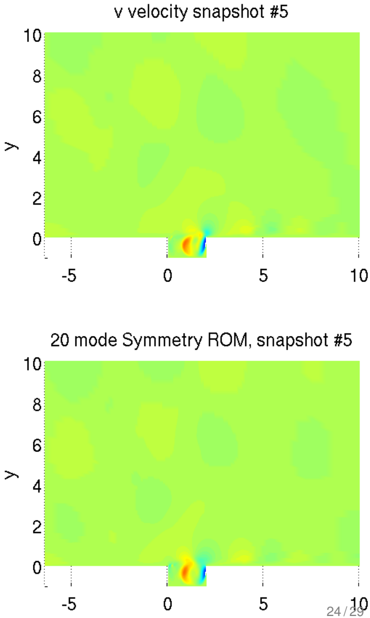

ROM based on Linearized Navier-Stokes Retaining $\nabla\bar{\mathbf{q}}$ Terms

$$\mathbf{q}'_{,t} + [\mathbf{A}_i(\bar{\mathbf{q}}) - \mathbf{K}_i^{vw}(\nabla\bar{\mathbf{q}})]\mathbf{q}'_{,i} - [\mathbf{K}_{ij}(\bar{\mathbf{q}})\mathbf{q}'_{,j}]_{,i} + \mathbf{C}(\nabla\bar{\mathbf{q}})\mathbf{q}' = \mathbf{F}$$

- Figure below shows:
  - ○: t vs. $a_i(t)$ (ROM coefficients).
  - −: t vs. $(\mathbf{q}'_{CFD}(\mathbf{x},t), \boldsymbol{\phi}_i(\mathbf{x}))$ (projection of snapshots onto modes).
- Movie on right shows v-velocity snapshot (top) vs. 20 mode symmetry ROM solution v (bottom).

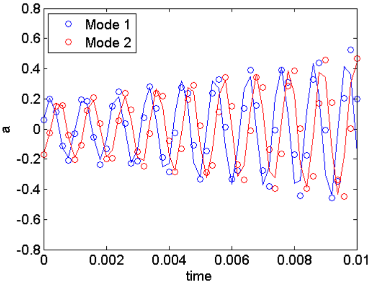

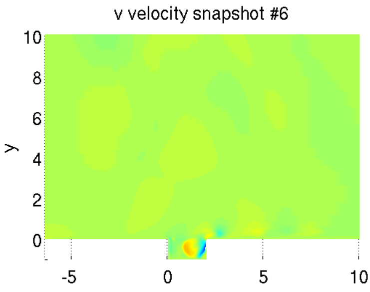

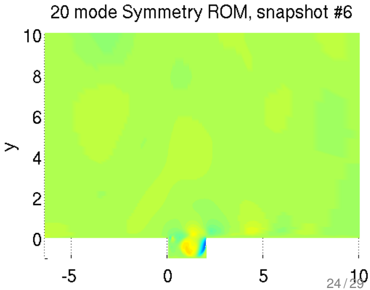

ROM based on Linearized Navier-Stokes Retaining $\nabla\bar{\mathbf{q}}$ Terms

$$\mathbf{q}'_{,t} + [\mathbf{A}_i(\bar{\mathbf{q}}) - \mathbf{K}_i^{vw}(\nabla\bar{\mathbf{q}})]\mathbf{q}'_{,i} - [\mathbf{K}_{ij}(\bar{\mathbf{q}})\mathbf{q}'_{,j}]_{,i} + \mathbf{C}(\nabla\bar{\mathbf{q}})\mathbf{q}' = \mathbf{F}$$

- Figure below shows:
  - ○: t vs. $a_i(t)$ (ROM coefficients).
  - $-$: t vs. $(\mathbf{q}'_{CFD}(\mathbf{x},t), \boldsymbol{\phi}_i(\mathbf{x}))$ (projection of snapshots onto modes).
- Movie on right shows v-velocity snapshot (top) vs. 20 mode symmetry ROM solution v (bottom).

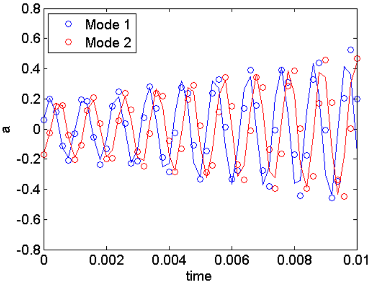

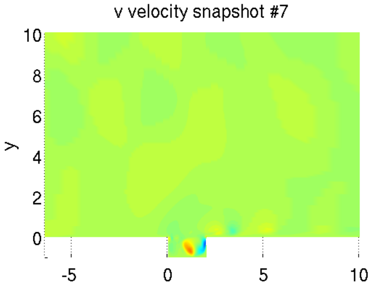

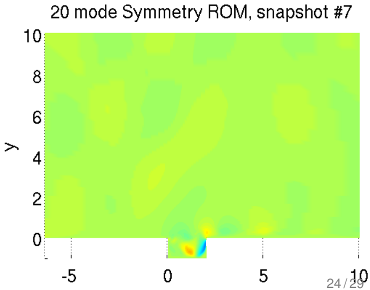

ROM based on Linearized Navier-Stokes Retaining $\nabla\bar{\mathbf{q}}$ Terms

$$\mathbf{q}'_{,t} + [\mathbf{A}_i(\bar{\mathbf{q}}) - \mathbf{K}_i^{vw}(\nabla\bar{\mathbf{q}})]\mathbf{q}'_{,i} - [\mathbf{K}_{ij}(\bar{\mathbf{q}})\mathbf{q}'_{,j}]_{,i}$$
$$+\mathbf{C}(\nabla\bar{\mathbf{q}})\mathbf{q}' = \mathbf{F}$$

- Figure below shows:
  - ○: t vs. $a_i(t)$ (ROM coefficients).
  - $-$: t vs. $(\mathbf{q}'_{CFD}(\mathbf{x},t), \boldsymbol{\phi}_i(\mathbf{x}))$ (projection of snapshots onto modes).
- Movie on right shows v-velocity snapshot (top) vs. 20 mode symmetry ROM solution v (bottom).

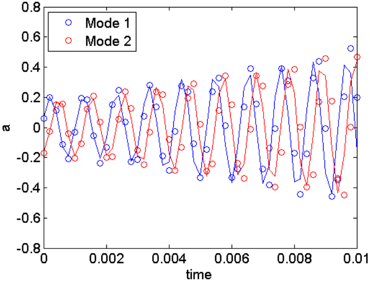

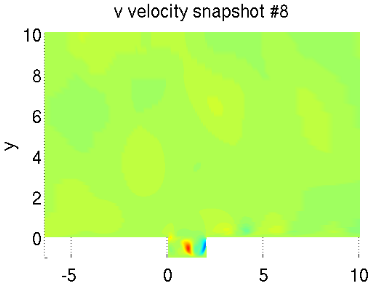

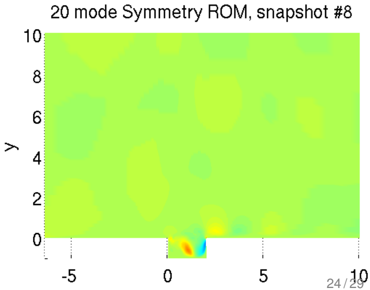

ROM based on Linearized Navier-Stokes Retaining $\nabla\bar{\mathbf{q}}$ Terms

$$\mathbf{q}'_{,t} + [\mathbf{A}_i(\bar{\mathbf{q}}) - \mathbf{K}_i^{vw}(\nabla\bar{\mathbf{q}})]\mathbf{q}'_{,i} - [\mathbf{K}_{ij}(\bar{\mathbf{q}})\mathbf{q}'_{,j}]_{,i} + \mathbf{C}(\nabla\bar{\mathbf{q}})\mathbf{q}' = \mathbf{F}$$

- Figure below shows:
  - ○: t vs. $a_i(t)$ (ROM coefficients).
  - $-$: t vs. $(\mathbf{q}'_{CFD}(\mathbf{x},t), \boldsymbol{\phi}_i(\mathbf{x}))$ (projection of snapshots onto modes).
- Movie on right shows v-velocity snapshot (top) vs. 20 mode symmetry ROM solution v (bottom).

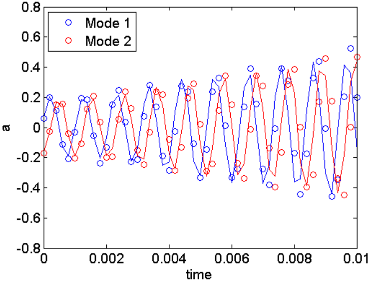

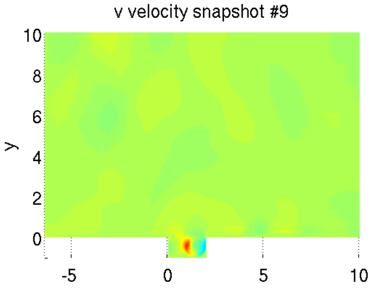

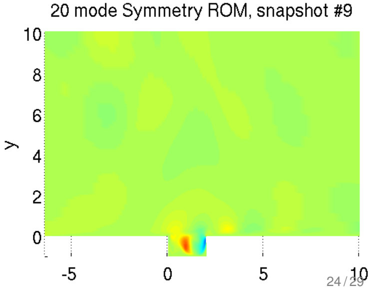

ROM based on Linearized Navier-Stokes Retaining $\nabla\bar{\mathbf{q}}$ Terms

$$\mathbf{q}'_{,t} + [\mathbf{A}_i(\bar{\mathbf{q}}) - \mathbf{K}_i^{vw}(\nabla\bar{\mathbf{q}})]\mathbf{q}'_{,i} - [\mathbf{K}_{ij}(\bar{\mathbf{q}})\mathbf{q}'_{,j}]_{,i}$$
$$+\mathbf{C}(\nabla\bar{\mathbf{q}})\mathbf{q}' = \mathbf{F}$$

- Figure below shows:
  - ○: t vs. $a_i(t)$ (ROM coefficients).
  - $-$: t vs. $(\mathbf{q}'_{CFD}(\mathbf{x},t), \boldsymbol{\phi}_i(\mathbf{x}))$ (projection of snapshots onto modes).
- Movie on right shows v-velocity snapshot (top) vs. 20 mode symmetry ROM solution v (bottom).

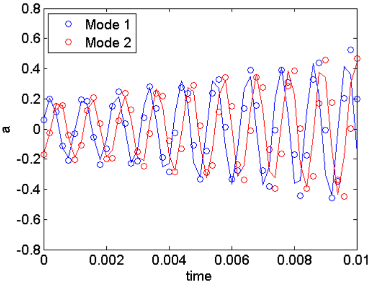

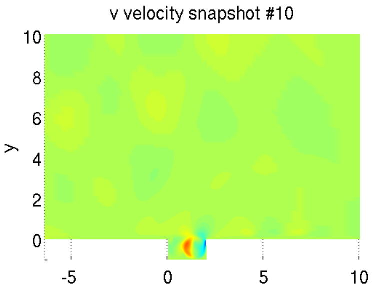

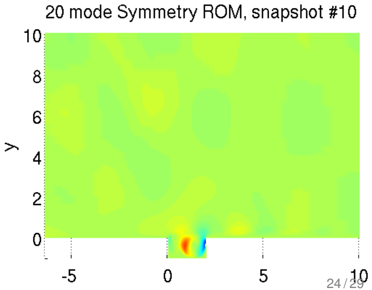

ROM based on Linearized Navier-Stokes Retaining $\nabla\bar{\mathbf{q}}$ Terms

$$\mathbf{q}'_{,t} + [\mathbf{A}_i(\bar{\mathbf{q}}) - \mathbf{K}_i^{vw}(\nabla\bar{\mathbf{q}})]\mathbf{q}'_{,i} - [\mathbf{K}_{ij}(\bar{\mathbf{q}})\mathbf{q}'_{,j}]_{,i}$$
$$+\mathbf{C}(\nabla\bar{\mathbf{q}})\mathbf{q}' = \mathbf{F}$$

- Figure below shows:
  - $\circ$: t vs. $a_i(t)$ (ROM coefficients).
  - $-$: t vs. $(\mathbf{q}'_{CFD}(\mathbf{x},t), \boldsymbol{\phi}_i(\mathbf{x}))$ (projection of snapshots onto modes).
- Movie on right shows v-velocity snapshot (top) vs. 20 mode symmetry ROM solution v (bottom).

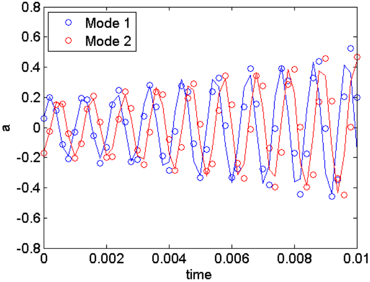

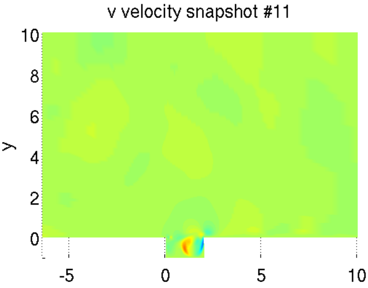

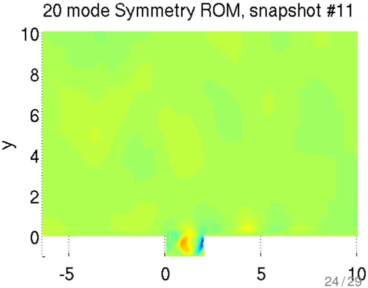

ROM based on Linearized Navier-Stokes Retaining $\nabla\bar{\mathbf{q}}$ Terms

$$\mathbf{q}'_{,t} + [\mathbf{A}_i(\bar{\mathbf{q}}) - \mathbf{K}_i^{vw}(\nabla\bar{\mathbf{q}})]\mathbf{q}'_{,i} - [\mathbf{K}_{ij}(\bar{\mathbf{q}})\mathbf{q}'_{,j}]_{,i} + \mathbf{C}(\nabla\bar{\mathbf{q}})\mathbf{q}' = \mathbf{F}$$

- Figure below shows:
  - $\circ$: t vs. $a_i(t)$ (ROM coefficients).
  - $-$: t vs. $(\mathbf{q}'_{CFD}(\mathbf{x},t), \boldsymbol{\phi}_i(\mathbf{x}))$ (projection of snapshots onto modes).
- Movie on right shows v-velocity snapshot (top) vs. 20 mode symmetry ROM solution v (bottom).

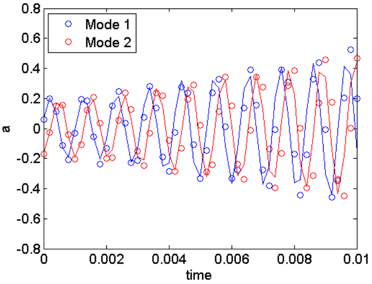

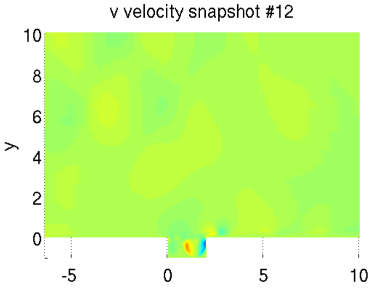

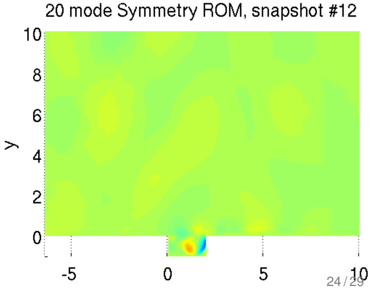

ROM based on Linearized Navier-Stokes Retaining $\nabla\bar{\mathrm{q}}$ Terms

$$\mathbf{q}'_{,t} + [\mathbf{A}_i(\bar{\mathbf{q}}) - \mathbf{K}_i^{vw}(\nabla\bar{\mathbf{q}})]\mathbf{q}'_{,i} - [\mathbf{K}_{ij}(\bar{\mathbf{q}})\mathbf{q}'_{,j}]_{,i} + \mathbf{C}(\nabla\bar{\mathbf{q}})\mathbf{q}' = \mathbf{F}$$

- Figure below shows:
  - $\circ$: t vs. $a_i(t)$ (ROM coefficients).
  - $-$: t vs. $(\mathbf{q}'_{CFD}(\mathbf{x},t), \boldsymbol{\phi}_i(\mathbf{x}))$ (projection of snapshots onto modes).
- Movie on right shows v-velocity snapshot (top) vs. 20 mode symmetry ROM solution v (bottom).

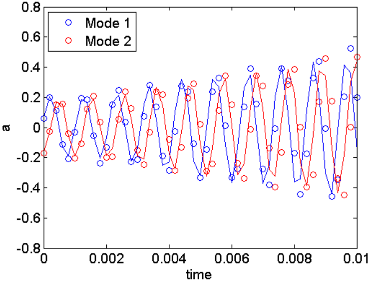

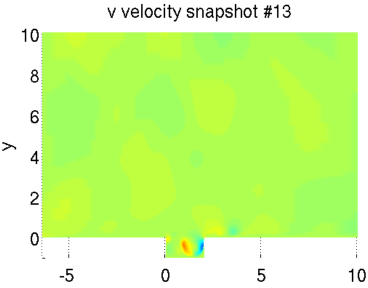

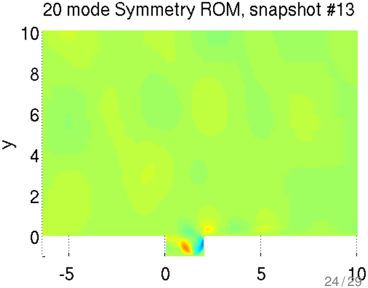

ROM based on Linearized Navier-Stokes Retaining $\nabla\bar{\mathbf{q}}$ Terms

$$\mathbf{q}'_{,t} + [\mathbf{A}_i(\bar{\mathbf{q}}) - \mathbf{K}_i^{vw}(\nabla\bar{\mathbf{q}})]\mathbf{q}'_{,i} - [\mathbf{K}_{ij}(\bar{\mathbf{q}})\mathbf{q}'_{,j}]_{,i} + \mathbf{C}(\nabla\bar{\mathbf{q}})\mathbf{q}' = \mathbf{F}$$

- Figure below shows:
  - $\circ$: t vs. $a_i(t)$ (ROM coefficients).
  - $-$: t vs. $(\mathbf{q}'_{CFD}(\mathbf{x},t), \boldsymbol{\phi}_i(\mathbf{x}))$ (projection of snapshots onto modes).
- Movie on right shows v-velocity snapshot (top) vs. 20 mode symmetry ROM solution v (bottom).

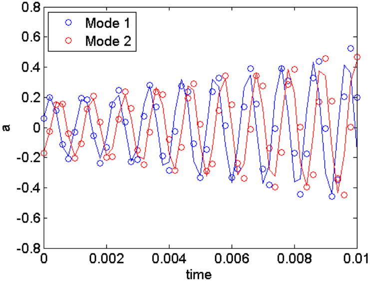

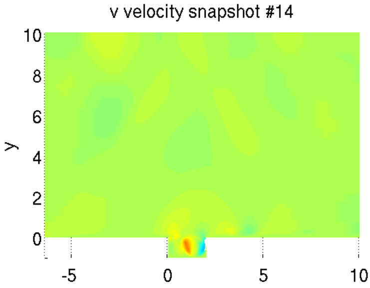

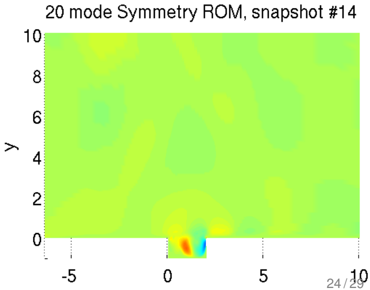

ROM based on Linearized Navier-Stokes Retaining $\nabla\bar{\mathbf{q}}$ Terms

$$\mathbf{q}'_{,t} + [\mathbf{A}_i(\bar{\mathbf{q}}) - \mathbf{K}_i^{vw}(\nabla\bar{\mathbf{q}})]\mathbf{q}'_{,i} - [\mathbf{K}_{ij}(\bar{\mathbf{q}})\mathbf{q}'_{,j}]_{,i} + \mathbf{C}(\nabla\bar{\mathbf{q}})\mathbf{q}' = \mathbf{F}$$

- Figure below shows:
  - $\circ$: t vs. $a_i(t)$ (ROM coefficients).
  - $-$: t vs. $(\mathbf{q}'_{CFD}(\mathbf{x},t), \boldsymbol{\phi}_i(\mathbf{x}))$ (projection of snapshots onto modes).
- Movie on right shows v-velocity snapshot (top) vs. 20 mode symmetry ROM solution v (bottom).

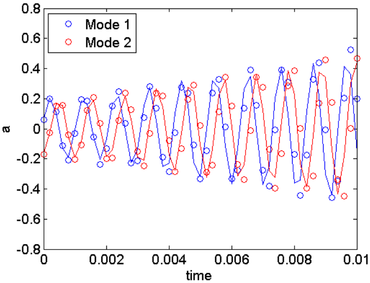

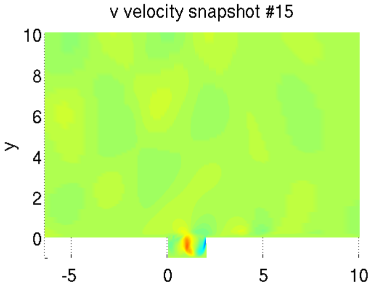

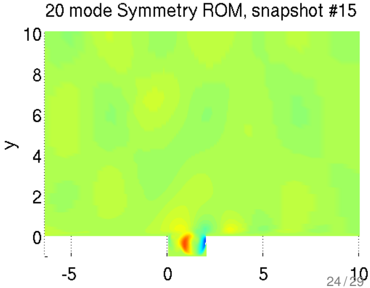

ROM based on Linearized Navier-Stokes Retaining $\nabla\bar{\mathrm{q}}$ Terms

$$\mathbf{q}'_{,t} + [\mathbf{A}_i(\bar{\mathbf{q}}) - \mathbf{K}_i^{vw}(\nabla\bar{\mathbf{q}})]\mathbf{q}'_{,i} - [\mathbf{K}_{ij}(\bar{\mathbf{q}})\mathbf{q}'_{,j}]_{,i} + \mathbf{C}(\nabla\bar{\mathbf{q}})\mathbf{q}' = \mathbf{F}$$

- Figure below shows:
  - ○: t vs. $a_i(t)$ (ROM coefficients).
  - $-$: t vs. $(\mathbf{q}'_{CFD}(\mathbf{x}, t), \boldsymbol{\phi}_i(\mathbf{x}))$ (projection of snapshots onto modes).
- Movie on right shows v-velocity snapshot (top) vs. 20 mode symmetry ROM solution v (bottom).

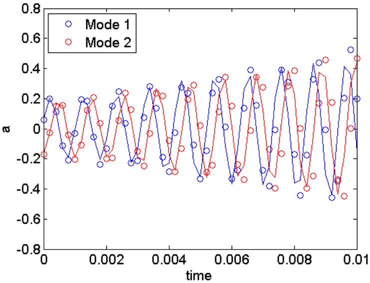

v velocity snapshot #16

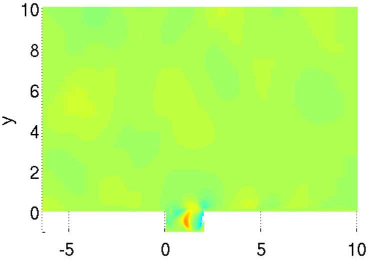

20 mode Symmetry ROM, snapshot #16

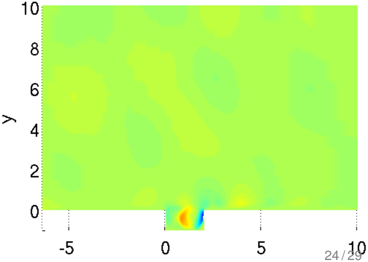

ROM based on Linearized Navier-Stokes Retaining $\nabla\bar{\mathbf{q}}$ Terms

$$\mathbf{q}'_{,t} + [\mathbf{A}_i(\bar{\mathbf{q}}) - \mathbf{K}_i^{vw}(\nabla\bar{\mathbf{q}})]\mathbf{q}'_{,i} - [\mathbf{K}_{ij}(\bar{\mathbf{q}})\mathbf{q}'_{,j}]_{,i} + \mathbf{C}(\nabla\bar{\mathbf{q}})\mathbf{q}' = \mathbf{F}$$

- Figure below shows:
  - $\circ$: t vs. $a_i(t)$ (ROM coefficients).
  - $-$: t vs. $(\mathbf{q}'_{CFD}(\mathbf{x},t), \boldsymbol{\phi}_i(\mathbf{x}))$ (projection of snapshots onto modes).
- Movie on right shows v-velocity snapshot (top) vs. 20 mode symmetry ROM solution v (bottom).

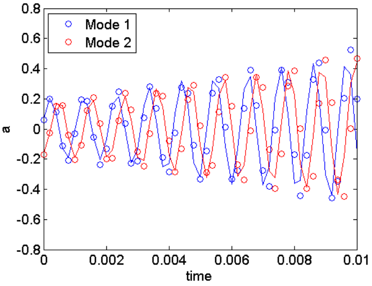

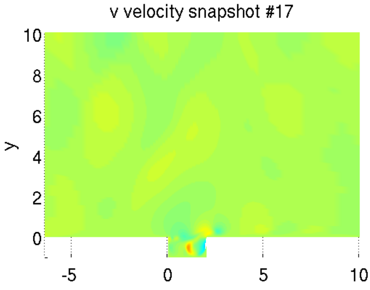

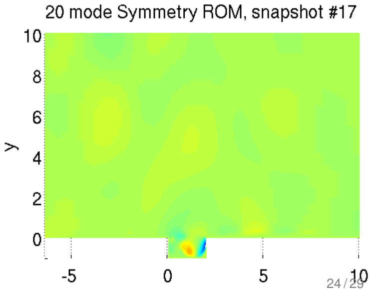

ROM based on Linearized Navier-Stokes Retaining $\nabla\bar{\mathbf{q}}$ Terms

$$\mathbf{q}'_{,t} + [\mathbf{A}_i(\bar{\mathbf{q}}) - \mathbf{K}_i^{vw}(\nabla\bar{\mathbf{q}})]\mathbf{q}'_{,i} - [\mathbf{K}_{ij}(\bar{\mathbf{q}})\mathbf{q}'_{,j}]_{,i}$$
$$+\mathbf{C}(\nabla\bar{\mathbf{q}})\mathbf{q}' = \mathbf{F}$$

- Figure below shows:
  - $\circ$: t vs. $a_i(t)$ (ROM coefficients).
  - $-$: t vs. $(\mathbf{q}'_{CFD}(\mathbf{x},t), \boldsymbol{\phi}_i(\mathbf{x}))$ (projection of snapshots onto modes).
- Movie on right shows v-velocity snapshot (top) vs. 20 mode symmetry ROM solution v (bottom).

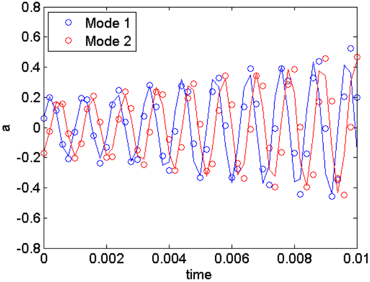

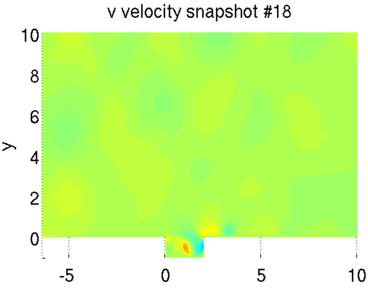

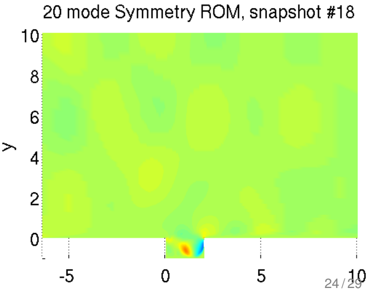

ROM based on Linearized Navier-Stokes Retaining $\nabla\bar{\mathbf{q}}$ Terms

$$\mathbf{q}'_{,t} + [\mathbf{A}_i(\bar{\mathbf{q}}) - \mathbf{K}_i^{vw}(\nabla\bar{\mathbf{q}})]\mathbf{q}'_{,i} - [\mathbf{K}_{ij}(\bar{\mathbf{q}})\mathbf{q}'_{,j}]_{,i} + \mathbf{C}(\nabla\bar{\mathbf{q}})\mathbf{q}' = \mathbf{F}$$

- Figure below shows:
  - $\circ$: t vs. $a_i(t)$ (ROM coefficients).
  - $-$: t vs. $(\mathbf{q}'_{CFD}(\mathbf{x}, t), \boldsymbol{\phi}_i(\mathbf{x}))$ (projection of snapshots onto modes).
- Movie on right shows v-velocity snapshot (top) vs. 20 mode symmetry ROM solution v (bottom).

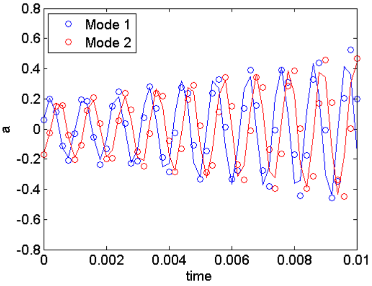

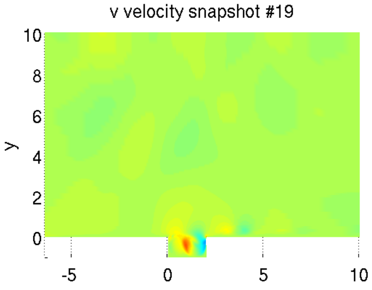

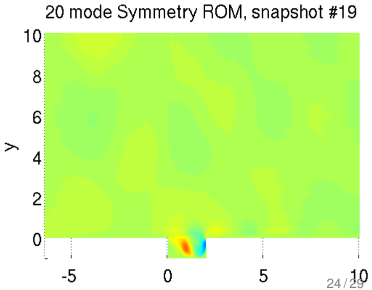

ROM based on Linearized Navier-Stokes Retaining $\nabla\bar{\mathbf{q}}$ Terms

$$\mathbf{q}'_{,t} + [\mathbf{A}_i(\bar{\mathbf{q}}) - \mathbf{K}_i^{vw}(\nabla\bar{\mathbf{q}})]\mathbf{q}'_{,i} - [\mathbf{K}_{ij}(\bar{\mathbf{q}})\mathbf{q}'_{,j}]_{,i} + \mathbf{C}(\nabla\bar{\mathbf{q}})\mathbf{q}' = \mathbf{F}$$

- Figure below shows:
  - ○: t vs. $a_i(t)$ (ROM coefficients).
  - $-$: t vs. $(\mathbf{q}'_{CFD}(\mathbf{x},t), \boldsymbol{\phi}_i(\mathbf{x}))$ (projection of snapshots onto modes).
- Movie on right shows v-velocity snapshot (top) vs. 20 mode symmetry ROM solution v (bottom).

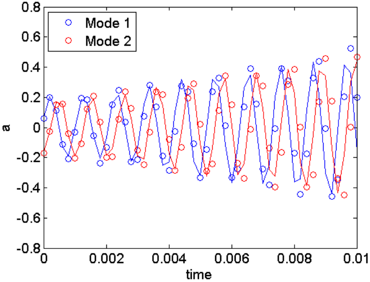

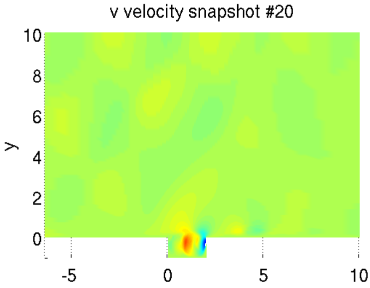

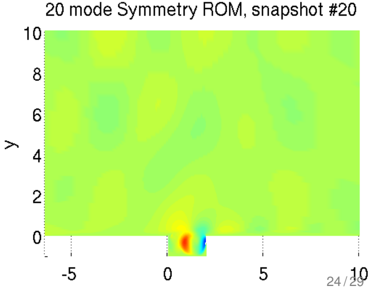

ROM based on Linearized Navier-Stokes Retaining $\nabla\bar{\mathbf{q}}$ Terms

$$\mathbf{q}'_{,t} + [\mathbf{A}_i(\bar{\mathbf{q}}) - \mathbf{K}_i^{vw}(\nabla\bar{\mathbf{q}})]\mathbf{q}'_{,i} - [\mathbf{K}_{ij}(\bar{\mathbf{q}})\mathbf{q}'_{,j}]_{,i} + \mathbf{C}(\nabla\bar{\mathbf{q}})\mathbf{q}' = \mathbf{F}$$

- Figure below shows:
  - ○: t vs. $a_i(t)$ (ROM coefficients).
  - $-$: t vs. $(\mathbf{q}'_{CFD}(\mathbf{x},t), \boldsymbol{\phi}_i(\mathbf{x}))$ (projection of snapshots onto modes).
- Movie on right shows v-velocity snapshot (top) vs. 20 mode symmetry ROM solution v (bottom).

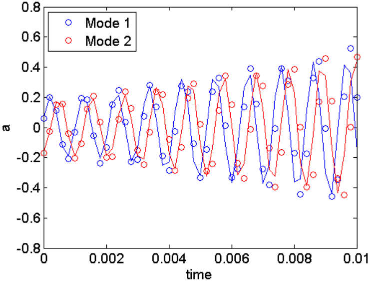

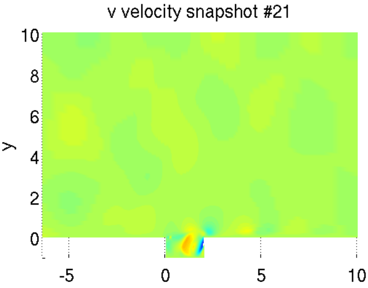

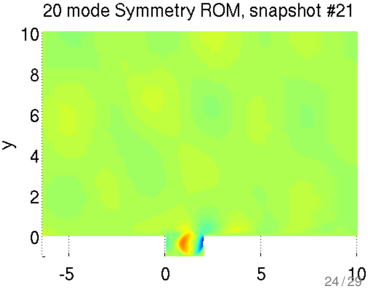

ROM based on Linearized Navier-Stokes Retaining $\nabla\bar{\mathbf{q}}$ Terms

$$\mathbf{q}'_{,t} + [\mathbf{A}_i(\bar{\mathbf{q}}) - \mathbf{K}_i^{vw}(\nabla\bar{\mathbf{q}})]\mathbf{q}'_{,i} - [\mathbf{K}_{ij}(\bar{\mathbf{q}})\mathbf{q}'_{,j}]_{,i} + \mathbf{C}(\nabla\bar{\mathbf{q}})\mathbf{q}' = \mathbf{F}$$

- Figure below shows:
  - $\circ$: t vs. $a_i(t)$ (ROM coefficients).
  - $-$: t vs. $(\mathbf{q}'_{CFD}(\mathbf{x},t), \boldsymbol{\phi}_i(\mathbf{x}))$ (projection of snapshots onto modes).
- Movie on right shows v-velocity snapshot (top) vs. 20 mode symmetry ROM solution v (bottom).

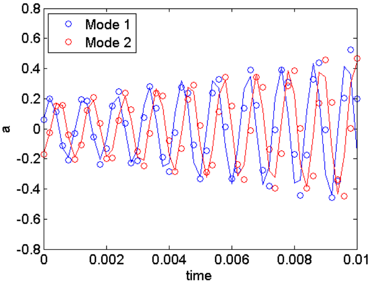

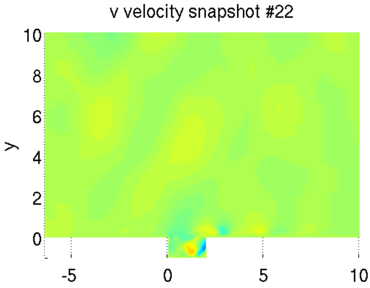

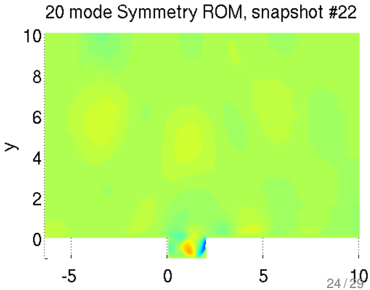

ROM based on Linearized Navier-Stokes Retaining $\nabla\bar{\mathbf{q}}$ Terms

$$\mathbf{q}'_{,t} + [\mathbf{A}_i(\bar{\mathbf{q}}) - \mathbf{K}_i^{vw}(\nabla\bar{\mathbf{q}})]\mathbf{q}'_{,i} - [\mathbf{K}_{ij}(\bar{\mathbf{q}})\mathbf{q}'_{,j}]_{,i} + \mathbf{C}(\nabla\bar{\mathbf{q}})\mathbf{q}' = \mathbf{F}$$

- Figure below shows:
  - $\circ$: t vs. $a_i(t)$ (ROM coefficients).
  - $-$: t vs. $(\mathbf{q}'_{CFD}(\mathbf{x},t), \boldsymbol{\phi}_i(\mathbf{x}))$ (projection of snapshots onto modes).
- Movie on right shows v-velocity snapshot (top) vs. 20 mode symmetry ROM solution v (bottom).

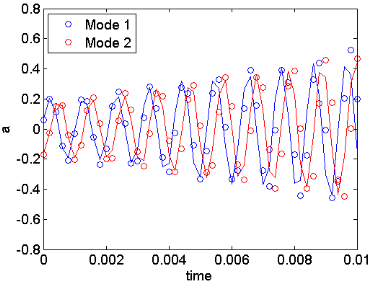

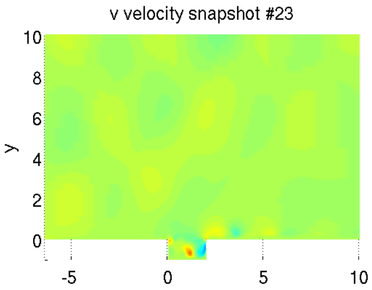

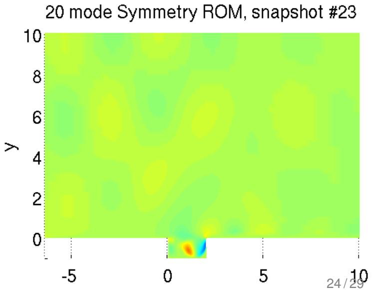

ROM based on Linearized Navier-Stokes Retaining $\nabla\bar{\mathbf{q}}$ Terms

$$\mathbf{q}'_{,t} + [\mathbf{A}_i(\bar{\mathbf{q}}) - \mathbf{K}_i^{vw}(\nabla\bar{\mathbf{q}})]\mathbf{q}'_{,i} - [\mathbf{K}_{ij}(\bar{\mathbf{q}})\mathbf{q}'_{,j}]_{,i}$$
$$+\mathbf{C}(\nabla\bar{\mathbf{q}})\mathbf{q}' = \mathbf{F}$$

- Figure below shows:
  - ○: t vs. $a_i(t)$ (ROM coefficients).
  - $-$: t vs. $(\mathbf{q}'_{CFD}(\mathbf{x},t), \boldsymbol{\phi}_i(\mathbf{x}))$ (projection of snapshots onto modes).
- Movie on right shows v-velocity snapshot (top) vs. 20 mode symmetry ROM solution v (bottom).

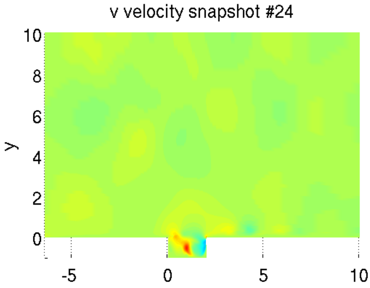

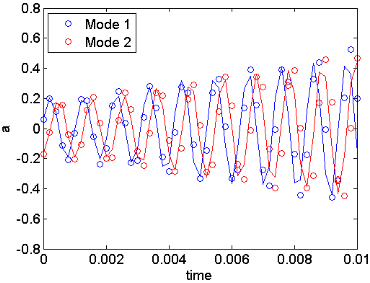

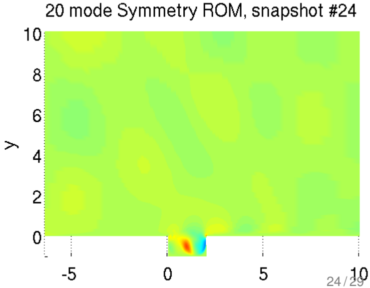

ROM based on Linearized Navier-Stokes Retaining $\nabla\bar{\mathbf{q}}$ Terms

$$\mathbf{q}'_{,t} + [\mathbf{A}_i(\bar{\mathbf{q}}) - \mathbf{K}_i^{vw}(\nabla\bar{\mathbf{q}})]\mathbf{q}'_{,i} - [\mathbf{K}_{ij}(\bar{\mathbf{q}})\mathbf{q}'_{,j}]_{,i}$$
$$+\mathbf{C}(\nabla\bar{\mathbf{q}})\mathbf{q}' = \mathbf{F}$$

- Figure below shows:
  - $\circ$: t vs. $a_i(t)$ (ROM coefficients).
  - $-$: t vs. $(\mathbf{q}'_{CFD}(\mathbf{x},t), \boldsymbol{\phi}_i(\mathbf{x}))$ (projection of snapshots onto modes).
- Movie on right shows v-velocity snapshot (top) vs. 20 mode symmetry ROM solution v (bottom).

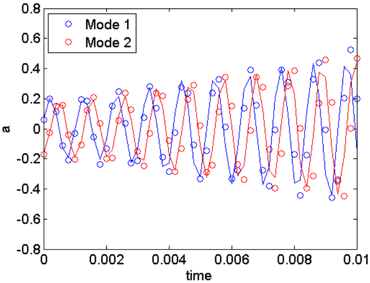

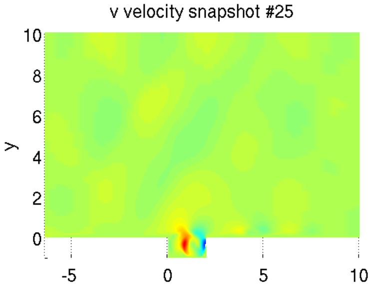

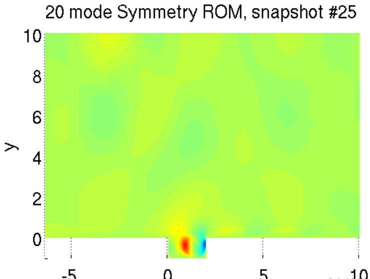

ROM based on Linearized Navier-Stokes Retaining $\nabla\bar{\mathbf{q}}$ Terms

$$\mathbf{q}'_{,t} + [\mathbf{A}_i(\bar{\mathbf{q}}) - \mathbf{K}_i^{vw}(\nabla\bar{\mathbf{q}})]\mathbf{q}'_{,i} - [\mathbf{K}_{ij}(\bar{\mathbf{q}})\mathbf{q}'_{,j}]_{,i}$$
$$+\mathbf{C}(\nabla\bar{\mathbf{q}})\mathbf{q}' = \mathbf{F}$$

- Figure below shows:
  - $\circ$: t vs. $a_i(t)$ (ROM coefficients).
  - $-$: t vs. $(\mathbf{q}'_{CFD}(\mathbf{x},t), \boldsymbol{\phi}_i(\mathbf{x}))$ (projection of snapshots onto modes).
- Movie on right shows v-velocity snapshot (top) vs. 20 mode symmetry ROM solution v (bottom).

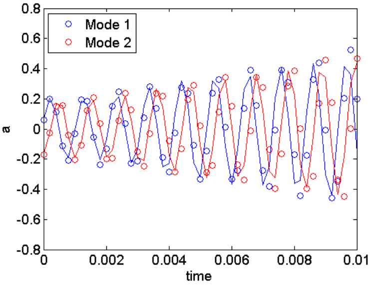

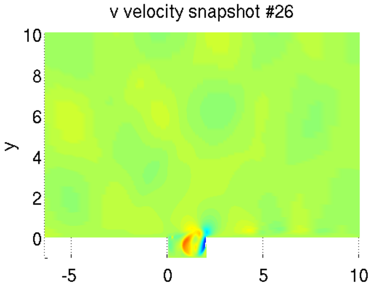

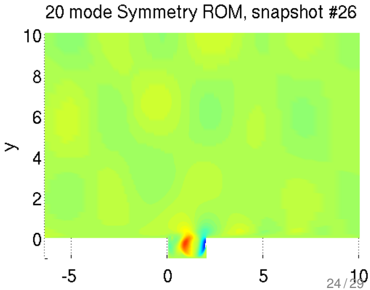

ROM based on Linearized Navier-Stokes Retaining $\nabla \bar{\mathbf{q}}$ Terms

$$\mathbf{q}'_{,t} + [\mathbf{A}_i(\bar{\mathbf{q}}) - \mathbf{K}_i^{vw}(\nabla\bar{\mathbf{q}})]\mathbf{q}'_{,i} - [\mathbf{K}_{ij}(\bar{\mathbf{q}})\mathbf{q}'_{,j}]_{,i} + \mathbf{C}(\nabla\bar{\mathbf{q}})\mathbf{q}' = \mathbf{F}$$

- Figure below shows:
  - $\circ$: t vs. $a_i(t)$ (ROM coefficients).
  - $-$: t vs. $(\mathbf{q}'_{CFD}(\mathbf{x},t), \boldsymbol{\phi}_i(\mathbf{x}))$ (projection of snapshots onto modes).
- Movie on right shows v-velocity snapshot (top) vs. 20 mode symmetry ROM solution v (bottom).

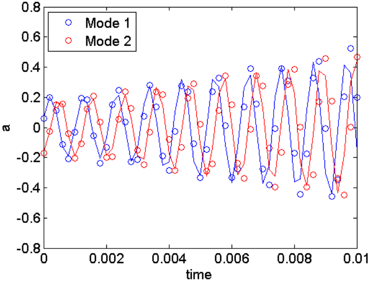

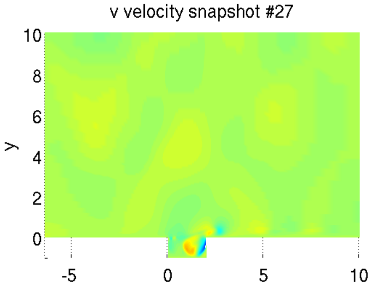

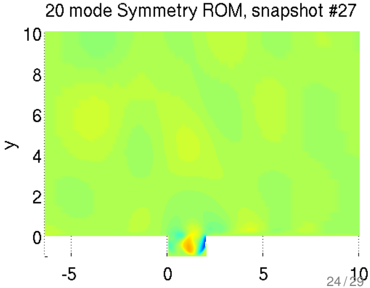

ROM based on Linearized Navier-Stokes Retaining $\nabla\bar{\mathbf{q}}$ Terms

$$\mathbf{q}'_{,t} + [\mathbf{A}_i(\bar{\mathbf{q}}) - \mathbf{K}_i^{vw}(\nabla\bar{\mathbf{q}})]\mathbf{q}'_{,i} - [\mathbf{K}_{ij}(\bar{\mathbf{q}})\mathbf{q}'_{,j}]_{,i}$$
$$+\mathbf{C}(\nabla\bar{\mathbf{q}})\mathbf{q}' = \mathbf{F}$$

- Figure below shows:
  - $\circ$: t vs. $a_i(t)$ (ROM coefficients).
  - $-$: t vs. $(\mathbf{q}'_{CFD}(\mathbf{x},t), \boldsymbol{\phi}_i(\mathbf{x}))$ (projection of snapshots onto modes).
- Movie on right shows v-velocity snapshot (top) vs. 20 mode symmetry ROM solution v (bottom).

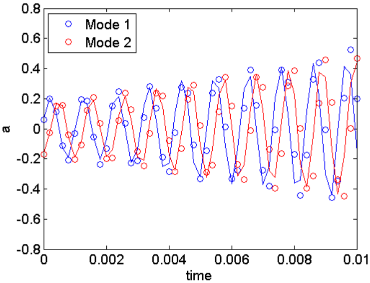

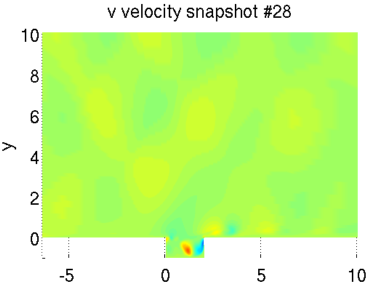

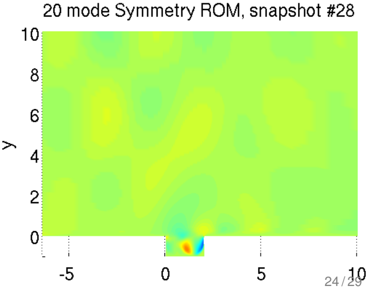

ROM based on Linearized Navier-Stokes Retaining $\nabla\bar{\mathbf{q}}$ Terms

$$\mathbf{q}'_{,t} + [\mathbf{A}_i(\bar{\mathbf{q}}) - \mathbf{K}_i^{vw}(\nabla\bar{\mathbf{q}})]\mathbf{q}'_{,i} - [\mathbf{K}_{ij}(\bar{\mathbf{q}})\mathbf{q}'_{,j}]_{,i} + \mathbf{C}(\nabla\bar{\mathbf{q}})\mathbf{q}' = \mathbf{F}$$

- Figure below shows:
  - $\circ$: t vs. $a_i(t)$ (ROM coefficients).
  - $-$: t vs. $(\mathbf{q}'_{CFD}(\mathbf{x},t), \boldsymbol{\phi}_i(\mathbf{x}))$ (projection of snapshots onto modes).
- Movie on right shows v-velocity snapshot (top) vs. 20 mode symmetry ROM solution v (bottom).

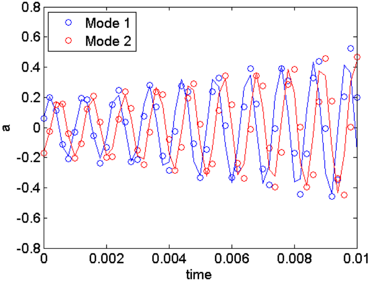

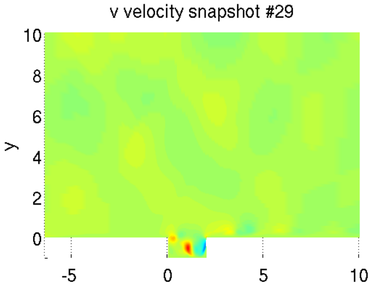

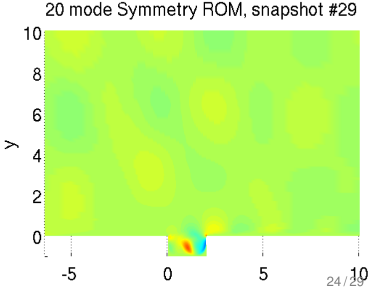

ROM based on Linearized Navier-Stokes Retaining $\nabla\bar{\mathbf{q}}$ Terms

$$\mathbf{q}'_{,t} + [\mathbf{A}_i(\bar{\mathbf{q}}) - \mathbf{K}_i^{vw}(\nabla\bar{\mathbf{q}})]\mathbf{q}'_{,i} - [\mathbf{K}_{ij}(\bar{\mathbf{q}})\mathbf{q}'_{,j}]_{,i} + \mathbf{C}(\nabla\bar{\mathbf{q}})\mathbf{q}' = \mathbf{F}$$

- Figure below shows:
  - ○: t vs. $a_i(t)$ (ROM coefficients).
  - $-$: t vs. $(\mathbf{q}'_{CFD}(\mathbf{x},t), \boldsymbol{\phi}_i(\mathbf{x}))$ (projection of snapshots onto modes).
- Movie on right shows v-velocity snapshot (top) vs. 20 mode symmetry ROM solution v (bottom).

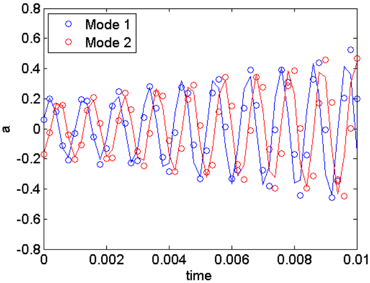

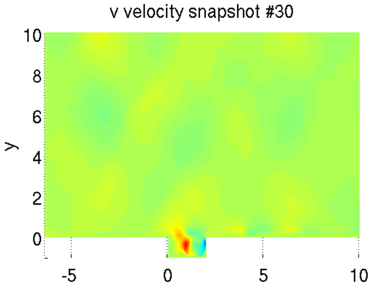

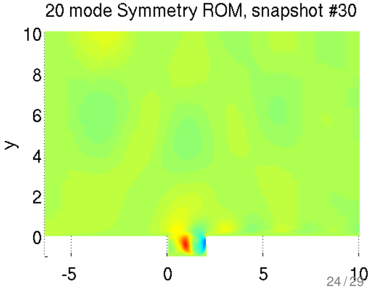

ROM based on Linearized Navier-Stokes Retaining $\nabla\bar{\mathbf{q}}$ Terms

$$\mathbf{q}'_{,t} + [\mathbf{A}_i(\bar{\mathbf{q}}) - \mathbf{K}_i^{vw}(\nabla\bar{\mathbf{q}})]\mathbf{q}'_{,i} - [\mathbf{K}_{ij}(\bar{\mathbf{q}})\mathbf{q}'_{,j}]_{,i} + \mathbf{C}(\nabla\bar{\mathbf{q}})\mathbf{q}' = \mathbf{F}$$

- Figure below shows:
  - ○: t vs. $a_i(t)$ (ROM coefficients).
  - $-$: t vs. $(\mathbf{q}'_{CFD}(\mathbf{x},t), \boldsymbol{\phi}_i(\mathbf{x}))$ (projection of snapshots onto modes).
- Movie on right shows v-velocity snapshot (top) vs. 20 mode symmetry ROM solution v (bottom).

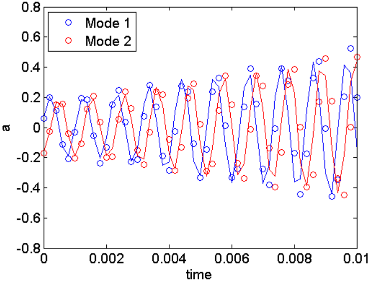

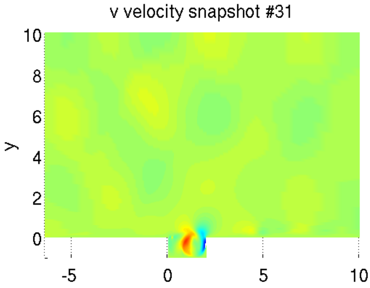

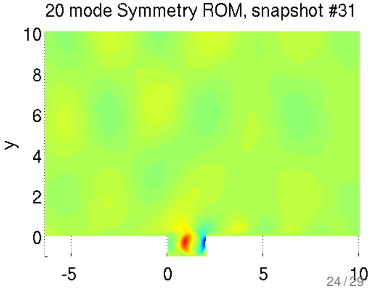

ROM based on Linearized Navier-Stokes Retaining $\nabla\bar{\mathbf{q}}$ Terms

$$\mathbf{q}'_{,t} + [\mathbf{A}_i(\bar{\mathbf{q}}) - \mathbf{K}_i^{vw}(\nabla\bar{\mathbf{q}})]\mathbf{q}'_{,i} - [\mathbf{K}_{ij}(\bar{\mathbf{q}})\mathbf{q}'_{,j}]_{,i} + \mathbf{C}(\nabla\bar{\mathbf{q}})\mathbf{q}' = \mathbf{F}$$

- Figure below shows:
  - $\circ$: t vs. $a_i(t)$ (ROM coefficients).
  - $-$: t vs. $(\mathbf{q}'_{CFD}(\mathbf{x},t), \boldsymbol{\phi}_i(\mathbf{x}))$ (projection of snapshots onto modes).
- Movie on right shows v-velocity snapshot (top) vs. 20 mode symmetry ROM solution v (bottom).

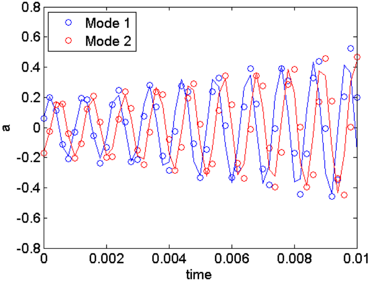

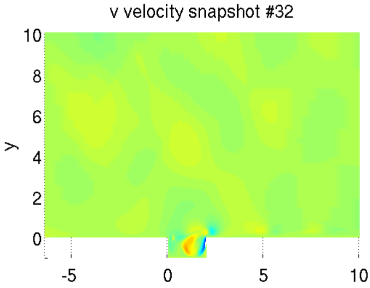

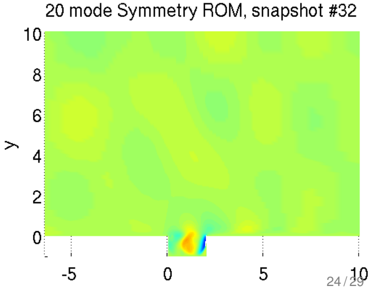

ROM based on Linearized Navier-Stokes Retaining $\nabla\bar{\mathrm{q}}$ Terms

$$\mathbf{q}'_{,t} + [\mathbf{A}_i(\bar{\mathbf{q}}) - \mathbf{K}_i^{vw}(\nabla\bar{\mathbf{q}})]\mathbf{q}'_{,i} - [\mathbf{K}_{ij}(\bar{\mathbf{q}})\mathbf{q}'_{,j}]_{,i}$$
$$+\mathbf{C}(\nabla\bar{\mathbf{q}})\mathbf{q}' = \mathbf{F}$$

- Figure below shows:
  - $\circ$: t vs. $a_i(t)$ (ROM coefficients).
  - $-$: t vs. $(\mathbf{q}'_{CFD}(\mathbf{x},t), \boldsymbol{\phi}_i(\mathbf{x}))$ (projection of snapshots onto modes).
- Movie on right shows v-velocity snapshot (top) vs. 20 mode symmetry ROM solution v (bottom).

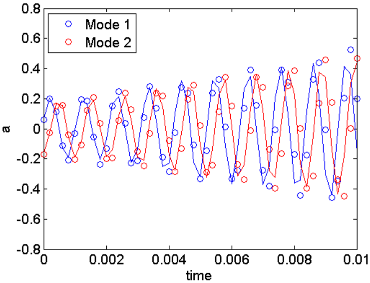

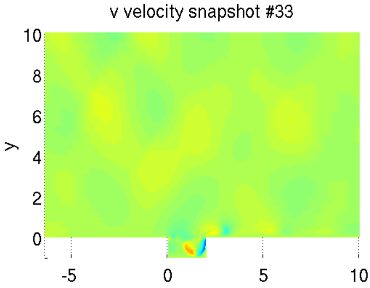

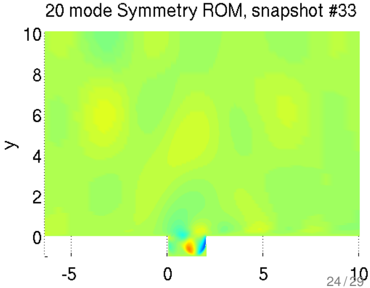

ROM based on Linearized Navier-Stokes Retaining $\nabla\bar{\mathrm{q}}$ Terms

$$\mathbf{q}'_{,t} + [\mathbf{A}_i(\bar{\mathbf{q}}) - \mathbf{K}_i^{vw}(\nabla\bar{\mathbf{q}})]\mathbf{q}'_{,i} - [\mathbf{K}_{ij}(\bar{\mathbf{q}})\mathbf{q}'_{,j}]_{,i} + \mathbf{C}(\nabla\bar{\mathbf{q}})\mathbf{q}' = \mathbf{F}$$

- Figure below shows:
  - $\circ$: t vs. $a_i(t)$ (ROM coefficients).
  - $-$: t vs. $(\mathbf{q}'_{CFD}(\mathbf{x}, t), \boldsymbol{\phi}_i(\mathbf{x}))$ (projection of snapshots onto modes).
- Movie on right shows v-velocity snapshot (top) vs. 20 mode symmetry ROM solution v (bottom).

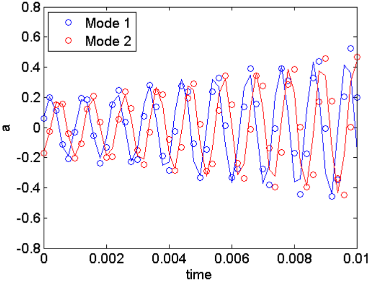

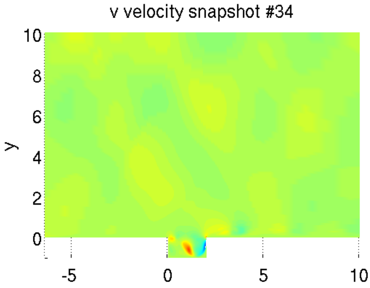

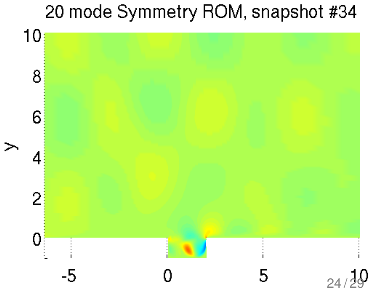

ROM based on Linearized Navier-Stokes Retaining $\nabla\bar{\mathbf{q}}$ Terms

$$\mathbf{q}'_{,t} + [\mathbf{A}_i(\bar{\mathbf{q}}) - \mathbf{K}_i^{vw}(\nabla\bar{\mathbf{q}})]\mathbf{q}'_{,i} - [\mathbf{K}_{ij}(\bar{\mathbf{q}})\mathbf{q}'_{,j}]_{,i} + \mathbf{C}(\nabla\bar{\mathbf{q}})\mathbf{q}' = \mathbf{F}$$

- Figure below shows:
  - $\circ$: t vs. $a_i(t)$ (ROM coefficients).
  - $-$: t vs. $(\mathbf{q}'_{CFD}(\mathbf{x},t), \boldsymbol{\phi}_i(\mathbf{x}))$ (projection of snapshots onto modes).
- Movie on right shows v-velocity snapshot (top) vs. 20 mode symmetry ROM solution v (bottom).

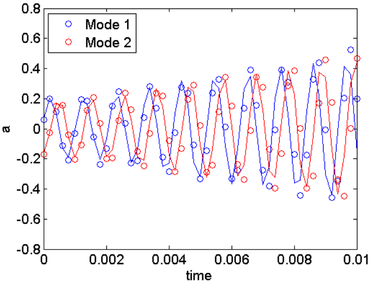

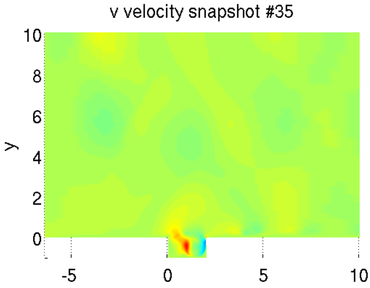

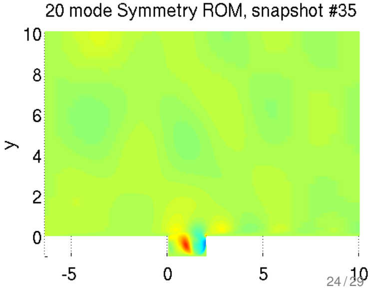

ROM based on Linearized Navier-Stokes Retaining $\nabla\bar{\mathbf{q}}$ Terms

$$\mathbf{q}'_{,t} + [\mathbf{A}_i(\bar{\mathbf{q}}) - \mathbf{K}_i^{vw}(\nabla\bar{\mathbf{q}})]\mathbf{q}'_{,i} - [\mathbf{K}_{ij}(\bar{\mathbf{q}})\mathbf{q}'_{,j}]_{,i} + \mathbf{C}(\nabla\bar{\mathbf{q}})\mathbf{q}' = \mathbf{F}$$

- Figure below shows:
  - $\circ$: t vs. $a_i(t)$ (ROM coefficients).
  - $-$: t vs. $(\mathbf{q}'_{CFD}(\mathbf{x},t), \boldsymbol{\phi}_i(\mathbf{x}))$ (projection of snapshots onto modes).
- Movie on right shows v-velocity snapshot (top) vs. 20 mode symmetry ROM solution v (bottom).

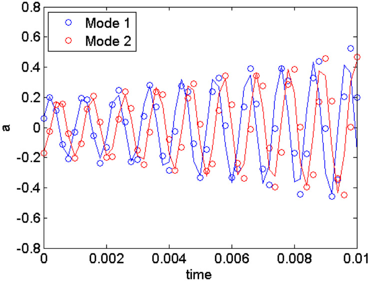

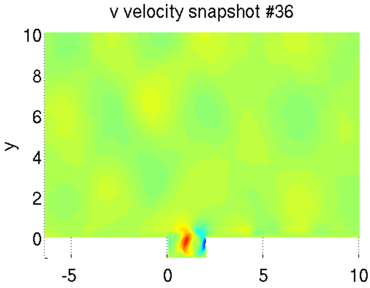

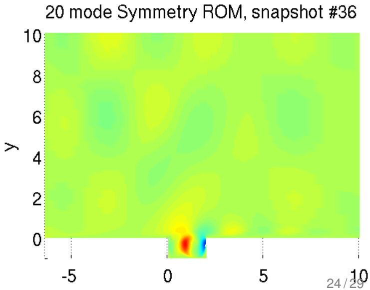

ROM based on Linearized Navier-Stokes Retaining $\nabla\bar{\mathbf{q}}$ Terms

$$\mathbf{q}'_{,t} + [\mathbf{A}_i(\bar{\mathbf{q}}) - \mathbf{K}_i^{vw}(\nabla\bar{\mathbf{q}})]\mathbf{q}'_{,i} - [\mathbf{K}_{ij}(\bar{\mathbf{q}})\mathbf{q}'_{,j}]_{,i}$$
$$+\mathbf{C}(\nabla\bar{\mathbf{q}})\mathbf{q}' = \mathbf{F}$$

- Figure below shows:
  - $\circ$: t vs. $a_i(t)$ (ROM coefficients).
  - $-$: t vs. $(\mathbf{q}'_{CFD}(\mathbf{x},t), \boldsymbol{\phi}_i(\mathbf{x}))$ (projection of snapshots onto modes).
- Movie on right shows v-velocity snapshot (top) vs. 20 mode symmetry ROM solution v (bottom).

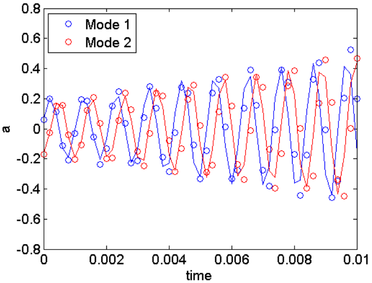

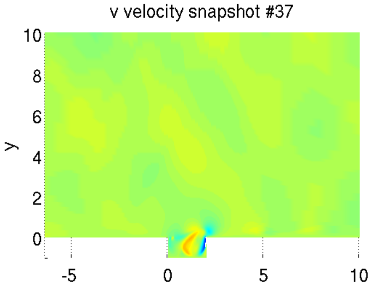

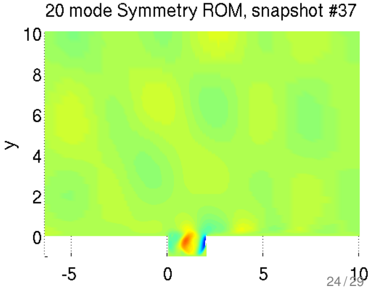

ROM based on Linearized Navier-Stokes Retaining $\nabla\bar{\mathbf{q}}$ Terms

$$\mathbf{q}'_{,t} + [\mathbf{A}_i(\bar{\mathbf{q}}) - \mathbf{K}_i^{vw}(\nabla\bar{\mathbf{q}})]\mathbf{q}'_{,i} - [\mathbf{K}_{ij}(\bar{\mathbf{q}})\mathbf{q}'_{,j}]_{,i} + \mathbf{C}(\nabla\bar{\mathbf{q}})\mathbf{q}' = \mathbf{F}$$

- Figure below shows:
  - $\circ$: t vs. $a_i(t)$ (ROM coefficients).
  - $-$: t vs. $(\mathbf{q}'_{CFD}(\mathbf{x},t), \boldsymbol{\phi}_i(\mathbf{x}))$ (projection of snapshots onto modes).
- Movie on right shows v-velocity snapshot (top) vs. 20 mode symmetry ROM solution v (bottom).

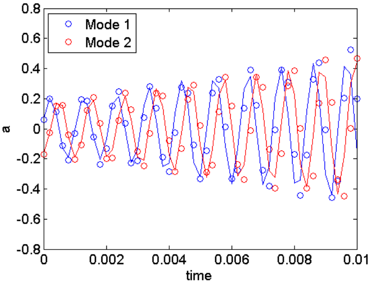

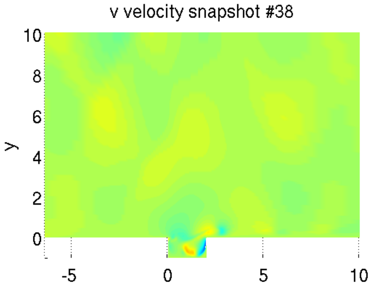

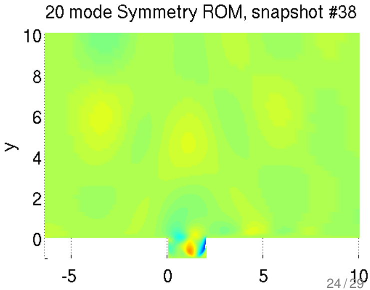

ROM based on Linearized Navier-Stokes Retaining $\nabla\bar{\mathbf{q}}$ Terms

$$\mathbf{q}'_{,t} + [\mathbf{A}_i(\bar{\mathbf{q}}) - \mathbf{K}_i^{vw}(\nabla\bar{\mathbf{q}})]\mathbf{q}'_{,i} - [\mathbf{K}_{ij}(\bar{\mathbf{q}})\mathbf{q}'_{,j}]_{,i}$$
$$+\mathbf{C}(\nabla\bar{\mathbf{q}})\mathbf{q}' = \mathbf{F}$$

- Figure below shows:
  - ○: t vs. $a_i(t)$ (ROM coefficients).
  - $-$: t vs. $(\mathbf{q}'_{CFD}(\mathbf{x},t), \boldsymbol{\phi}_i(\mathbf{x}))$ (projection of snapshots onto modes).
- Movie on right shows v-velocity snapshot (top) vs. 20 mode symmetry ROM solution v (bottom).

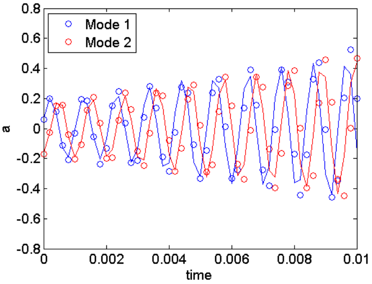

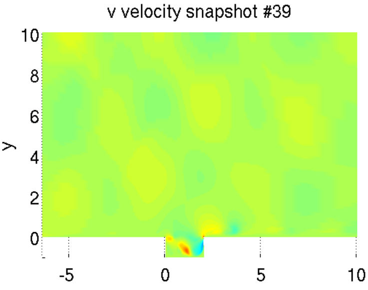

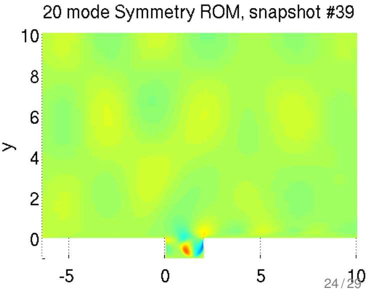

ROM based on Linearized Navier-Stokes Retaining $\nabla\bar{\mathbf{q}}$ Terms

$$\mathbf{q}'_{,t} + [\mathbf{A}_i(\bar{\mathbf{q}}) - \mathbf{K}_i^{vw}(\nabla\bar{\mathbf{q}})]\mathbf{q}'_{,i} - [\mathbf{K}_{ij}(\bar{\mathbf{q}})\mathbf{q}'_{,j}]_{,i} + \mathbf{C}(\nabla\bar{\mathbf{q}})\mathbf{q}' = \mathbf{F}$$

- Figure below shows:
  - ○: t vs. $a_i(t)$ (ROM coefficients).
  - $-$: t vs. $(\mathbf{q}'_{CFD}(\mathbf{x}, t), \boldsymbol{\phi}_i(\mathbf{x}))$ (projection of snapshots onto modes).
- Movie on right shows v-velocity snapshot (top) vs. 20 mode symmetry ROM solution v (bottom).

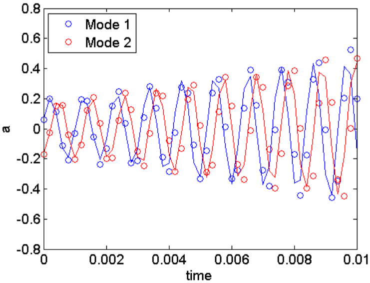

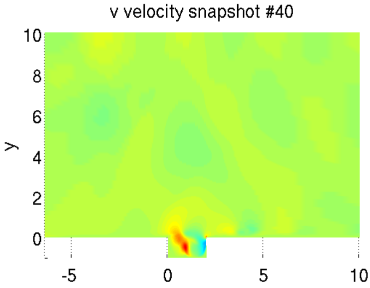

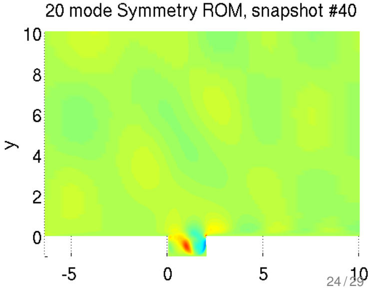

ROM based on Linearized Navier-Stokes Retaining $\nabla\bar{\mathbf{q}}$ Terms

$$\mathbf{q}'_{,t} + [\mathbf{A}_i(\bar{\mathbf{q}}) - \mathbf{K}_i^{vw}(\nabla\bar{\mathbf{q}})]\mathbf{q}'_{,i} - [\mathbf{K}_{ij}(\bar{\mathbf{q}})\mathbf{q}'_{,j}]_{,i}$$
$$+\mathbf{C}(\nabla\bar{\mathbf{q}})\mathbf{q}' = \mathbf{F}$$

- Figure below shows:
  - $\circ$: t vs. $a_i(t)$ (ROM coefficients).
  - $-$: t vs. $(\mathbf{q}'_{CFD}(\mathbf{x},t), \boldsymbol{\phi}_i(\mathbf{x}))$ (projection of snapshots onto modes).
- Movie on right shows v-velocity snapshot (top) vs. 20 mode symmetry ROM solution v (bottom).

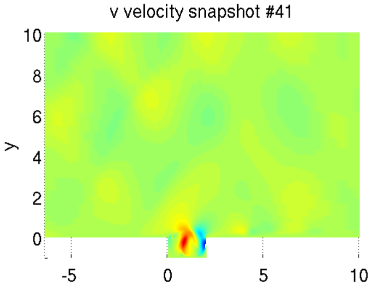

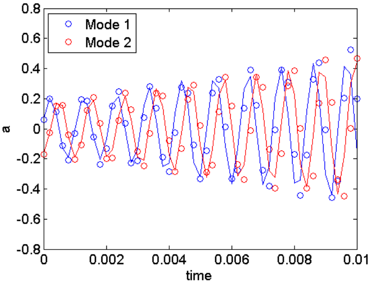

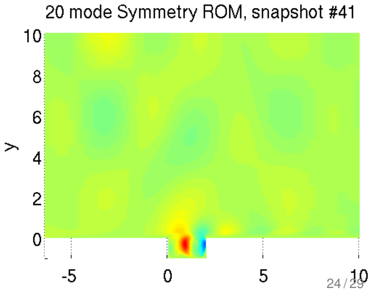

ROM based on Linearized Navier-Stokes Retaining $\nabla\bar{\mathbf{q}}$ Terms

$$\mathbf{q}'_{,t} + [\mathbf{A}_i(\bar{\mathbf{q}}) - \mathbf{K}_i^{vw}(\nabla\bar{\mathbf{q}})]\mathbf{q}'_{,i} - [\mathbf{K}_{ij}(\bar{\mathbf{q}})\mathbf{q}'_{,j}]_{,i} + \mathbf{C}(\nabla\bar{\mathbf{q}})\mathbf{q}' = \mathbf{F}$$

- Figure below shows:
  - $\circ$: t vs. $a_i(t)$ (ROM coefficients).
  - $-$: t vs. $(\mathbf{q}'_{CFD}(\mathbf{x},t), \boldsymbol{\phi}_i(\mathbf{x}))$ (projection of snapshots onto modes).
- Movie on right shows v-velocity snapshot (top) vs. 20 mode symmetry ROM solution v (bottom).

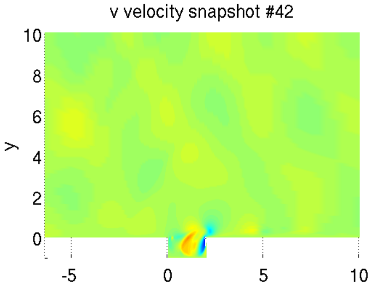

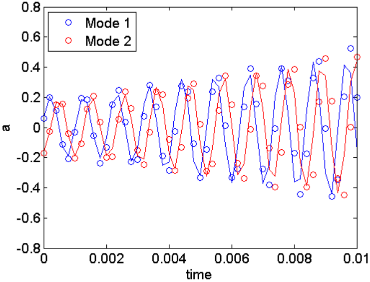

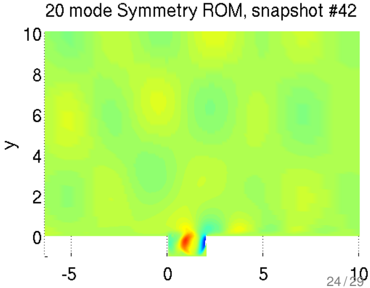

ROM based on Linearized Navier-Stokes Retaining $\nabla\bar{\mathbf{q}}$ Terms

$$\mathbf{q}'_{,t} + [\mathbf{A}_i(\bar{\mathbf{q}}) - \mathbf{K}_i^{vw}(\nabla\bar{\mathbf{q}})]\mathbf{q}'_{,i} - [\mathbf{K}_{ij}(\bar{\mathbf{q}})\mathbf{q}'_{,j}]_{,i} + \mathbf{C}(\nabla\bar{\mathbf{q}})\mathbf{q}' = \mathbf{F}$$

- Figure below shows:
  - $\circ$: t vs. $a_i(t)$ (ROM coefficients).
  - $-$: t vs. $(\mathbf{q}'_{CFD}(\mathbf{x}, t), \boldsymbol{\phi}_i(\mathbf{x}))$ (projection of snapshots onto modes).
- Movie on right shows v-velocity snapshot (top) vs. 20 mode symmetry ROM solution v (bottom).

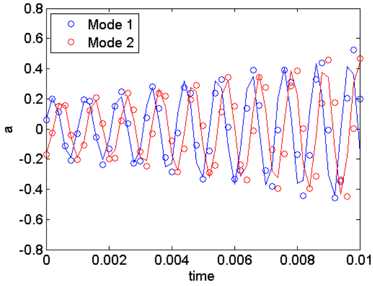

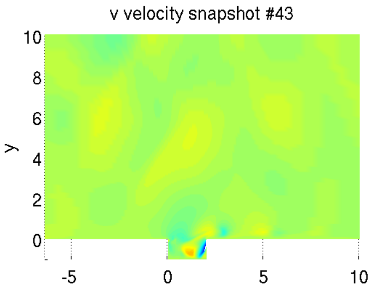

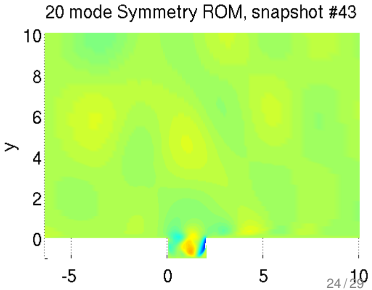

ROM based on Linearized Navier-Stokes Retaining $\nabla\bar{\mathbf{q}}$ Terms

$$\mathbf{q}'_{,t} + [\mathbf{A}_i(\bar{\mathbf{q}}) - \mathbf{K}_i^{vw}(\nabla\bar{\mathbf{q}})]\mathbf{q}'_{,i} - [\mathbf{K}_{ij}(\bar{\mathbf{q}})\mathbf{q}'_{,j}]_{,i}$$
$$+\mathbf{C}(\nabla\bar{\mathbf{q}})\mathbf{q}' = \mathbf{F}$$

- Figure below shows:
  - $\circ$: t vs. $a_i(t)$ (ROM coefficients).
  - $-$: t vs. $(\mathbf{q}'_{CFD}(\mathbf{x}, t), \boldsymbol{\phi}_i(\mathbf{x}))$ (projection of snapshots onto modes).
- Movie on right shows v-velocity snapshot (top) vs. 20 mode symmetry ROM solution v (bottom).

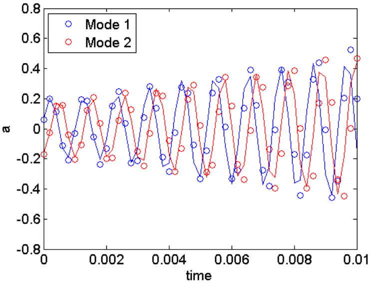

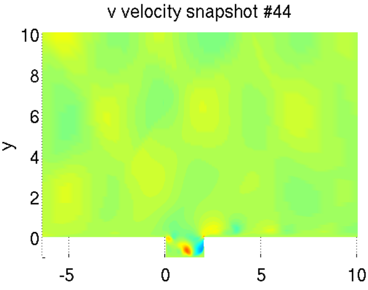

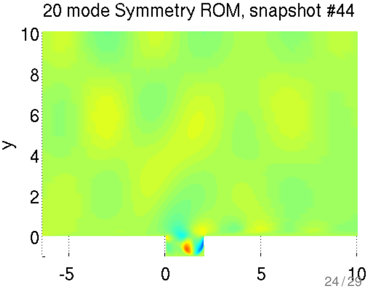

ROM based on Linearized Navier-Stokes Retaining $\nabla\bar{\mathbf{q}}$ Terms

$$\mathbf{q}'_{,t} + [\mathbf{A}_i(\bar{\mathbf{q}}) - \mathbf{K}_i^{vw}(\nabla\bar{\mathbf{q}})]\mathbf{q}'_{,i} - [\mathbf{K}_{ij}(\bar{\mathbf{q}})\mathbf{q}'_{,j}]_{,i} + \mathbf{C}(\nabla\bar{\mathbf{q}})\mathbf{q}' = \mathbf{F}$$

- Figure below shows:
  - $\circ$: t vs. $a_i(t)$ (ROM coefficients).
  - $-$: t vs. $(\mathbf{q}'_{CFD}(\mathbf{x},t), \boldsymbol{\phi}_i(\mathbf{x}))$ (projection of snapshots onto modes).
- Movie on right shows v-velocity snapshot (top) vs. 20 mode symmetry ROM solution v (bottom).

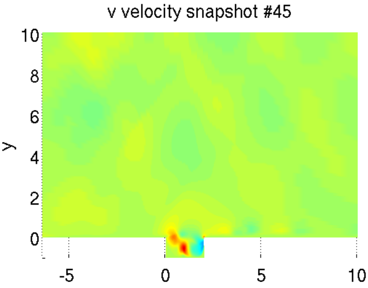

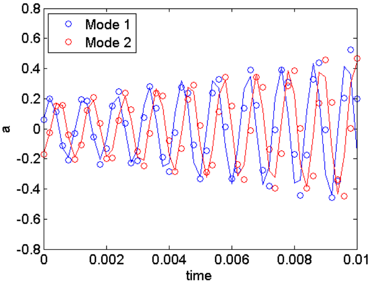

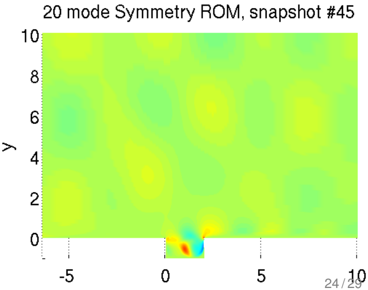

ROM based on Linearized Navier-Stokes Retaining $\nabla\bar{\mathbf{q}}$ Terms

$$\mathbf{q}'_{,t} + [\mathbf{A}_i(\bar{\mathbf{q}}) - \mathbf{K}_i^{vw}(\nabla\bar{\mathbf{q}})]\mathbf{q}'_{,i} - [\mathbf{K}_{ij}(\bar{\mathbf{q}})\mathbf{q}'_{,j}]_{,i} + \mathbf{C}(\nabla\bar{\mathbf{q}})\mathbf{q}' = \mathbf{F}$$

- Figure below shows:
  - $\circ$: t vs. $a_i(t)$ (ROM coefficients).
  - $-$: t vs. $(\mathbf{q}'_{CFD}(\mathbf{x},t), \boldsymbol{\phi}_i(\mathbf{x}))$ (projection of snapshots onto modes).
- Movie on right shows v-velocity snapshot (top) vs. 20 mode symmetry ROM solution v (bottom).

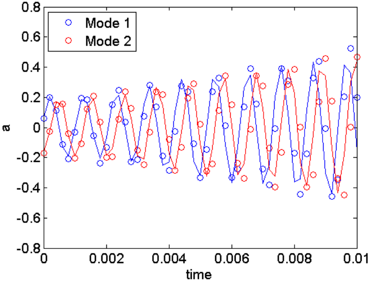

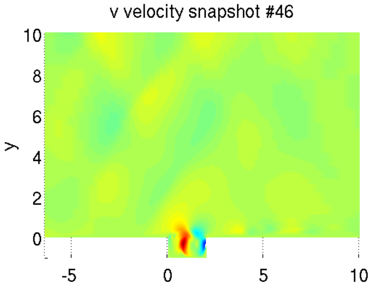

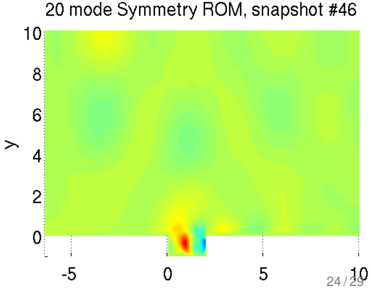

ROM based on Linearized Navier-Stokes Retaining $\nabla\bar{\mathbf{q}}$ Terms

$$\mathbf{q}'_{,t} + [\mathbf{A}_i(\bar{\mathbf{q}}) - \mathbf{K}_i^{vw}(\nabla\bar{\mathbf{q}})]\mathbf{q}'_{,i} - [\mathbf{K}_{ij}(\bar{\mathbf{q}})\mathbf{q}'_{,j}]_{,i} + \mathbf{C}(\nabla\bar{\mathbf{q}})\mathbf{q}' = \mathbf{F}$$

- Figure below shows:
  - $\circ$: t vs. $a_i(t)$ (ROM coefficients).
  - $-$: t vs. $(\mathbf{q}'_{CFD}(\mathbf{x},t), \boldsymbol{\phi}_i(\mathbf{x}))$ (projection of snapshots onto modes).
- Movie on right shows v-velocity snapshot (top) vs. 20 mode symmetry ROM solution v (bottom).

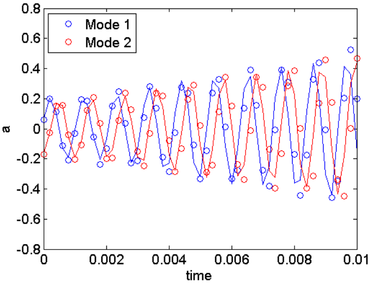

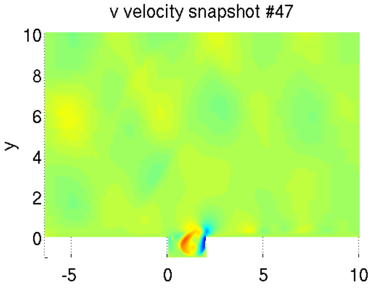

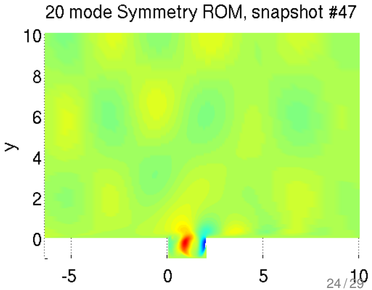

ROM based on Linearized Navier-Stokes Retaining $\nabla\bar{\mathbf{q}}$ Terms

$$\mathbf{q}'_{,t} + [\mathbf{A}_i(\bar{\mathbf{q}}) - \mathbf{K}_i^{vw}(\nabla\bar{\mathbf{q}})]\mathbf{q}'_{,i} - [\mathbf{K}_{ij}(\bar{\mathbf{q}})\mathbf{q}'_{,j}]_{,i} + \mathbf{C}(\nabla\bar{\mathbf{q}})\mathbf{q}' = \mathbf{F}$$

- Figure below shows:
  - ○: t vs. $a_i(t)$ (ROM coefficients).
  - −: t vs. $(\mathbf{q}'_{CFD}(\mathbf{x},t), \boldsymbol{\phi}_i(\mathbf{x}))$ (projection of snapshots onto modes).
- Movie on right shows v-velocity snapshot (top) vs. 20 mode symmetry ROM solution v (bottom).

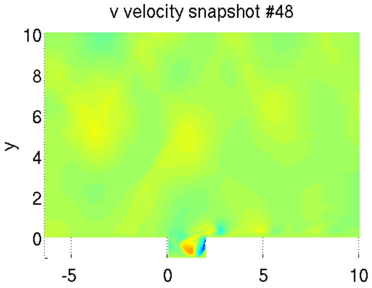

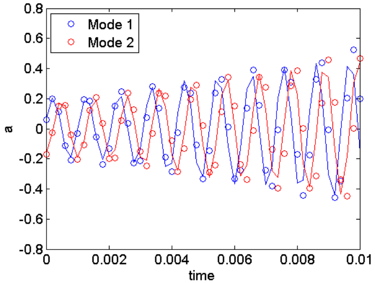

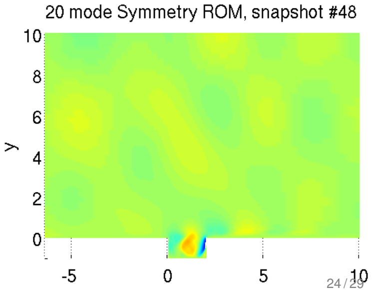

ROM based on Linearized Navier-Stokes Retaining $\nabla\bar{\mathbf{q}}$ Terms

$$\mathbf{q}'_{,t} + [\mathbf{A}_i(\bar{\mathbf{q}}) - \mathbf{K}_i^{vw}(\nabla\bar{\mathbf{q}})]\mathbf{q}'_{,i} - [\mathbf{K}_{ij}(\bar{\mathbf{q}})\mathbf{q}'_{,j}]_{,i} + \mathbf{C}(\nabla\bar{\mathbf{q}})\mathbf{q}' = \mathbf{F}$$

- Figure below shows:
  - $\circ$: t vs. $a_i(t)$ (ROM coefficients).
  - $-$: t vs. $(\mathbf{q}'_{CFD}(\mathbf{x}, t), \boldsymbol{\phi}_i(\mathbf{x}))$ (projection of snapshots onto modes).
- Movie on right shows v-velocity snapshot (top) vs. 20 mode symmetry ROM solution v (bottom).

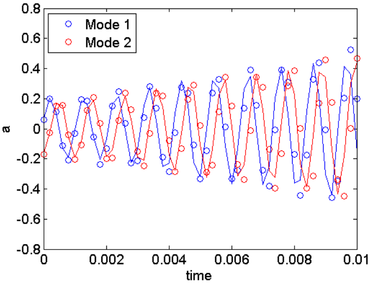

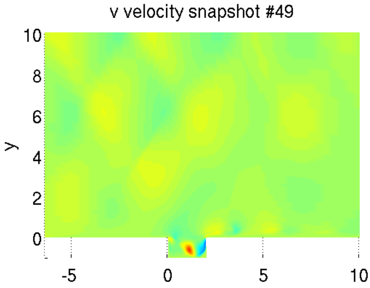

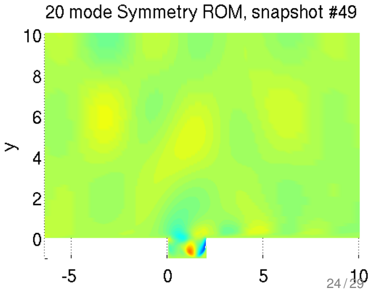

ROM based on Linearized Navier-Stokes Retaining $\nabla\bar{\mathbf{q}}$ Terms

$$\mathbf{q}'_{,t} + [\mathbf{A}_i(\bar{\mathbf{q}}) - \mathbf{K}_i^{vw}(\nabla\bar{\mathbf{q}})]\mathbf{q}'_{,i} - [\mathbf{K}_{ij}(\bar{\mathbf{q}})\mathbf{q}'_{,j}]_{,i} + \mathbf{C}(\nabla\bar{\mathbf{q}})\mathbf{q}' = \mathbf{F}$$

- Figure below shows:
  - $\circ$: t vs. $a_i(t)$ (ROM coefficients).
  - $-$: t vs. $(\mathbf{q}'_{CFD}(\mathbf{x},t), \boldsymbol{\phi}_i(\mathbf{x}))$ (projection of snapshots onto modes).
- Movie on right shows v-velocity snapshot (top) vs. 20 mode symmetry ROM solution v (bottom).

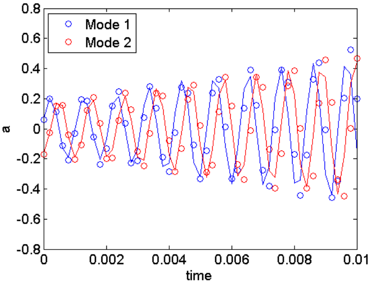

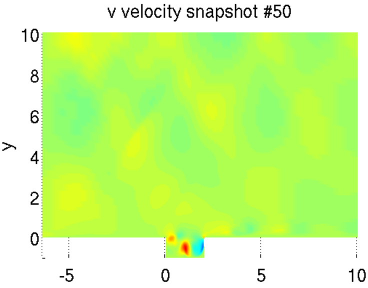

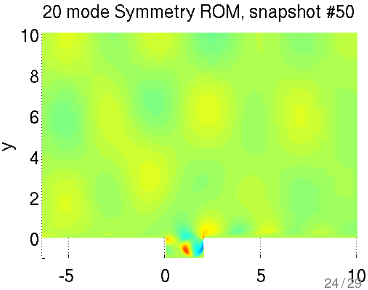

ROM based on Linearized Navier-Stokes Retaining $\nabla\bar{\mathrm{q}}$ Terms

Summary & Future Work

- A Galerkin ROM in which the *continuous* equations are projected onto the basis modes in a *continuous* inner product is proposed.
- The choice of inner product for the Galerkin projection step is crucial to stability of the ROM.
  - For linearized compressible flow, Galerkin projection in the "symmetry" inner product leads to a ROM that is stable for any choice of basis.
  - Continuous "symmetry" inner product has discrete counterpart that can be determined in a black box fashion for *any* stable linear system.
- Extensions to non-linear compressible flows based on a local linearization of the governing equations prior to projection is described.
- Performance of the proposed POD/Galerkin ROM is examined on a linear as well as a non-linear test case.
  - LQR controller design/performance demonstrated on linear test case (driven inviscid pulse).
  - Importance of retaining velocity gradient terms in ROM equations illustrated on non-linear test case (driven cavity)

Future Work: Controller design for non-linear cavity problems

References (www.sandia.gov/$\sim$ikalash)

[1] **I. Kalashnikova**, S. Arunajatesan. “A Stable Galerkin Reduced Order Model (ROM) for Compressible Flow”. *WCCM Paper No. 2012-18407*, 10th World Congress for Computational Mechanics (WCCM), Sao Paulo, Brazil (July 2012).

[2] **I. Kalashnikova**, M.F. Barone. “On the Stability and Convergence of a Galerkin Reduced Order Model (ROM) of Compressible Flow with Solid Wall and Far-Field Boundary Treatment”. *Int. J. Numer. Meth. Engng.* **83** (2010) 1345-1375.

[3] M.F. Barone, **I. Kalashnikova**, D.J. Segalman, H. Thornquist. “Stable Galerkin Reduced Order Models for Linearized Compressible Flow”. *J. Comput. Phys.* **288** (2009) 1932-1946.

[4] **I. Kalashnikova**, M.F. Barone. “Stable and Efficient Galerkin Reduced Order Model for Non-Linear Fluid Flow”. *AIAA Paper No. 2011–3110, 6th AIAA Theoretical Fluid Mechanics Conference*, Honolulu, HI (June 2011).

[5] J.S. Hesthaven, D. Gottlieb. “A stable penalty method for the compressible Navier-Stokes equations: I. Open boundary conditions.” *SIAM J. Sci. Comput.* **17**(3) 579–612 (1996).

[6] V. Sankaran, S. Menon. “LES of Scalar Mixing in Supersonic Shear Layers.” *Proceedings of the Combustion Institute*, **30**(2) 2835–2842 (2004).

[7] M.A. Heroux, R.A. Bartlett, V.E. Howle, R.J. Hoekstra, J.J. Hu, T.G. Kolda, R.B. Lehoucq, K.R. Long, R.P. Pawlowski, E.T. Phipps, A.G. Salinger, H.K. Thornquist, R.S. Tuminaro, J.M. Willenbring, A. Williams, K.S. Stanley. “An overview of the Trilinos project”. *ACM Trans. Math. Softw.* **31**(3) (2005).

[8] R.M. Murray, K.J. Astrom. “Feedback systems: an introduction for scientists and engineers.” Princeton University Press, 2008.

Sandia National Laboratories

References (www.sandia.gov/∼ikalash)

[1] **I. Kalashnikova**, S. Arunajatesan. “A Stable Galerkin Reduced Order Model (ROM) for Compressible Flow”. *WCCM Paper No. 2012-18407*, 10th World Congress for Computational Mechanics (WCCM), Sao Paulo, Brazil (July 2012).

[2] **I. Kalashnikova**, M.F. Barone. “On the Stability and Convergence of a Galerkin Reduced Order Model (ROM) of Compressible Flow with Solid Wall and Far-Field Boundary Treatment”. *Int. J. Numer. Meth. Engng.* **83** (2010) 1345-1375.

[3] M.F. Barone, **I. Kalashnikova**, D.J. Segalman, H. Thornquist. “Stable Galerkin Reduced Order Models for Linearized Compressible Flow”. *J. Comput. Phys.* **288** (2009) 1932-1946.

[4] **I. Kalashnikova**, M.F. Barone. “Stable and Efficient Galerkin Reduced Order Model for Non-Linear Fluid Flow”. *AIAA Paper No. 2011–3110, 6th AIAA Theoretical Fluid Mechanics Conference*, Honolulu, HI (June 2011).

[5] J.S. Hesthaven, D. Gottlieb. “A stable penalty method for the compressible Navier-Stokes equations: I. Open boundary conditions.” *SIAM J. Sci. Comput.* **17**(3) 579–612 (1996).

[6] V. Sankaran, S. Menon. “LES of Scalar Mixing in Supersonic Shear Layers.” *Proceedings of the Combustion Institute*, **30**(2) 2835–2842 (2004).

[7] M.A. Heroux, R.A. Bartlett, V.E. Howle, R.J. Hoekstra, J.J. Hu, T.G. Kolda, R.B. Lehoucq, K.R. Long, R.P. Pawlowski, E.T. Phipps, A.G. Salinger, H.K. Thornquist, R.S. Tuminaro, J.M. Willenbring, A. Williams, K.S. Stanley. “An overview of the Trilinos project”. *ACM Trans. Math. Softw.* **31**(3) (2005).

[8] R.M. Murray, K.J. Astrom. “Feedback systems: an introduction for scientists and engineers.” Princeton University Press, 2008.

Thank you! Questions?

ikalash@sandia.gov

Sandia National Laboratories

Linearized ROM System Matrices

$$
\mathbf{A}_1 = \begin{pmatrix} \bar{u}_1 & 0 & 0 & R & \frac{R\bar{T}}{\bar{\rho}} \\ 0 & \bar{u}_1 & 0 & 0 & 0 \\ 0 & 0 & \bar{u}_1 & 0 & 0 \\ \bar{T}(\gamma-1) & 0 & 0 & \bar{u}_1 & 0 \\ \bar{\rho} & 0 & 0 & 0 & \bar{u}_1 \end{pmatrix}, \quad \mathbf{A}_2 = \begin{pmatrix} \bar{u}_2 & 0 & 0 & 0 & 0 \\ 0 & \bar{u}_2 & 0 & R & \frac{R\bar{T}}{\bar{\rho}} \\ 0 & 0 & \bar{u}_2 & 0 & 0 \\ 0 & \bar{T}(\gamma-1) & 0 & \bar{u}_2 & 0 \\ 0 & \bar{\rho} & 0 & 0 & \bar{u}_2 \end{pmatrix}
$$

$$
\mathbf{A}_3 = \begin{pmatrix} \bar{u}_3 & 0 & 0 & 0 & 0 \\ 0 & \bar{u}_3 & 0 & 0 & 0 \\ 0 & 0 & \bar{u}_3 & R & \frac{R\bar{T}}{\bar{\rho}} \\ 0 & 0 & \bar{T}(\gamma-1) & \bar{u}_3 & 0 \\ 0 & 0 & \bar{\rho} & 0 & \bar{u}_3 \end{pmatrix}, \quad \mathbf{K}_{11} \equiv \frac{1}{\bar{\rho}Re} \begin{pmatrix} 2\mu+\lambda & 0 & 0 & 0 & 0 \\ 0 & \mu & 0 & 0 & 0 \\ 0 & 0 & \mu & 0 & 0 \\ 0 & 0 & 0 & \frac{\gamma\kappa}{Pr} & 0 \\ 0 & 0 & 0 & 0 & 0 \end{pmatrix},
$$

$$
\mathbf{K}_{12} \equiv \frac{1}{\bar{\rho}Re} \begin{pmatrix} 0 & \lambda & 0 & 0 & 0 \\ \mu & 0 & 0 & 0 & 0 \\ 0 & 0 & 0 & 0 & 0 \\ 0 & 0 & 0 & 0 & 0 \\ 0 & 0 & 0 & 0 & 0 \end{pmatrix}, \quad \mathbf{K}_{13} \equiv \frac{1}{\bar{\rho}Re} \begin{pmatrix} 0 & 0 & \lambda & 0 & 0 \\ 0 & 0 & 0 & 0 & 0 \\ \mu & 0 & 0 & 0 & 0 \\ 0 & 0 & 0 & 0 & 0 \\ 0 & 0 & 0 & 0 & 0 \end{pmatrix}
$$

$$
\mathbf{K}_{21} \equiv \frac{1}{\bar{\rho}Re} \begin{pmatrix} 0 & \mu & 0 & 0 & 0 \\ \lambda & 0 & 0 & 0 & 0 \\ 0 & 0 & 0 & 0 & 0 \\ 0 & 0 & 0 & 0 & 0 \\ 0 & 0 & 0 & 0 & 0 \end{pmatrix}, \quad \mathbf{K}_{22} \equiv \frac{1}{\bar{\rho}Re} \begin{pmatrix} \mu & 0 & 0 & 0 & 0 \\ 0 & 2\mu+\lambda & 0 & 0 & 0 \\ 0 & 0 & \mu & 0 & 0 \\ 0 & 0 & 0 & \frac{\gamma\kappa}{Pr} & 0 \\ 0 & 0 & 0 & 0 & 0 \end{pmatrix}
$$

Linearized ROM System Matrices (continued)

$$\mathbf{K}_{23} \equiv \frac{1}{\bar{\rho} Re}\begin{pmatrix} 0 & 0 & 0 & 0 & 0 \\ 0 & 0 & \lambda & 0 & 0 \\ 0 & \mu & 0 & 0 & 0 \\ 0 & 0 & 0 & 0 & 0 \\ 0 & 0 & 0 & 0 & 0 \end{pmatrix}, \quad \mathbf{K}_{31} \equiv \frac{1}{\bar{\rho} Re}\begin{pmatrix} 0 & 0 & \mu & 0 & 0 \\ 0 & 0 & 0 & 0 & 0 \\ \lambda & 0 & 0 & 0 & 0 \\ 0 & 0 & 0 & 0 & 0 \\ 0 & 0 & 0 & 0 & 0 \end{pmatrix}$$

$$\mathbf{K}_{32} \equiv \frac{1}{\bar{\rho} Re}\begin{pmatrix} 0 & 0 & 0 & 0 & 0 \\ 0 & 0 & \mu & 0 & 0 \\ 0 & \lambda & 0 & 0 & 0 \\ 0 & 0 & 0 & 0 & 0 \\ 0 & 0 & 0 & 0 & 0 \end{pmatrix}, \quad \mathbf{K}_{33} \equiv \frac{1}{\bar{\rho} Re}\begin{pmatrix} \mu & 0 & 0 & 0 & 0 \\ 0 & \mu & 0 & 0 & 0 \\ 0 & 0 & 2\mu + \lambda & 0 & 0 \\ 0 & 0 & 0 & \frac{\gamma\kappa}{Pr} & 0 \\ 0 & 0 & 0 & 0 & 0 \end{pmatrix}$$

$$\mathbf{K}_1^{vw} \equiv \begin{pmatrix} 0 & 0 & 0 & 0 & 0 \\ 0 & 0 & 0 & 0 & 0 \\ 0 & 0 & 0 & 0 & 0 \\ \frac{(\gamma-1)}{R\bar{\rho}}\bar{\tau}_{11} & \frac{(\gamma-1)}{R\bar{\rho}}\bar{\tau}_{12} & \frac{(\gamma-1)}{R\bar{\rho}}\bar{\tau}_{13} & 0 & 0 \\ 0 & 0 & 0 & 0 & 0 \end{pmatrix}, \quad \mathbf{K}_2^{vw} \equiv \begin{pmatrix} 0 & 0 \\ 0 & 0 \\ 0 & 0 \\ \frac{(\gamma-1)}{R\bar{\rho}}\bar{\tau}_{21} & \frac{(\gamma-1)}{R\bar{\rho}}\bar{\tau}_{22} \\ 0 & 0 \end{pmatrix}$$

$$\mathbf{K}_3^{vw} \equiv \begin{pmatrix} 0 & 0 & 0 & 0 & 0 \\ 0 & 0 & 0 & 0 & 0 \\ 0 & 0 & 0 & 0 & 0 \\ \frac{(\gamma-1)}{R\bar{\rho}}\bar{\tau}_{31} & \frac{(\gamma-1)}{R\bar{\rho}}\bar{\tau}_{32} & \frac{(\gamma-1)}{R\bar{\rho}}\bar{\tau}_{33} & 0 & 0 \\ 0 & 0 & 0 & 0 & 0 \end{pmatrix}$$

Linearized ROM System Matrices (continued)

$$\mathbf{C} = \begin{pmatrix} \frac{\partial \bar{u}}{\partial x} & \frac{\partial \bar{u}}{\partial y} & \frac{\partial \bar{u}}{\partial z} & \frac{R}{\bar{\rho}}\frac{\partial \bar{\rho}}{\partial x} & \frac{1}{\bar{\rho}}\left(\bar{\mathbf{u}} \cdot \nabla \bar{u} + R\frac{\partial \bar{T}}{\partial x}\right) \\ \frac{\partial \bar{v}}{\partial x} & \frac{\partial \bar{v}}{\partial y} & \frac{\partial \bar{v}}{\partial z} & \frac{R}{\bar{\rho}}\frac{\partial \bar{\rho}}{\partial y} & \frac{1}{\bar{\rho}}\left(\bar{\mathbf{u}} \cdot \nabla \bar{v} + R\frac{\partial \bar{T}}{\partial y}\right) \\ \frac{\partial \bar{w}}{\partial x} & \frac{\partial \bar{w}}{\partial y} & \frac{\partial \bar{w}}{\partial z} & \frac{R}{\bar{\rho}}\frac{\partial \bar{\rho}}{\partial z} & \frac{1}{\bar{\rho}}\left(\bar{\mathbf{u}} \cdot \nabla \bar{w} + R\frac{\partial \bar{T}}{\partial z}\right) \\ \frac{\partial \bar{T}}{\partial x} & \frac{\partial \bar{T}}{\partial y} & \frac{\partial \bar{T}}{\partial z} & (\gamma - 1)\nabla \cdot \bar{\mathbf{u}} & \frac{1}{\bar{\rho}}\left(\bar{\mathbf{u}} \cdot \nabla \bar{T} + (\gamma - 1)\bar{T}\nabla \cdot \bar{\mathbf{u}}\right) \\ \frac{\partial \bar{\rho}}{\partial x} & \frac{\partial \bar{\rho}}{\partial y} & \frac{\partial \bar{\rho}}{\partial z} & 0 & \nabla \cdot \bar{\mathbf{u}} \end{pmatrix}$$